TRANSPORTATION RESEARCH

RECORD

No. 1335

Materials and Construction

Concrete Technology

A peer-reviewed publication of the Transportation Research Board

TRANSPORTATION RESEARCH BOARD
NATIONAL RESEARCH COUNCIL
WASHINGTON, D.C. 1992

Transportation Research Record 1335
Price: $20.00

Subscriber Category
IIIB materials and construction

TRB Publications Staff
Director of Publications: Nancy A. Ackerman
Senior Editor: Naomi C. Kassabian
Associate Editor: Alison G. Tobias
Assistant Editors: Luanne Crayton, Norman Solomon
Production Coordinator: Karen W. McClain
Office Manager: Phyllis D. Barber
Production Assistant: Betty L. Hawkins

Printed in the United States of America

Library of Congress Cataloging-in-Publication Data
National Research Council. Transportation Research Board.

Concrete technology.
p. cm.—(Transportation research record ISSN 0361-1981 ; no. 1335)
"A peer-reviewed publication of the Transportation Research Board."
Includes bibliographical references.
ISBN 0-309-05173-8
1. Pavements, Concrete—Testing. 2. Bridges, Concrete—Floors—Testing. 3. Pavements, Reinforced concrete—Testing. I. National Research Council (U.S.). Transportation Research Board. II. Series Transportation research record ; 1335.
TE7.H5 no. 1335
[TE278]
388 s—dc20
[625.8'4] 92-19392
CIP

Sponsorship of Transportation Research Record 1335

GROUP 2—DESIGN AND CONSTRUCTION OF TRANSPORTATION FACILITIES
Chairman: Charles T. Edson, New Jersey Department of Transportation

Concrete Section
Chairman: Thomas J. Pasko, Jr., Federal Highway Administration

Committee on Performance of Concrete
Chairman: Donald J. Janssen, University of Washington
M. Arockiasamy, Philip D. Cady, William P. Chamberlin, James R. Clifton, Glen William De Puy, Philip H. Decabooter, John W. Figg, Kenneth C. Hover, Inam Jawed, Joseph F. Lamond, Richard C. Meininger, Roger P. Northwood, John T. Paxton, Steven A. Ragan, V. Ramakrishnan, John Ryell, Charles F. Scholer, David Stark, Richard Edwin Weyers

Committee on Mechanical Properties of Concrete
Chairman: Michael M. Sprinkel, Virginia Transportation Research Council
Archie F. Carter, Jr., J. Harold Deatherage, James T. Dikeou, Wilbur Charles Greer, Jr., Lloyd E. Hackman, Inam Jawed, Louis A. Kuhlmann, Joseph F. Lamond, V. M. Malhotra, Richard C. Meininger, Edward G. Nawy, Sandor Popovics, Steven A. Ragan, V. Ramakrishnan, Masood Rasoulian, David R. Reidenouer, Gary L. Robson, Robert R. Santoro, Ernest Schrader, Raymond J. Schutz, S. P. Shah, Parviz Soroushian, Peter C. Tatnall, Dan G. Zollinger

Committee on Chemical Additions and Admixtures for Concrete
Chairman: H. Celik Ozyildirim, Virginia Transportation Research Council
Bernard C. Brown, John W. Bugler, Ramon L. Carrasquillo, Henry H. Duval, Jr., Richard D. Gaynor, R. Douglas Hooton, Kenneth C. Hover, Inam Jawed, Daniel P. Johnston, Kamal Henri Khayat, T. J. Larsen, Mosongo Moukwa, Michael F. Pistilli, V. Ramakrishnan, Jere Rose, Maris A. Sermolins, A. Haleem Tahir, Samuel S. Tyson, Suneel N. Vanikar, Thomas G. Weil, David Whiting

Frederick D. Hejl, Transportation Research Board staff

Sponsorship is indicated by a footnote at the end of each paper. The organizational units, officers, and members are as of December 31, 1991.

Transportation Research Record 1335

Contents

Foreword

The papers in this Record, on various facets of concrete technology, should be of interest to state and local construction, design, materials, and research engineers as well as contractors and material producers.

Chang describes the evaluation of six generic types of sealer and coating systems considered for use on nonwearing concrete surfaces in Indiana. After subjecting the systems to accelerated weathering, water absorption and vapor transmission, and rapid chloride ion permeability tests, he concluded that the epoxies and straight penetrants performed better than the others.

Smith describes the repair of delaminated bridge decks by epoxy injection. She concludes that timely epoxy repair on a delaminated bridge deck can extend the service life of the deck up to four years. McGhee and Ozyildirim describe the Virginia Department of Transportation's successful experience with the construction of thin-bonded portland cement concrete overlays of existing concrete pavements using fast-track paving. They also found that the overlay concrete bonds to the base concrete with or without the use of a bonding grout.

Sprinkel reports on a study to evaluate the performance of latex-modified concrete overlays on bridge decks in Virginia during a 20-year period. He found that latex-modified concrete overlays placed on decks with less than 2 lb/yd^3 of chloride ion at the rebar can be expected to have a service life greater than 20 years. Temple et al. describe a study on the design and construction of a bonded steel fiber reinforced concrete overlay on an existing 8-in. continuously reinforced concrete pavement in Louisiana.

Salami proposes and utilizes a constitutive model based on the theory of plasticity to characterize the behavior of plain concrete and steel-fiber-reinforced concrete. Alungbe et al. report on a study to determine the coefficient of linear thermal expansion of Florida concrete to be used in modeling and analysis of concrete pavement response and performance. In his second paper, Salami develops analytical expressions for determining the uniaxial tensile strength of plain concrete in terms of its uniaxial compressive strength.

Whiting and Mitchell describe the conception, development, and applications of the rapid chloride permeability test (AASHTO T 277-89 and ASTM C 1202-91) used to estimate a bridge's susceptibility to corrosion. Armaghani et al. present the results of the first phase of research to study strength and durability of concrete in Florida. Findings affirm the need to develop specifications for concrete durability based on requirements for both compressive strength and permeability of concrete.

Rezansoff et al. describe the nondestructive evaluation of the long-term performance of 25-year-old concrete blocks that anchored guy wires used for bracing telecommunication towers.

Laboratory Evaluation of Generic Concrete Sealer and Coating Systems

LUH-MAAN CHANG

Research was conducted to evaluate generic types of sealer and coating systems for use on nonwearing concrete surfaces in Indiana. Although significant variations exist among six generic classes of coating systems subject to accelerated weathering, water absorption and vapor transmission, and rapid chloride ion permeability tests, certain generic chemical formulations of coating systems appear to exhibit comparatively better performance than others. The epoxies were comparatively better barriers to chloride and water absorption but deteriorated and discolored sightly in the accelerated weathering test. The straight penetrants (straight silanes, silicone, and siloxane) were relatively good in terms of their ability to resist water and chloride absorption and showed little sign of deterioration in the weathering test. The materials that were combinations of the above penetrants did not perform as well as the straight penetrants. Masonry coatings were ineffective chloride barriers, but they did have aesthetic qualities. The urethane and methyl methacrylate did not perform consistently across all tests.

The deterioration of concrete structures is accelerated when damaging chemical substances and moisture are allowed to penetrate the concrete. In recent years, attempts to eliminate this problem have been made by applying surface coatings and sealers to the concrete. Although use of sealers and coatings has met with varying degrees of success, it is not uncommon for them to cause earlier failure and uneven discoloration of the concrete surface, thereby degrading the aesthetics of the structure (*1,2*). In addition, new coating systems emerge on the market almost every day. Many highway engineers continually face the challenge of selecting a proper coating system for construction projects.

Research was conducted at Purdue University to evaluate generic types of sealer and coating systems for use on nonwearing concrete surfaces in Indiana (*3*). The effectiveness of different surface sealers and coatings when applied on nonwearing concrete surface and subjected to different laboratory experiments was studied. Effectiveness was established by determining if these materials could minimize or prevent the intrusion of chloride ions into the concrete while maintaining structural and aesthetic integrity. The purpose of this paper is to present the research results and methodologies.

The paper will begin with a discussion of the methodology used in the research. Three different types of laboratory experiments will be illustrated. The analysis of the experimental data will be explained, and the results will be presented.

Division of Construction Engineering and Management, School of Civil Engineering, Purdue University, West Lafayette, Ind. 47907.

RESEARCH METHODOLOGY

A literature search was completed at Purdue University using *Thomas' Register* and *Sweets Manual* to identify the promising sealers and coatings for experimental tests and testing methods. Information and literature received from the Florida, Illinois, Indiana, Kentucky, Ohio, Tennessee, and Texas state departments of transportation were also reviewed. This review revealed the concrete sealers and coatings currently used by those states. A questionnaire regarding the technical data of concrete sealers was sent to 119 chemical companies. Product information received from 54 suppliers of coatings was analyzed. Of the 54 chemical companies that responded, 42 companies suggested 120 different materials.

After the information and literature received from the departments of transportation and the surrounding states was reviewed, 24 coatings or penetrants were selected from different chemical companies; they generally include all of the generic types of materials in use most widely. The selected materials for evaluation in this project are listed in Table 1. The reader should be aware that solids and ingredients are the same, but different material manufacturers use different names for them. They are the elements of the material composition that are left behind and constitute the dryfilm after drying. There are also differences in definition among sealers, coatings, and penetrants. However, they are used interchangeably here.

These materials were classified into six general groups. The first group includes all of the epoxies. This group contains epoxies with varying percent of solids, ranging from 20 to 100 percent (tests 1–4 and 25). The second group includes all four of the silanes, a silicone, and a siloxane (tests 7–11 and 14). The third group contains the siloxane/silicone mixture, the polysiloxane/hydrophobic-fumed silica, and the blend of many silanes (tests 15, 18, and 21). The fourth group includes all seven of the masonry coatings (tests 16, 19, 20, and 22–24). Test 17 was masonry coating. After trial rapid permeability test, it was removed from the study. The fifth group contains urethanes (tests 5 and 6). The last is methyl methacrylates (tests 12 and 13).

Three laboratory experiments were conducted on the selected penetrants and coatings: water absorption and vapor transmission test, accelerated weathering test, and rapid chlo-

TABLE 1 MATERIALS SELECTED FOR TESTING

Test No.	Chemical Composition	Percent Solids/ Ingredients	Penetrant or Coating
1	Epoxy (polyamine)	50	P
2	Epoxy (polyamine)	20	P
3	Epoxy (polysulfide)	50	P
4	Epoxy (polyamine)	50	P
5	Chemically-Cured Urethane	55	C
6	Moisture-Cured Urethane	30	P
7	Alkyl-Alkoxy Silane	40	P
8	Alkyl-Alkoxy Silane	<20	P
9	Alkyl-Alkoxy Silane	20	P
10	Alkyl-Alkoxy Silane	40	P
11	Silicone	5	P
12	Methyl Methacrylate with Silane Primer	20	P
13	Methyl Methacrylate	30	P
14	Siloxane	20	P
15	Silaxane/Silicone Mixture	10	P
16	Styrene/Acrylic Copolymer	75	C
18	Blend of Silanes	30	P
19	Vinyl Acrylic Latex	58	C
20	Polyester Resin	60	C
21	Poly-Siloxane/Hydrophobic Fumed Silica	7	P
22	Styrene/Acrylic Copolymer	61	C
23	Elastomeric Resin		C
24	Acrylic Resin		C
25	Epoxy	100	C

ride ion permeability test. The procedures for these three experiments are discussed in the following sections.

WATER ABSORPTION AND VAPOR TRANSMISSION TEST

Test Objectives

The objectives of this phase of the project were to evaluate the differences between water and chloride ion absorption for concrete coated with the 24 materials and then soaked in saltwater solution (15 percent sodium chloride) and the water vapor permeability characteristics of these coated specimens during an air-drying period (*4*). The following parameters were evaluated: (a) water absorption-vapor transmission characteristics of surface-coated concretes and (b) chloride ion penetration into surface-coated concretes.

The less water absorbed by the concrete, the better the sealing ability of the concrete material. Conversely, the more water the coated concrete absorbed, the worse the sealing ability. In contrast, the more water transmitted out during the drying process the better because less water is trapped inside the concrete. Therefore, the higher the weight loss

or weight gain, the higher the sealing ability of the painted material.

Sample Preparations

Twenty-five 4-in. cubes and two control cubes were cast for testing. The molds for the 4-in. cubes were constructed of steel and were coated with a thin film of oil to allow for easy removal of the concrete cube after an adequate curing period. The fresh concrete was placed in the molds in approximately three equal layers. Each layer was compacted by rodding using 25 strokes with a 3/8-in.-diameter steel rod. The molds were then covered with a sheet of plastic to prevent excess drying on the surface.

The prepared concrete cubes were stored for 24 hr in a laboratory environment. At the end of the 24-hr period, the molds were opened and the samples were placed in lime-saturated water for the next 4 days. Soaking the cubes in the lime-saturated water helped prevent leaching of calcium hydroxide, which breaks down the internal structure and ultimately reduces the strength of the concrete. All six sides of the cubes were lightly sandblasted after the moisture curing period at an age of 5 days to remove any foreign materials that may have been present on the surfaces.

Test Procedures

The 24 cubes were coated at an age of 28 days after an air-drying period of 22 days.

The sealers and coatings were all applied at the rate of 100 ft^2/gal. The reason for this was to try to eliminate as many variables as possible from the test in an effort to concentrate on the different paint materials. The amount of material for each cube was calculated using the weight of the material in pounds per gallon, the surface area of the cube, and the 100 ft^2/gal coverage rate. The sealers and coatings were applied by brush. The cubes were then stored in a laboratory environment. Two control specimens were prepared with which to compare the coated cubes.

After the drying period for the coatings, the cubes were weighed and immersed in a 15 percent NaCl solution. The cubes were then at the age of 35 days.

All cubes were placed in a plastic container with approximately 6 gal of 15 percent NaCl solution. About an inch cover of the solution was maintained over the tops of the cubes. During the soaking period, the gain in the saturated surface dry cube weight after 3, 6, 9, 12, 15, 18, and 21 days of soaking was determined to the nearest 0.001 lb. Immediately after each weighing, the cubes were returned to the solution. The solution was stirred periodically to eliminate settling. After 21 days of soaking in the solution, each cube was removed from the water bath and moved to a climate-controlled room (70°F and around 65 percent relative humidity). They were stored on steel racks and moved periodically to reduce the effect of variations in air circulation. During the following 24-day air-drying period, the loss in weight at 3, 6, 9, 12, 15, 18, 21, and 24 days was determined by weighing to the nearest 0.001 lb. After the air-drying period, the cubes were moved to another environmentally controlled room for 12 more days (100°F and 20 percent relative humidity). The loss in weight at 27, 30, 33, and 36 days was determined by weighing to the nearest 0.001 lb.

After the water absorption and vapor transmission testing, powder samples were taken from each of the 24 coated cubes and the 2 untreated control specimens. In order to extract the powder samples, two holes were drilled in opposite sides of each of the cubes. Three powder samples were taken from both of the holes in each cube, for a total of six samples from each cube. The first powder sample was taken at a depth of 1/2 in., the second at 1 in., and the third at 1 1/2 in. All six of the powder samples were tested for chloride content; the values were averaged together and are presented here. The total chloride content was determined using an acid-digestion potentiometric titration procedure.

ACCELERATED WEATHERING TEST

The objective of this test was to determine the influence of 14 weeks of accelerated laboratory weathering on the performance of sealers and coatings when applied to concrete. The performance was judged by making periodical visual observations of the surface conditions by measuring the chloride ion contents in the concrete at the end of the test and by measuring the gloss of the surface with a glossmeter every 2 weeks.

The accelerated weathering method used in this study was similar to the northern climate method described in NCHRP Report 244 (*4*). This accelerated weathering cycle was designed to expose the slabs to a wide range of environmental factors, including acid, saltwater, thermal heat, ultraviolet exposure, fresh water rinse, and overnight freezing and thawing.

Sample Preparation

Twenty-five concrete slabs and two control slabs were cast in wood frames coated with shellac for easy removal. The test slabs were 4-in. thick and 11-in. square. A dike about 1-in. high was formed on the test surface so that the saltwater could be pounded during testing.

The slabs were covered with a sheet of plastic and allowed to cure for 1 day in a laboratory environment. After curing, the slabs were stripped from their forms and transferred to a moisture curing room for 4 additional days. At the end of this curing period, the slabs were lightly sandblasted to remove any foreign material.

The slabs were allowed to air dry in a laboratory environment for different lengths of time. The sealers and coatings were then applied according to the manufacturers' recommendations. Nine samples were coated at the age of 7 days, 3 at the age of 14 days, 2 at the age of 21 days, and 11 at the age of 28 days. The amount of material for each slab was calculated using the weight of the material in pounds per gallon, the recommended coverage rates, and the surface area of the slabs. The sealers and coatings were applied by brush in a laboratory environment. The second coat, if required, was applied after 24 hr. The slabs were then stored in a laboratory environment for 7 days.

Ultraviolet Light Apparatus

The monthly total for normal ultraviolet radiation (with wave lengths from 2950 to 3950 A') for winter months in Indianapolis is approximately 2460 W-hr/m^2/month. The ultraviolet source used during this phase of the testing consisted of a standard 48-in.-long fluorescent fixture with two 40-W ultraviolet lamps (W-F40BL) on the fixture. Four slabs were positioned 9 in. under two fixtures, which provided 14 to 18 W/m^2.

By using average values of monthly winter and summer ultraviolet radiation for northern regions along with the average number of hours of daylight per month, 166.7 W-hr/m^2/day was calculated to be the approximate normal radiation from the sun for a typical yearly average day. This value was taken from NCHRP Report 244 (*4*).

The test slabs received 3 hr of ultraviolet exposure per day for 5 weekdays and 66 hr of ultraviolet exposure between 5 p.m. Friday and 8 a.m. Monday. Thus, the slabs received approximately 1,280 W-hr/m^2/week for the entire 24-week period. The total cumulative ultraviolet light exposure during the 24-week testing was slightly more than 30,000 W-hr/m^2, which is roughly equivalent to 185 average northern days of ultraviolet radiation exposure per year.

Northern Climate Test Procedure

This test method was based on a daily cycle, with limited activity extending through the weekends. The following 24-hr cycle was repeated for the 5 weekdays for 24 weeks:

- 15-hr overnight freeze at 0°F; the diked test surface was empty.
- 2-hr thaw at 73 to 83°F; the diked test surface was empty.
- 3-hr exposure to ultraviolet radiation and thermal heat at 95°F (+/- 5°F); the test surface was empty.
- 3-hr soaking period with 15 percent NaCl and 0.02 molar sulfurous avid water solution on the test surface (fresh solution every other day).
- Test solution poured off, slab rinsed with fresh water and drained.
- Slab returned to freezer.

On weekends the specimens were exposed to the ultraviolet radiation and the 95°F temperature. The diked test surface remained empty during weekends.

The northern climate test solution contained a 15 percent NaCl and 0.02 molar sulfurous acid solution component to represent the salts that are spread over the highways throughout the winter and the acids found in the rains and atmosphere in northern industrial regions.

During the 24-week test period, visual inspections, photographs, and notes of the condition of the slabs were recorded biweekly. Glossmeter measurements were also taken to show the loss in gloss of the surfaces during the entire testing period using a 60-degree glossmeter.

Chloride Ion Content Procedure

Following the 24-week testing period, powder samples were taken from each of the 24 coated slabs and the untreated control slabs. Two holes were drilled in each of the slabs in order to extract the powder samples. Four powder samples were taken from both of the holes in each slab, for a total of eight samples from each slab. The first powder sample was taken at a depth of 1/2 in., the second at 1 in., the third at 1 1/2 in., and the fourth at 2 in. All eight of the powder samples were tested for chloride content, and the values were averaged together and are presented here. The total chloride content was determined using an acid-digestion potentiometric titration procedure. This testing was done at the Indiana Department of Highways (IDOH) Materials and Testing Lab with the help of IDOH personnel.

Glossmeter Data

The glossiness of the test surfaces is one of indexes to the overall appearance of the concrete and can be measured with a glossmeter. Four readings were taken on each surface every 2 weeks and then averaged to obtain a mean value for that particular day.

RAPID CHLORIDE ION PERMEABILITY TEST

The objective of the chloride ion permeability test was to determine the ability of the sealers and coatings to prevent penetration of chloride ions.

It has been shown in recent studies that chloride can be caused to migrate out of a concrete slab quite rapidly by applying an external electric field across the slab (*5*). This technique can be used as a chloride permeability method if the polarity is reversed by placing a sodium hydroxide solution (+) on one side and a sodium chloride solution (−) on the other. The chloride ions thus migrate into the concrete under the influence of an electric field. As the electrical resistivity of the concrete decreases with the increasing chloride ion concentration, a measure of the increase in current with the time can be correlated with the amount of chloride entering the concrete.

The fresh concrete was placed inside oiled molds 3.75 in. in diameter and 6 in. tall. Three layers were made, and each layer was rodded 25 times with a 3/8-in.-diameter rod.

The cylinders were cured for 24 hr in the molds. They were then removed from the molds and placed in lime-saturated water for 3 days. At the age of 5 days the cylinders were cut into 2-in. disks. The flat surfaces of the cylinders were lightly sandblasted.

The cylinders were allowed to cure until the age of 28 days, at which time 24 disks were coated with the materials. Two control disks remained. The amount of material used to coat all of the cylinders was 100 ft^2/gal. All the coated cylinders were allowed to cure for an additional 7 days in a laboratory environment before the testing began.

Concrete Mixture Design

The concrete was designed to meet the requirements of the IDOH specifications for Class A concrete (*6*). All the concrete specimens were designed to have a water to cement ratio no greater than 0.66, (564 lbs. cement), an air content

between 5 and 8 percent, a ratio of fine aggregate to total aggregate between 35 and 45 percent (by weight), and a slump of 3.0 in.

Source of Errors

Readers should be cautious interpreting the results because of the following several possible sources for errors.

1. No replicates for each individual type of sealer or coating system were made. This could limit the evaluation of validity and reliability of the experimental data obtained from the research. However, many replicates were provided for each generic type of sealer or coating.

were not followed precisely in either the accelerated weathering test or the water absorption and vapor transmission test. Some procedures were adjusted slightly to suit the limited environment.

2. Because of the limitation of testing space and instruments, the procedures discussed in NCHRP Report 244 (*4*)

3. Each individual type of sealer or coating has its own special formula. Although each was grouped into a certain generic type, a slightly different ingredient in the formula could make a big difference in performance when applied to the concrete surface.

RESULTS OF INDIVIDUAL TYPE AND DISCUSSION

Water Absorption and Vapor Transmission

The objectives of this phase of the project were to evaluate the differences in water and chloride ion absorption for concrete coated with the 24 materials and soaked in a 15 percent NaCl solution. The subsequent water vapor transmission characteristics were also compared during an air-drying period, which followed the soaking period.

The chloride absorption characteristics and the ratios of weight loss to weight gain for all 24 materials are shown in Table 2. Seven materials exhibited a greater than 80 percent reduction of chlorides compared with the control [two silanes (8 and 10), a silicone (11), a methyl methacrylate (12), a siloxane (14), a siloxane/silicone mixture (15), and a masonry coating (16)]. Materials 8, 10, 11, and 14 all lost more than

TABLE 2 WATER ABSORPTION AND VAPOR TRANSMISSION TEST RESULTS

Generic Type	Test #	Individual Type (% Solids or Ingredients)	AVERAGE CHLORIDE Percent Reduction	WEIGHT GAIN Percent by Weight	WEIGHT GAIN Percent Reduction	Weight Loss Percent by Wt	Wt. Loss Wt. Gain Ratio, %
EPOXIES	1	Epoxy (50)	77.28	0.42	80.91(a)	0.95	227.3(b)
	2	Epoxy (20)	79.29	0.42	80.91	1.45	345.5
	3	Epoxy (50)	34.27	0.94	57.27	1.39	248.0
	4	Epoxy (50)	69.72	0.49	77.73	0.83	169.2
	25	Epoxy (100)	74.73	0.29	86.82	0.14	50.0
STRAIGHT PENETRANTS	7	Silane (40)	61.82	0.38	82.73	1.60	420.0
	8	Silane (<20)	85.11	0.30	86.36	1.40	462.5
	9	Silane (20)	40.46	0.53	75.91	1.56	292.9
	10	Silane (40)	81.46	0.27	87.73	1.29	485.7
	11	Silicone (5)	82.79	0.34	84.55	1.55	455.6
	14	Siloxane (20)	85.37	0.34	84.55	1.52	444.4
BLEND OF PENETRANTS	15	Siloxane/Silic (10)	84.73	0.49	77.73	1.62	330.8
	18	Blend of Silanes (30)	76.52	0.49	77.73	1.48	300.0
	21	Poly-Siloxane/ Silica (7)	23.25	1.99	9.55	2.40	120.8
MASONRY COATING	16	Styrene/Acrylic Co. (75)	81.19	0.95	56.82	1.65	173.1
	19	Vinyl Acrylic (58)	39.13	1.71	22.27	2.07	121.3
	20	Polyester Resin (60)	63.34	1.34	39.09	2.11	167.7
	22	Styrene/Acrylic Co. (61)	57.18	1.34	39.09	1.97	147.2
	23	Elastomeric Acrylic	17.06	1.91	13.18	1.99	103.8
	24	Acrylic Resin	25.04	1.67	24.09	2.03	121.7
URETHANE	5	Urethane (55)	63.26	0.79	64.09	0.87	104.8
	6	Urethane (30)	-16.64	2.05	6.82	2.05	100.0
METHACRY-LATE	12	Methyl Methacrylate (20)	87.54	0.19	91.36	1.40	740.0
	13	Methyl Methacrylate (30)	73.48	0.87	60.45	1.63	187.0
CONTROL		No Coating	0.00	2.20	0.00	2.54	115.5
	(a)	(2.2 - 0.42) 2.2 = 80.91,		(b) 0.95	0.42 x 100 % = 227.3 %		

four times the weight that they gained. Five materials were between 70 and 80 percent more effective against chloride intrusion than were the controls [three epoxies (1, 2, and 25), a methyl methacrylate (13), and a blend of silanes (18)]. Materials 2 and 18 both lost more than three times the weight that they gained. Five materials had average chloride content reduction values from 50 to 70 percent of that of the untreated control [an epoxy (4), a urethane (5), a silane (7), and two masonry coatings (20 and 22)]. The silane also lost more than four times what it gained but was only around 61 percent more effective against chloride intrusion.

Accelerated Weathering

The objective of this test was to determine the influence of 24 weeks of accelerated laboratory weathering tests on the performance of the selected sealers and coatings when applied to small concrete slabs. The northern climate test (3) method included an accelerated weathering cycle in which the coated slabs were exposed to a wide range of environmental conditions, including ultraviolet light, high temperatures, acid/salt-water, fresh water rinse, freezing, and thawing.

The performance of the sealers and coatings was judged by making periodical visual inspections of the surface conditions (this included taking photographs), measuring the gloss of the surface with a glossmeter every 2 weeks, and measuring the chloride ion content in the concrete at the end of the testing period.

All specimens exhibited some degree of surface deterioration or discoloration, except for the chemically-cured urethane and four of the masonry coatings. The epoxy formulations exhibited varying degrees of discoloration and deterioration from the effects of this testing. The 100 percent solids epoxy discolored slightly but did not deteriorate. The 20 percent solids epoxy demonstrated the worst deterioration of all the epoxies. The performance of the epoxy seems to be directly related to the amount of solids present. Only a slight deterioration occurred on the surface of the slabs coated with the penetrants (silane, siloxane, silicone, and combinations of the three). Only one silane (less than 20 percent solids), the combination of siloxane and silicone, and the blend of silanes exhibited significant surface deterioration. The moisture-cured urethane, straight methyl methacrylate, and one of the styrene acrylic copolymers (75 percent solids) also had deep etching over their entire surfaces. The other styrene acrylic copolymer (61 percent solids) exhibited minor surface deterioration, and the methyl methacrylate with the silane primer showed some slight discoloration of the surface coating. The untreated control specimen exhibited uniform deep etching over the entire surface and had many coarse aggregates showing.

The glossmeter values at weeks 0 and 24 of the accelerated weathering test are presented in Table 3. All materials ex-

TABLE 3 GLOSS REDUCTION

Generic Type	Test #	Individual Type (% Solids or Ingredients)	Week 0	Week 24	Percent Reduction
EPOXIES	1	Epoxy (50)	5.95	0.78	86.89
	2	Epoxy (20)	0.75	0.02	97.33
	3	Epoxy (50)	1.55	0.08	94.84
	4	Epoxy (50)	9.53	0.48	94.96
	25	Epoxy (100)	14.20	0.73	94.86
STRAIGHT PENETRANTS	7	Silane (40)	0.23	0.08	65.22
	8	Silane (<20)	0.25	0.00	100.00
	9	Silane (20)	0.13	0.13	0.00
	10	Silane (40)	0.23	0.23	0.00
	11	Silicone (5)	0.15	0.03	80.00
	14	Siloxane (20)			86.30
BLEND OF PENETRANTS	15	Siloxane/Silicone (10)	0.53	0.00	100.00
	18	Blend of Silanes (30)	0.25	0.05	80.00
	21	Poly-Siloxane/Silica (7)	0.55	0.00	100.00
MASONRY COATING	16	Styrene/Acrylic Copolymer (75)	0.58	0.00	100.00
	19	Vinyl Acrylic (58)	1.35	1.15	14.81
	20	Polyester Resin (60)	0.30	0.03	90.00
	22	Styrene/Acrylic Copolymer (61)	1.55	1.05	32.26
	23	Elastomeric Acrylic	1.20	0.93	22.50
	24	Acrylic Resin	0.08	0.70	20.45
URETHANE	5	Urethane (55)	3.93	1.85	52.93
	6	Urethane (30)	1.90	0.10	94.74
METHACRY-LATE	12	Methyl Methacrylate (20)	4.15	1.50	63.86
	13	Methyl Methacrylate (30)	1.88	0.28	85.11
CONTROL			0.20	0.00	100.00

hibited a decrease in their gloss except the slabs coated with silane. The coatings that experienced any deterioration or discoloration also had a subsequent loss of gloss.

The chloride content values for the 24 tested materials and the control specimen are presented in Table 4. The chloride content of the untreated control specimens was extremely high at the end of the test, 0.423 percent by weight of concrete. The two masonry coatings that were based on the styrene acrylic copolymer (samples 16 and 22) actually exhibited higher chloride contents than the control. Five materials that reduced the chloride content by more than 90 percent of that of the untreated control [three silanes (10, 8, and 7), a siloxane, and the blend of silanes]. Six materials were between 80 and 90 percent more effective than the control specimen [a silicone, a silane (9), three epoxies (1, 3, and 25), and the siloxane-silica mixture]. Two of the 24 tested materials were between 50 and 80 percent more effective than the control [an epoxy (4) and a urethane (5)]. Eight materials were less than twice as effective as the untreated control [four masonry coatings (19, 20, 23, and 24), an epoxy (2), a urethane (6), and both methyl methacrylates (12 and 13)].

The rapid chloride ion permeability results for all 24 materials (coated at age 28 days) are shown in Table 5. Two materials reduced the chloride intrusion by more than 90 percent compared with the control, and one of them (the 100 percent solids epoxy) had a negligible permeability rating. The other material (a chemically cured urethane with a 55 percent solids content) had a low rating. Six of the materials exhibited low permeability values between 58 and 80 percent compared with the control specimens. The last six materials exhibited moderate permeability values between 35 and 54 percent of that of the untreated concrete. The rapid chloride permeability testing is a quick method. In this study, the test took about 8 weeks to complete, whereas a simple water absorption vapor transmission test required 13 weeks to finish and an accelerating weathering test lasted for 24 weeks.

Five of the top seven materials were epoxy formulations. The comparatively best material was the 100 percent solids epoxy. The other four materials were the 50 percent solids epoxies. The next best generic type was the silane. The silanes with the higher solids contents were much more effective than the ones with 20 percent or less solids. Both methyl methacrylates exhibited a reduction of about 77 percent from the uncoated control specimen. Siloxane, silicone, and the combination of the two had permeability values between 65 and 74 percent of that of the untreated concrete. The rest of the

TABLE 4 AVERAGE CHLORIDE CONTENT FOR PONDING SLABS

Generic Type	Test #	Individual Type (& Solids or Ingredients)	Average % Chloride	Percent Reduction
EPOXIES	1	Epoxy (50)	0.075	82.26
	2	Epoxy (20)	0.408	3.64
	3	Epoxy (50)	0.055	86.91
	4	Epoxy (50)	0.125	70.56
	25	Epoxy (100)	0.045	89.39
STRAIGHT PENETRANTS	7	Silane (40)	0.038	91.10
	8	Silane (<20)	0.034	91.75
	9	Silane (20)	0.049	88.26
	10	Silane (40)	0.029	93.02
	11	Silicone (5)	0.044	89.51
	14	Siloxane (20)	0.041	90.19
BLEND OF PENETRANTS	15	Siloxane/ Silicone (10)	0.293	30.48
	18	Blend of Silanes (30)	0.031	92.46
	21	Poly-Siloxane/Silica (7)	0.081	80.76
MASONRY COATING	16	Styrene/Acrylic Copolymer (75)	0.482	-14.03
	19	Vinyl Acrylic (58)	0.286	32.34
	20	Polyester Resin (60)	0.289	31.57
	22	Styrene/Acrylic Copolymer (61)	0.528	-24.86
	23	Elastomeric Acrylic	0.292	30.89
	24	Acrylic Resin	0.348	17.71
URETHANE	5	Urethane (55)	0.136	67.78
	6	Urethane (30)	0.295	30.18
METHACRY-LATE	12	Methyl Methacrylate (20)	0.230	45.46
	13	Methyl Methacrylate (30)	0.409	3.08
CONTROL			0.422	0.00

TABLE 5 RAPID CHLORIDE PERMEABILITY RESULTS (AASHTO T 277–83I)

Generic Type	Test #	Individual Type (& Solids or Ingredients)	Coulombs Passed	Percent Reduction	AASHTO Designation
EPOXIES	1	Epoxy (50)	661	85.81	very low
	2	Epoxy (20)	1829	60.73	low
	3	Epoxy (50)	467	89.97	very low
	4	Epoxy (50)	546	88.28	very low
	25	Epoxy (100)	66	98.58	negligible
STRAIGHT PENETRANTS	7	Silane (40)	792	82.99	very low
	8	Silane (<20)	1002	78.48	low
	9	Silane (20)	1812	61.09	low
	10	Silane (40)	538	88.45	very low
	11	Silicone (5)	1369	70.60	low
	14	Siloxane (20)	1226	73.67	low
BLEND OF PENETRANTS	15	Siloxane/Silicone Silicone (10)	1623	65.15	low
	18	Blend of Silanes (30)	2521	48.01	moderate
	21	Poly-Siloxane/ Silica (7)	2680	42.45	moderate
MASONRY COATING	16	Styrene Acrylic Cop. (61)	1939	58.36	low
	19	Vinyl Acrylic (58)	1788	61.61	low
	20	Polyester Resin (60)	1853	60.21	low
	22	Styrene Acrylic Cop. (75)	2470	46.96	moderate
	23	Elastomeric Acrylic	2255	51.58	moderate
	24	Acrylic Resin	2170	53.40	moderate
URETHANE	5	Urethane (55)	258	94.46	very low
	6	Urethane (30)	3006	35.45	moderate
METHACRY-LATE	12	Methyl Methacry-late (20)	1117	76.01	low
	13	Methyl Methacry-late (30)	997	78.59	very low
CONTROL			4657	0.00	high

materials, all six of the masonry coatings, a blend of silanes, a polysiloxane/silica, and a moisture-cured urethane, had permeability values below 62 percent of that of the control specimen.

RESULTS OF GENERIC TYPE AND DISCUSSION

The results presented in Tables 1 – 5 are summarized in Table 6. The mean values of percent chloride ion reduction from the three tests indicate that epoxy and straight penetrants consistently stopped chloride ion penetration well. Masonry coatings and blend penetrants were comparatively weak barriers, whereas urethane and methyl methacrylate exhibited mixed results. In the water absorption and vapor transmission test, epoxy, straight penetrants, and methyl methacrylate had significant moisture reduction value in contrast to blend penetrants, masonry coating, and urethane. The calculation of weight loss to weight gain ratios indicated that straight penetrants, methyl methacrylate, and blend penetrants benefitted the coated concrete substantially more than the epoxy, masonry coating, and urethane. Herein, the epoxy demonstrated that it could block the water out of concrete as well as trap water inside the concrete. It was especially true of the 100 percent solid epoxy. Data on the reduction of gloss after the coated concrete was subjected to 24 weeks of the accelerated weathering test are presented in the last row of Table 6. Combined with the visual inspection, masonry coating and straight penetrants sustained the attack of severe weather better than the other generic types of sealers and penetrants.

TABLE 6 SUMMARY RESULTS FOR GENERIC TYPE

DESCRIPTION OF PROPERTIES COMPARING WITH CONTROL SPECIMEN (uncoated concrete)	EPOXY	STRAIGHT PENETRANT	BLEND PENETRANT	MASONRY COATING	URETHANE	METHYL METHCRYL
Percent of Chloride Ion Reduction						
1. From Rapid Permeability Test	84.67 (14.22)	75.88 (9.66)	51.87 (11.83)	55.35 (5.66)	64.96 (41.73)	77.30 (1.82)
2. From Water Absorption/Vapor Vapor Transmission Test	67.06 (18.67)	72.84 (18.17)	61.50 (33.38)	47.16 (24.41)	23.31 (56.50)	80.51 (9.94)
3. From Accelerating Weathering Test	66.54 (35.91)	90.64 (1.69)	67.90 (32.93)	12.27 (25.38)	48.98 (26.59)	24.27 (29.97)
Percent of Moisture Reduction from Water Absorption Test (Weight Gain)	76.73 (11.36)	83.64 (4.16)	55.00 (39.36)	32.42 (15.66)	35.46 (40.50)	75.91 (21.86)
Weight Loss/Weight Gains Ratio from Water Absorption/ Vapor Transmission Test	208.00 (78.87)	426.85 (63.87)	250.53 (113.40)	118.18 (28.76)	102.40 (3.39)	463.55 (391.03)
Gloss Diminishing from Accelerating Weathering Test	93.78 (3.99)	55.25 (44.24)	93.33 (11.55)	46.67 (37.99)	73.84 (29.56)	74.49 (44.24)

CONCLUSION

Because of limited resources, the experiments in this study were designed with no replicates for each individual coating system, and the testings did not exactly follow NCHRP testing procedures. Compounded with a slightly different ingredient on the formula of each individual sealer and coating, this could result in a drastic difference on their behavior. Therefore, definite conclusions cannot be made at this point. More laboratory and field testings are needed to verify the differences among various generic sealers and coatings. Nevertheless, the following phenomena are apparent.

1. The epoxies were comparatively better chloride and water absorption barriers, but they deteriorated and discolored slightly in the accelerated weathering test.
2. The penetrants (straight silanes, silicone, and siloxane) resisted water and chloride absorption quite well. They also showed little sign of deterioration in the weathering test. The materials that were combinations of penetrants did not perform as consistently as the straight penetrants.
3. Masonry coatings were comparatively ineffective barriers to chloride ions, but they did offer aesthetic benefits.
4. The urethane and methyl methacrylate results varied dramatically from one test to another.

ACKNOWLEDGMENT

The research described in this paper was funded by IDOH under Joint Highway Research Project C-36-67BB. IDOH support is gratefully acknowledged. Special thanks are extended to Richard Smutzer, Don Scott, Tony Zander, and Peter Garner.

REFERENCES

1. P. Maslow. *Chemical Materials for Construction.* McGraw-Hill, Inc., New York, N.Y., 1982, pp. 433–472.
2. C. G. Munger. *Corrosion Prevention by Protective Coatings.* National Association of Corrosion Engineers, Houston, Tex., 1984, pp. 287–303.
3. L.-M. Chang and P. S. Garner. *An Investigation of Surface Coatings on Exposed Concrete.* Indiana Department of Highways, Indianapolis, May 1989.
4. *NCHRP Report 244: Concrete Sealers for Protection of Bridge Structures.* TRB, National Research Council, Washington, D.C., 1979.
5. D. Whiting. *Rapid Determination of the Chloride Permeability of Concrete.* FHWA/RD-81/119. FHWA, U.S. Department of Transportation, 1981.
6. Indiana Department of Highways Specifications. Section 702 Structural Concrete, Indianapolis, 1986, pp. 286–287.

Publication of this paper sponsored by Committee on Performance of Concrete.

Epoxy Injection of Bridge Deck Delamination

BARBARA J. SMITH

Four delaminated bridges were epoxy injected and compared with bridges that were not injected. The injection history, cores, and condition reports for the bridges demonstrated that a plane of delamination, once repaired, stayed repaired, and that the surface of the deck remained intact with a frequency of injection of once every 4 years. Continued observation for 7 years after the last injection of the decks validated that delamination can be effectively repaired and can remain serviceable up to approximately 4 years, when additional injections or another type of repair can be scheduled. The use of timely epoxy repair for a bridge undergoing untimely delamination extends the useful life of the original deck.

Epoxy injection repair of delaminated bridges was first proposed by Kansas researchers in 1974 (*1*). The 5-year program for testing the benefits and limitations of epoxy repair began in 1979 and ended in 1984 (*2*). Observation continued until three of the four bridges chosen were removed in spring 1991 for upgrading to current specifications for that portion of Interstate.

THE PROGRAM

The test and control bridges were three pairs of bridges on I-470 west of Topeka, one unpaired bridge in the same area, and one unpaired bridge in a neighboring county on I-70. The westbound bridges of each pair and the bridge on I-70 were test bridges. The eastbound bridges of each pair and the unpaired bridge on I-470 were control bridges. The original program was modified so that instead of each bridge being injected annually or biennially on the test program, all test bridges were quartered. One portion of each was injected annually, one portion every 3 years, and one portion every 4 years. These bridges had been injected before 1979 (Table 1). The 1S bridge is in the neighboring county. Other conditions of this bridge remove it from comparison with the others in this paper. The complete injection history for each is given in Figures 1–4. Companion bridges used for direct comparison control were available until 1980. The control bridges were those bridges in the better condition within each pair when epoxy injection was begun. The equipment and procedure for injection had been developed before this study and reported in 1974 (*1*).

The problems encountered were (a) obtaining the correct epoxy A and B component ratios inside the deck for good polymerization by crosslinking, (b) polymerization occurring too quickly, resulting in a hardened foam, (c) mapping the hollow planes, and (d) procuring epoxy components each year on competitive bids. The problems of mapping and early polymerization were solved as the study progressed. Because the epoxy injection equipment was hand built the solutions for problems were also hand built and are discussed by Smith and Stratton (*2*). Commercial epoxy injection equipment now available has been relatively trouble free since its purchase. The commercial equipment eliminates some of the mixing and polymerization problems encountered with the older handmade equipment.

Each year corrosion potential and delaminated areas were mapped for each deck, the scheduled injections were performed, and each injected section was remapped for hollow planes at least 30 days after injection. The areas of delamination and injection were counted for tabulation and comparison. Plotting of hollow plane areas by bridge deck sections for each year indicated that factors other than the repairs being done were important in hollow plane areas. Delamination varied in quantity from year to year. The effects seemed to be independent of injection or noninjection, the bridge, and the interval of injection.

Through the use of the climatological data summarized monthly by the National Weather Service Forecast Office at the Topeka Municipal Philip Billard Airport the frequency of occurrence for several weather phenomena was tabulated (Figure 5). Further discussion is provided elsewhere (*2*). Plotting the frequency of occurrences of each phenomenon between injection dates for each deck versus area of hollow planes allowed the analysis of weather factors in affecting areas of delamination (Figures 6–9).

DISCUSSION OF RESULTS

In addition to the observations that were made during the test period and extension (1979–1986) and reported in 1988 (*2*), observations that were made through spring 1991 are included. Several questions are addressed in the following discussion. Do the repaired delaminations bond and stay bonded? Were there some delaminations that did not repair, and if so, were those delaminations different from the others? Is epoxy injection repair a long-term benefit or detriment to the deck? What epoxy injection schedule should be used for the most effective benefits? Are other problems or questions that were not known before the study known now?

Bonding depends on getting epoxy into the delamination. The type of delamination often determines whether epoxy can be injected. There is ample evidence in preinjection and

Materials and Research Center, Kansas Department of Transportation, 2300 Van Buren, Topeka, Kans. 66611.

TABLE 1 BRIDGE DESCRIPTIONS

I.D.[1]	YEAR BUILT	BRIDGE # AS OF 1987	LOCATION	SIZE	TYPE	HISTORY
1S	1962	70-99-10.45	WB I-70 over Spring Creek	132.6' x 40.0'	RBSH[2]	Seal[3, 5]
2S	1959	470-89-0.370	WB I-470 over 10th Street	194.5' x 40.0'	RBGC[4]	Epoxy[5]
2C	1959	470-89-0.360	EB I-470 over 10th Street	230.5' x 30.0'	RBGC	Overlay[6]
3S	1960	470-89-1.050	WB I-470 over Huntoon	304.5' x 30.0'	RBGC	Epoxy[5]
3C	1959	470-89-1.040	EB I-470 over Huntoon	30.45' x 30.0'	RBGC	Overlay
4S	1960	470-89-1.210	WB I-470 over Wanamaker	222.5' x 30.2'	RVSH[7]	Epoxy[5]
4C	1960	470-89-1.200	EB I-470 over Wanamaker	222.5' x 30.0'	RVSH	Seal[5] Overlay
5C	1959	470-89.0-15	WB I-470 over I-70	398.5' x 30.2'	RBGC	Seal

1 S denotes an epoxy injected bridge, C denotes a comparison bridge.
2 Reinforced concrete slab continuous and haunched.
3 Unmaintained asphalt slurry seal.
4 Reinforced concrete box girder continuous.
5 Epoxy injection history given in separate figure for each bridge.
6 Iowa system overlay emplaced in 1980.
7 Reinforced concrete voided slab continuous and haunched.

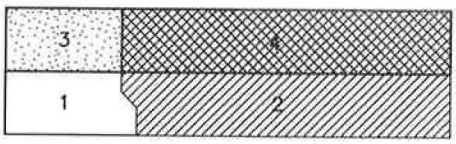

70-99-10-45 I-70 WB over Spring Creek,
Wabaunsee County, Reinforced Concrete Slab
Continuous & Haunched
Deck Completed 1962

1 AREA INJECTED (1972), (1974), 1979, 1980, 1981, 1982, 1983 (annually)

2 AREA INJECTED (1972), (1974), 1979, 1981, 1983 (biennially)

3 AREA INJECTED (1972), (1974), 1979, 1980, 1983 (triennially)

4 AREA INJECTED (1972), (1974), 1979, 1983 (quadrennially)

(1972) Year bridge injected prior to current report
1979 Year bridge injected for current report
Bridge Dimensions 132.6' x 40.0'

FIGURE 1 Bridge 1S with injection schedule indicated for portions of the bridge deck.

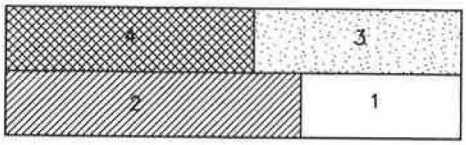

470-89-0.37 I-470 WB over Tenth Street
Shawnee County, Reinforced Concrete
Box Girder Continuous
Deck Completed 1959

1 AREA INJECTED (1974), (1978), 1979, 1980, 1981, 1982, 1983 (annually)

2 AREA INJECTED (1974), (1978), 1979, 1981, 1983 (biennially)

3 AREA INJECTED (1974), (1978), 1979, 1980, 1983 (triennially)

4 AREA INJECTED (1974), (1978), 1979, 1983 (quadrennially)

(1974) Year bridge injected prior to current report
1979 Year bridge injected for current report
Bridge Dimensions 230.5' x 30.0'

FIGURE 2 Bridge 2S with injection schedule indicated for portions of the bridge deck.

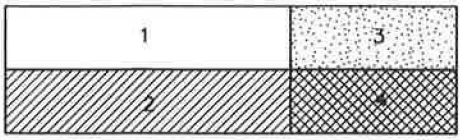

470-89-1.050 I-470 WB over Huntoon
Shawnee County, Reinforced Concrete
Box Girder Continuous
Deck Completed 1960

1 AREA INJECTED (1972), (1974), (1978), 1980, 1981, 1982, 1983, 1984 (annually)

2 AREA INJECTED (1972), (1973), (1978), 1980, 1982, 1984 (biennially)

3 AREA INJECTED (1972), (1973), (1978), 1980, 1983 (triennially)

4 AREA INJECTED (1972), (1973), (1978), 1980, 1984 (quadrennially)

(1978) Year bridge injected prior to current report
1980 Year bridge injected for current report
Bridge Dimensions 304.5' x 30.0'

FIGURE 3 Bridge 3S with injection schedule indicated for portions of the bridge deck.

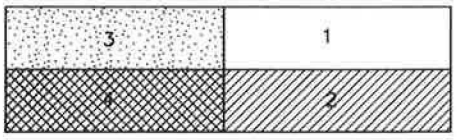

470-89-1.210 I-470 WB over Wanamaker Rd.
Shawnee County, Reinforced Concrete
Voided Slab Continuous & Haunched
Deck Completed 1960

1 AREA INJECTED (1972), (1973), (1976), (1978), 1980, 1981, 1982, 1983, 1984 (annually)

2 AREA INJECTED (1972), (1973), (1976), (1978), 1980, 1982, 1984 (biennially)

3 AREA INJECTED (1972), (1973), (1976), (1978), 1980, 1983 (triennially)

4 AREA INJECTED (1972), (1973), (1976), (1978), 1980, 1984 (quadrennially)

(1972) Year bridge injected prior to current report
1980 Year bridge injected for current report
Bridge Dimensions 222.5' x 30.0'

FIGURE 4 Bridge 4S with injection schedule indicated for portions of the bridge deck.

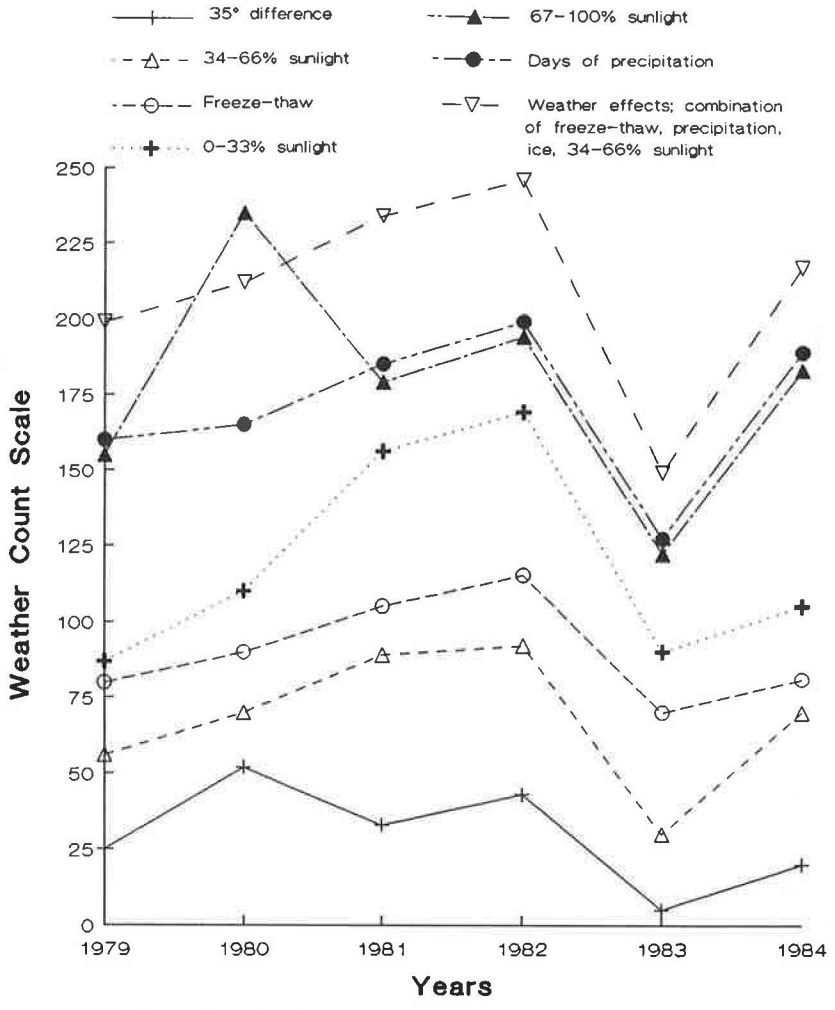

FIGURE 5 Several weather factors, including the derived weather effects curve.

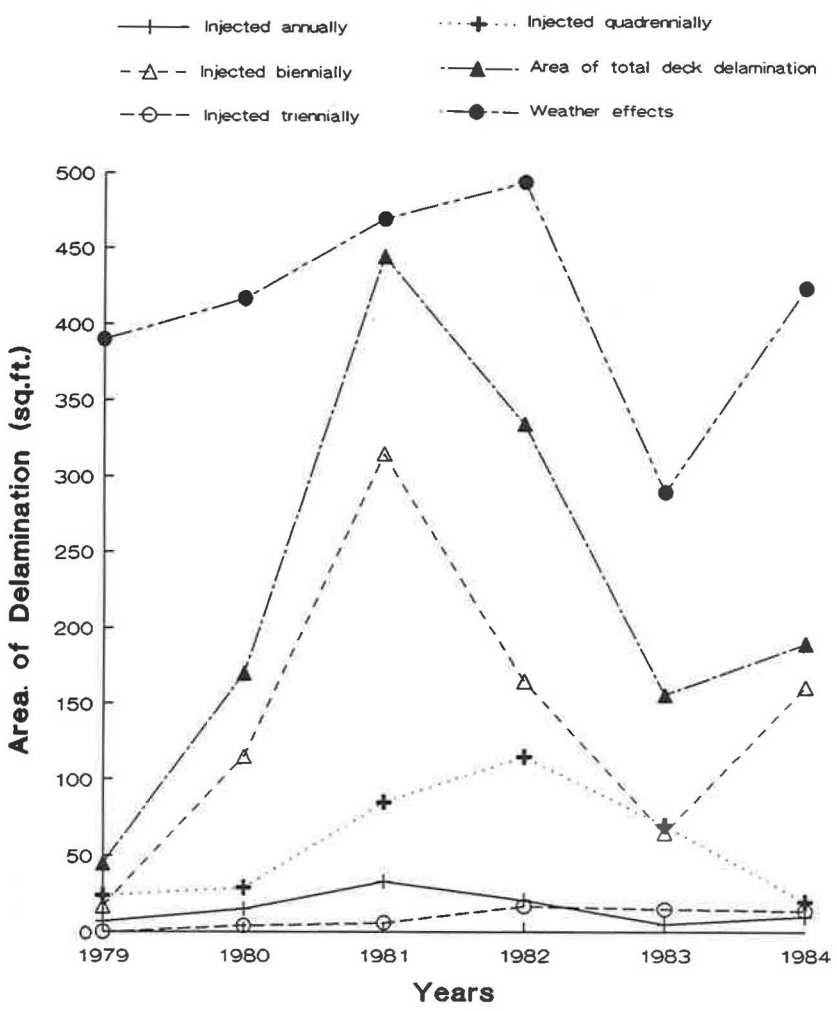

FIGURE 6 Bridge 1S delamination areas, by portions injected on research schedule, total deck delamination, and weather effects by injection year.

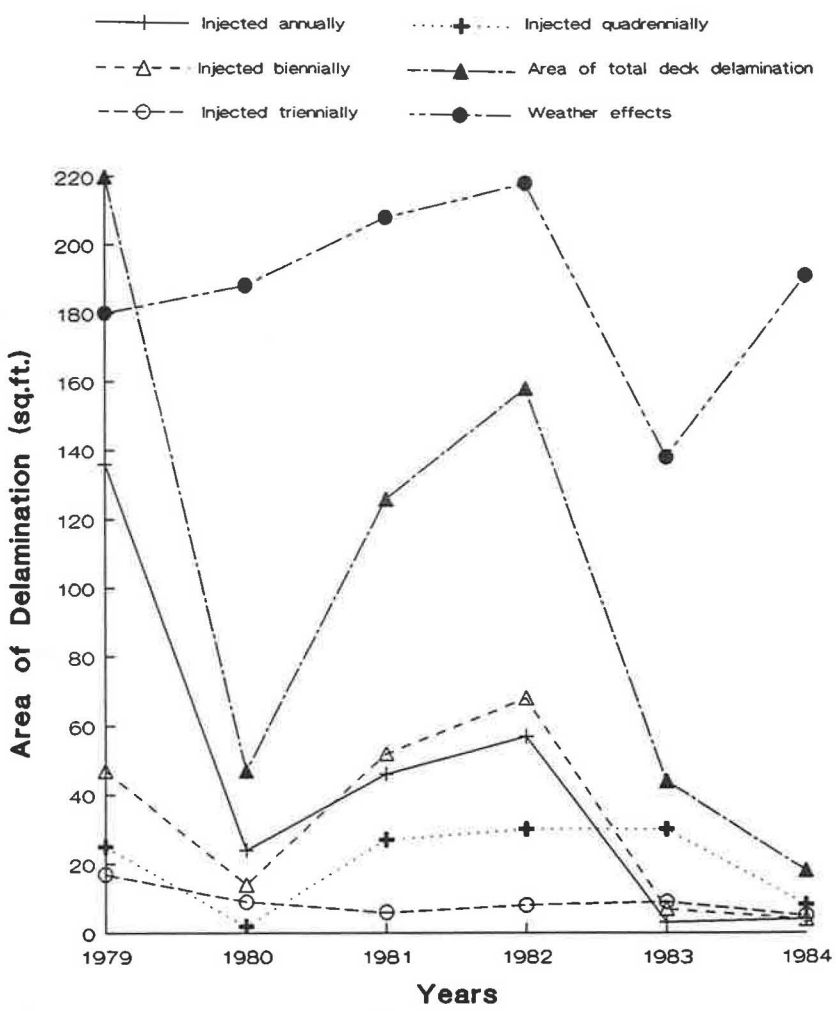

FIGURE 7 Bridge 2S delamination areas, by portions injected on research schedule, total deck delamination, and weather effects by injection year.

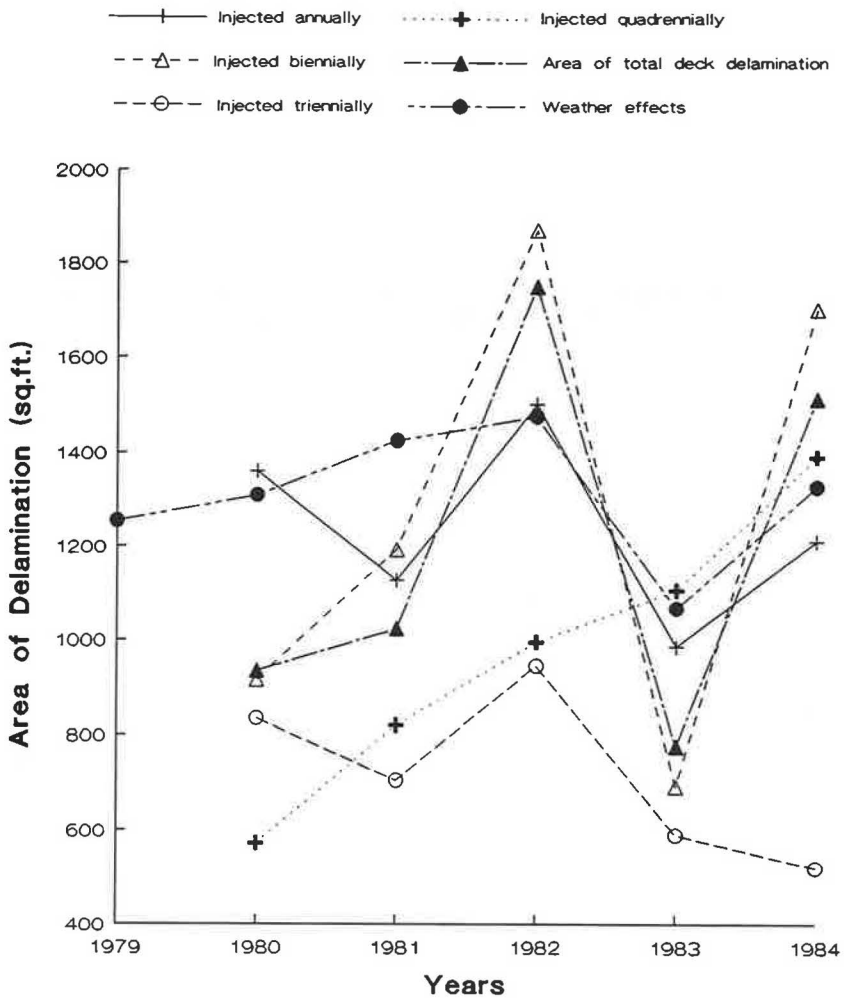

FIGURE 8 Bridge 3S delamination areas by portions injected on research schedule, total deck delamination, and weather effects by injection year.

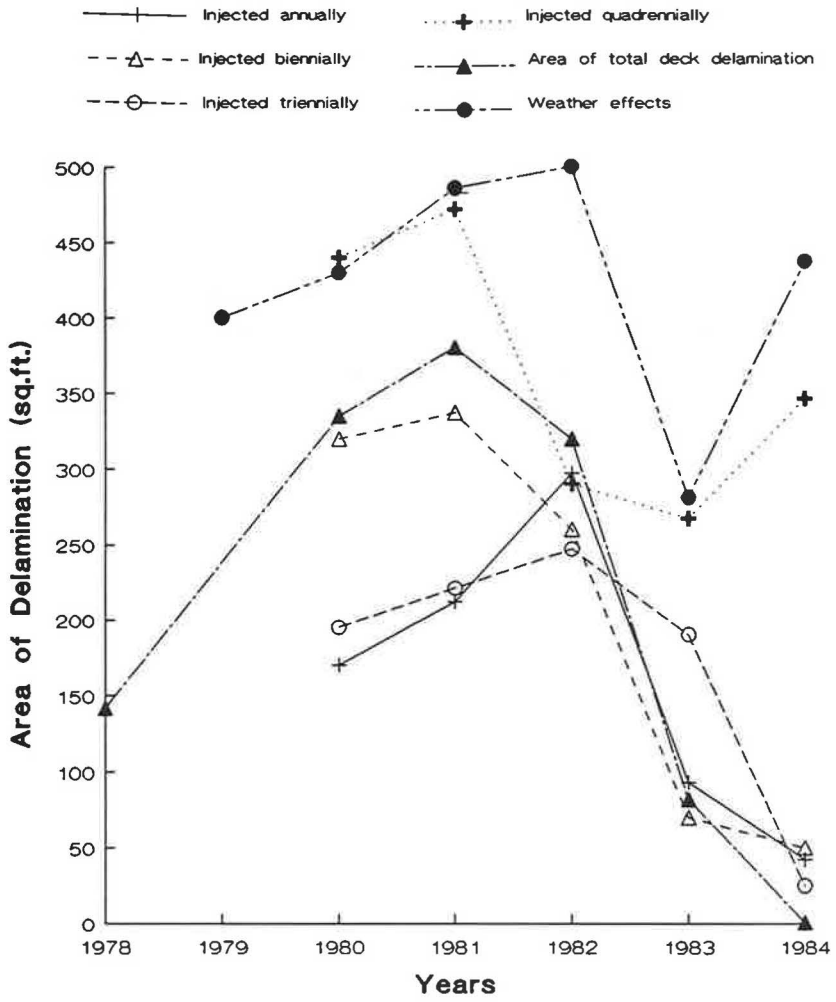

FIGURE 9 Bridge 4S delamination areas, by portion injected on research schedule, total deck delamination, and weather effects by injection year.

postinjection maps to show that not all hollow planes are alike. Shallow planes, related to hollow scaling of the deck surface, were not easy (and were sometimes impossible) to inject. Long thin planes above rebar steel with little concrete cover were sometimes too shallow to inject or required frequent change of injection sites. Large areas of delamination were generally easy to inject and required few site changes.

Evidence from maps and cores taken at repaired areas and observation since the end of the project indicate that once epoxy has been injected into a hollow plane, the plane is bonded and stays bonded. Maps and cores also indicate that a few hollow planes become "ghosts" by disappearing before repair, then reappearing at a later date. Discussion of the problems they may cause is included in work by Smith and Stratton (*2*).

Analysis of many possible weather factors indicated that weather phenomena that seem to influence increased delamination were precipitation, freeze-thaw, 0 to 66 percent sunlight, thunderstorms, and freeze-thaw with wind chill. Other factors were opposed to the trend in delamination. Some are shown in Figure 5. Combining some of the factors into a derived curve that could then be projected into the graphs of areas of delaminated deck allowed the weather effects on the bridges to be taken for what they were and not to be confused with injection or noninjection effects. In Figures 6–9 the derived weather effects curve is shown but should be considered only for its shape in comparison with the other curves. These figures also show the delaminated areas with frequency of injection for each of the four study bridges during the injection study period. The most apparent conclusion from studying these figures is that injection every year or 2 had no definite benefit in maintenance over injection every 3 or 4 years. Observation after the last injections to 1991 when the decks were demolished indicated that in 3 or 4 years little or no spalling occurred; in 7 or 8 years increased spalling occurred. Had the decks been injected at the 4-year interval, the increased surface spalling that was noted without injection in the 8th year probably would not have occurred.

Salting of bridges is known to be detrimental to the longevity of the decks. Information from the maintenance supervisor indicates that of the bridges in this study, no bridge is more or less likely than the others for needing salt treatments. Because they are in the same vicinity, the same Topeka climate and weather prevailed for all. Salt sampling (Table 2) for the study bridges from 1979 through 1991 reveals that the ratio of samples surpassing 1 lb/yd^3 of chloride has increased continually throughout the observation periods. This finding was expected.

At the beginning of the project the proposed study bridges had noninjected companion or control bridges that could be evaluated for direct comparison. Those who have attempted research in the field know the difficulties of controlling and evaluating the actual process of the research. The encroachment of maintenance was encountered during this project. The test bridges remained untouched, but maintenance forces evaluated the control bridges and proceeded to emplace Iowa system concrete overlays. These repairs resulted in the removal of the bridges from direct comparison in 1980. Condition reports were made before the overlays. When condition reports were later made on the study bridges, direct comparisons could be made of the decks at different ages. Now that the overlays are more than 10 years old the conditions of the repairs can be compared and analyzed. Another complication in evaluation of the research was the presence of slurry seal on one comparison bridge that was overlaid. Another bridge was included of the same age and vicinity that also had a seal but had not been overlaid. Both sealed bridges are included here to provide a comparison of the slurry sealed and overlaid bridge with the slurry sealed bridge. Condition reports are not available for the 1S bridge or its companion. Consequently few poststudy comparisons can be made. The 1S bridge is included for reference only and is discussed more fully in the report by Smith and Stratton (*2*).

In the evaluation of this repair procedure it was decided to use area of delamination, corrosion potential, chloride content, and spalled or patched areas. Area of delamination and corrosion potential were obtained each year directly from the deck. Chloride content required taking powdered samples to be evaluated in the chemical laboratory. They were taken in conjunction with cores during some years. This test provides a limited indication of the overall deck condition. Areas of spalls and patches can be observed directly and were reported in the condition reports. Because the control bridges were overlaid in 1980, the 1979 condition reports became quite useful for comparisons not anticipated at the beginning of the study.

If one compares the averages of the study bridges to the averages of the comparison bridges, taking into consideration that the observations have been taken at different times for each group of bridges and that the control bridges themselves vary, several things can be noted (Tables 2 and 3). The 1989 averages for the injected bridges on the whole compare favorably to the 1979 (preoverlay) averages for the comparison bridges.

In Table 2, the companion bridges are grouped in several ways, all the companion decks (2C, 3C, 4C, 5C), bare deck bridges only (2C, 3C), slurry sealed decks (4C, 5C), and bare deck bridges and the slurry sealed deck with no overlay (3C, 3C, 5C). This grouping accounts for the various treatment and repair histories of the companion decks. Using 1986 or 1989 averages for the study bridges and considering the percent of area of delamination for the comparison bridges for 1979 shows that the averages are similar for the study bridges and the bare deck bridges or the three bridges 2C, 3C, and 5C. The two bridges with slurry seals show much lower areas of delamination, which causes the average of all four decks to be lower. Separation of the averages highlights the effect of the slurry seals for deck protection even when they were not maintained but had been worn through by the time the study began. This effect also can be seen in the other measures. Because this effect is so prominent, the remainder of the discussion will deal with the study decks compared with the three decks 2C, 3C, and 5C, or the two bare decks 2C and 3C.

Corrosion potential as measured with the copper/copper sulfate half cell described by ASTM (ASTM C876) shows that corrosion potential was similar for the study bridges in the late 1980s and the comparison bridges in 1979. The 1991 values for the comparison bridges reflect the effects of the overlay on this measure; the concrete had had few years to accumulate salt to bring about the corrosion potential. Notice that the 1991 values are similar to the 1979 values of the two

TABLE 2 DECK CONCRETE CONDITIONS

Bridge Grps.	Bridge & Date	% of Area Delamination	Corrosive Potential over -0.35	Chloride in #/Cu.Yd. 3/4"	1-1/2"	2-1/4"
	2S					
	1986	23	35.0%	12.7	6.2	3.5
	1989	24.8	42.0%	10.5	4.9	2.0
	1991	25.6	54.3%	13.96	9.43	4.83
	2C					
	1979	34	47.0%	7.05	3.61	2.51
	1991	30.7	12.2%	8.68	2.86	1.81
	3S					
	1986	11	47.0%	11.1	3.7	1.2
	1989	38	59.0%	10.6	5.77	2.66
	3C[1]					
	1979	39	61.0%	11.1	6.94	4.35
	1990	25	10.0%	7.96	2.15	1.62
	1991	33.1	10.0%	N/A[4]	N/A[4]	N/A[4]
	4S					
	1986	59	81.0%	10.5	7.2	3.09
	1989	45.7	43.0%	10.3	7.2	3.09
	4C[2]					
	1979	5	20.0%	2.14	1.46	0.82
	1990	5	1.5%	6.0	2.5	1.4
	5C[3]					
	1986	22	35.0%	1.90	1.48	1.14
	1989	23	44.0%	3.63	2.52	1.35
Study Br.	1986	31.0	54.3%	11.4	5.4	2.5
2S, 3S, 4S	1989	36.2	48.0%	10.5	6.0	2.6
Comparison	1979	36.5	54.0%	9.1	5.3	3.4
Br. 2C & 3C[1]	1991(+1990)	29.6	10.7%	8.3	2.5	1.7
Comparison	1979(+1986)	13.5	27.5%	2.0	1.5	1.0
Br. 4C[2] & 5C[3]	1991	12.5	22.8%	4.8	2.5	1.4
4 Br. - 2C,	1979(+1986)	25	40.8%	5.5	3.4	2.2
3C, 4C & 5C	1991	20.2	16.7%	6.6	2.5	1.5
3 Bridges	1979(+1986)	31.7	44.7%	6.7	4.0	2.7
2C, 3C & 5C	1991	26.2	22.1%	6.8	2.5	1.6

1 No Slurry seal, Iowa System overlay in 1980.
2 Unmaintained slurry seal, Iowa System overlay in 1980.
3 Unmaintained slurry seal only.
4 Not available.

TABLE 3 DECK SURFACE CONDITIONS

Bridge & Date and Average	Total Spall & Patch Area ft^2	Total Spall & Patch Area/1000ft^2	Average Depth of Steel (1979)
2S			1.92"
1986	23	2.96	
1989	112	14.40	
3S			1.71"
1986	54	5.91	
1989	167	18.30	
4S			2.16"
1986	7	1.05	
1989	86	12.90	
2C[1]			NA
1979	370	53.50	
3C[1]			1.83"
1979	490	53.60	
1990	19	2.08	
4C[2]			1.81"
1979	8	1.20	
1990	1	0.15	
5C[3]			1.46"
1986	769	64.30	
1989	940	78.60	
2S, 3S, 4S average			
1986	28	3.31	
1989	122	15.20	
2C, 3C, 5C average			
1979 + 1986	543	57.10	
3C 5C average			
1989, 1990	479.5	40.30	

1 Iowa System overlay in 1980.
2 Both overlay and slurry seal.
3 Unmaintained slurry seal only.

sealed decks. Chloride contents drive these trends. The severity of cold wet weather and the total amount of precipitation each year affect the total chloride accumulation as it is measured at any given time. Epoxy injection of bare decks and slurry seals emplaced before traffic slowed the ingress of salt to the steel, as compared with the untreated companion decks. In Table 3 the surface conditions of the decks are compared. The average total spalled and patched area per 1000 ft^2 is less for the study bridges in 1989 than for the companion bridges in 1979. Again, observations of the injected decks indicate that had the study bridges been injected 4 years after the last injection, the extent of spalling and the need for patching would have been considerably less.

Projections of repair needs and costs made in 1988 (*2*) were based on observations at the time. The extension of observations to spring 1991 added validity to the conclusions of that study: if begun in a timely manner when delamination is 5 percent or less and continued as a routine program every 4 years, the injection of epoxy can be effective in preserving the deck surface of a bridge undergoing delamination. The cost-effectiveness will depend on the area to be repaired, with greater benefits accruing if injection is begun earlier. Other reasons to choose epoxy injection repair include the relative patch-free maintenance of the driving surface resulting in less exposure of work crews to traffic hazards and of the public to spalls and potholes; the ability to repair one lane of a deck at a time, leaving other lanes to bear the traffic load; and the capability of the newly repaired area for handling traffic at the end of each daily work period, allowing construction-free driving at peak periods or at night. Also, the repair can "buy

time" for a deck surface; therefore repair of a moderately delaminated deck can be a shorter term program to extend the life of the deck until final repairs can be made.

Although not intended in the original study goals, the inclusion of slurry sealed decks made possible their evaluation compared with nonsealed decks. The decks were sealed before traffic was allowed and salting began. The results show this treatment to be an effective one. The epoxy injection repair is available before the salting of a bridge deck. The lesser amount of delamination indicates the greater cost-effectiveness for each deck. Other factors already discussed can emphasize or offset the cost of epoxy repair for a given bridge.

CONCLUSION

The study of epoxy injection repair of hollow planes in bridge decks was undertaken to test the durability, frequency of application, and general effectiveness of the procedure. The data from four test bridges with comparisons with companion bridges indicate that initiating a program of delamination injection and continuing the injection as a routine maintenance program every 4 years will preserve the driving surface of the deck. Weather factors are important contributors to the amount of delamination that occurs each year and may be important in the disappearance and reappearance of delamination. Whether the injection repair program is begun early in the life of the deck or later when delamination is more severe, general benefits from the choice of epoxy injection repair result, such as being able to open the deck to traffic after each repair work period, closing only the lane undergoing repair, and maintaining a spall- and patch-free deck, which provides a safer driving surface. The repair can "buy time" for a deck until final repairs or options can be scheduled.

ACKNOWLEDGMENTS

The study was conducted with the cooperation of FHWA. Those who assisted in the preparation of this paper are Karen A. Clowers, John B. Wojakowski, Jeffrey V. Hunt, and Dick Hoch.

REFERENCES

1. F. W. Stratton and B. F. McCollom. *Repair of Hollow or Softened Areas in Bridge Decks by Rebonding with Injected Epoxy Resin or Other Polymers.* Final Report K-F-72-5. State Highway Commission of Kansas, July 1974, 104 pp.
2. B. J. Smith and F. W. Stratton. *1988 Bridge Deck Hollow Repair Using Injected Epoxy.* FHWA-KS-8811. FHWA, U.S. Department of Transportation; Kansas Department of Transportation, Topeka, Feb. 1988, 57 pp.

Publication of this paper sponsored by Committee on Mechanical Properties of Concrete.

Construction of a Thin-Bonded Portland Cement Concrete Overlay Using Accelerated Paving Techniques

K. H. McGhee and Celik Ozyildirim

The Virginia Department of Transportation's first modern experience with the construction of thin-bonded portland cement concrete overlays of existing concrete pavements through the use of fast-track paving is described. The study was conducted in cooperation with FHWA, and paving mixtures tested in a FHWA mobile laboratory were used. The study showed that the pavement could be overlaid and opened to traffic within 48 hr. Of special interest was the finding that the overlay concrete bonds to the base concrete with or without the use of a bonding grout.

The placement of new portland cement concrete (PCC) overlays on old PCC pavements is not a new technology. In fact, several such overlays were constructed in Virginia as early as the 1920s (*1*). Even thin-bonded overlays are not particularly new; they have been used for a number of years as an acceptable rehabilitation alternative for old PCC pavement, both jointed and continuously reinforced (*2*). A general requirement is that the underlying (old) concrete should be in reasonably good structural condition to adequately support the overlay. Thus, thin-bonded overlays typically have been used to structurally enhance sound pavements in anticipation of increased traffic volumes and loads.

The construction of such overlays using slip form pavers in a fast-track mode (rapid construction) is a relatively new technology that was first introduced in Iowa in 1986 (*3,4*). The promoters of this technology are candid in admitting that a major impetus to its development is an attempt to provide and demonstrate a construction window (lane closure time) that would compete favorably with that of asphaltic concrete overlays and would, therefore, make PCC overlays more acceptable to both the traveling public and maintenance engineers.

Recognizing that a competitive climate between the two paving industries is an important economic issue, the Virginia Department of Transportation (VDOT), through the Virginia Transportation Research Council and in cooperation with FHWA, selected a suitable Virginia location on which to try a thin-bonded PCC overlay. Among a number of sites considered were several on Interstate routes on which the limited access feature lends itself well to the construction operations involved. Sites with high traffic volumes were not considered acceptable because of the experimental nature of the work. The site selected was an old PCC pavement on U.S. Route 13 in Northampton County. This pavement was still in reasonably good condition with moderate traffic volume. The 1-mi section chosen for the fast-track project has only one side entrance to be accommodated during construction of the overlay.

Virginia Transportation Research Council, Box 3817 University Station, Charlottesville, Va. 22903-0817.

PURPOSE

The major purpose of the project was to evaluate the feasibility of constructing a thin-bonded portland cement concrete overlay of an existing concrete pavement in a fast-track mode to minimize lane closure times. A secondary purpose was to evaluate the performance of the overlay during a 5-year period. Unfortunately, the experimental nature of the project prohibited any realistic evaluation of costs that might apply to a similar nonexperimental project.

HISTORY OF EXISTING PAVEMENT

The existing PCC pavement on the fast-track project was constructed in 1965. The original design consisted of a native sand and gravel subgrade topped with a sand and gravel select material used as a subbase. The concrete pavement was 8-in. thick with transverse joints spaced at 20 ft. No dowels were used in the joints, which were sealed with a hot-poured rubberized asphalt. Traffic records indicate that the section had sustained approximately 2.2 million 18-kip equivalent single axle loads (ESALs) in the outside lane. Although project records did not indicate the design ESAL, traffic records indicate a rather modest growth of approximately 2.5 percent annually since 1980.

The major distresses manifested by the old pavement were joint faulting and a few instances of joint spalling. Some slabs had failed because of longitudinal cracking. Preliminary distress surveys available in VDOT files provided background material for evaluation of the performance of the overlay.

SPECIFICATION DEVELOPMENT

The development of construction specifications for the project was a cooperative effort of VDOT, FHWA, and the American Concrete Paving Association (ACPA). Because of the time constraints inherent in the process, several iterations were necessary before an acceptable specification was realized and

made available for bidding purposes. A list of the major elements of the project, many of which will be discussed in more detail, follows.

1. The project consisted of the design and placement of a nominal 3 ½-in.-thick thin-bonded overlay applied to the prepared surface of the old pavement.
2. The old pavement was repaired to restore any areas of structural failure in order to give the overlay a more uniform foundation.
3. The paving portion of the project was constructed in a fast-track mode with a lane closure time of 48 hr, beginning with the initiation of concrete placement and ending with the removal of the curing blanket.

PRELIMINARY TESTING

Trial Concrete Batches

For the fast-track overlay, the following concrete specifications were required:

- Minimum compressive strength at 24 hr: 3,000 psi,
- Aggregate size number: 57 or 68,
- Nominal maximum aggregate size: 1,
- Minimum cement content: 750 lb/yd^3,
- Maximum w/c: 0.42,
- Slump: 0 to 3 in.,
- Air content: 6 ± 2 percent, and
- Water-reducing admixture: AASHTO M194.

Special provisions stated that for bonding the overlay to the base concrete, a grout (portland cement and water) should be applied on the clean dry surface when the ambient temperature was 90°F or below. At higher temperatures, the base concrete surface should be in a saturated surface dry condition. The grout should contain the same portland cement as the overlay and should have a maximum water/cement ratio (w/c) of 0.45. Thus, the grout quality would approximate that of the paving concrete. Curing of the overlay should be with a liquid membrane seal applied at a dosage of 1.5 times the standard rate. The membrane seal was followed by insulating blankets consisting of closed-cell polystyrene foam having a minimum *R* value of 0.5 and protected on one side by a plastic film.

The contractor selected a prestressing plant at Cape Charles, Virginia, close to the job site, to furnish the concrete. Two sets of trial batches were used to develop mixture proportions and evaluate the bonding of the overlay.

The first trial set was made in April 1989 in cooperation with the FHWA Demonstration Projects division using the council's laboratory facilities and FHWA's mobile concrete laboratory and included a trip to the plant with the mobile laboratory and some batching at the plant. The second set of trial batches was made in May 1990 at the plant.

First Set of Trial Batches

In the first set, 11 batches of concrete were prepared using the materials furnished by the plant at Cape Charles as well as materials available in the laboratory. These batches are explained in detail in the FHWA report on the study (*5*). Two cements were used. One was a finely ground Type II cement obtained from the plant; the other was a Type III cement available in the laboratory. The coarse aggregate furnished by the plant was crushed granite from Stafford County, and the fine aggregate was siliceous sand from King George County. The w/c was variable, with a maximum of 0.42. Either a water-reducing admixture (WR) or a water-reducing and retarding admixture (WR + R) with minimal retardation at low dosages (as claimed by the producer) was used. Experimental batches were made using the previously mentioned materials and admixtures. Some of these included a sand having a better particle shape than the one used in normal plant production. Others contained a high-range water-reducing admixture (HRWR) or fly ash in order to provide the range of workability and strength that could be achieved at early ages with the available materials. All of the batches contained a neutralized vinsol resin as an air-entraining admixture to provide the specified air content (6 ± 2 percent). Compressive strengths were determined at different early ages by testing 4-in. × 8-in. cylinders in accordance with AASHTO T 22 using neoprene pads in retaining rings. The results indicated that the various combinations of w/c and HRWRs with the job materials were capable of reaching the required strength of 3,000 psi within 24 hr. This strength was attained as early as 12 hr with a w/c of 0.35 and an HRWR. However, because of economy, better control of workability, and a close resemblance to a mixture commonly used at the plant, trial mixture TB 11 (see following table) was chosen for the experimental installation. The w/c of 0.415 and the 3-in. slump were attained without the use of an HRWR. This mixture attained 3,000 psi in about 23 hr. The following table presents the mixture proportions (lb/yd^3).

	TB11	*Job*
Cement	750	750
Maximum water	311	315
Coarse aggregate	1,902	1,877
Fine aggregate	1,065	1,045

Subsequently, the mobile concrete laboratory was moved to the plant, and a 2-yd^3 batch with the same proportions as TB11 was prepared using a 4-yd^3 capacity stationary concrete mixer. The results indicated that 3,000 psi was achieved with this batch in 24 hr.

Both at the laboratory and at the plant, the maturity method (ASTM C 1074) and the pulse-velocity method (ASTM C 597) were used to predict the strength of the concrete. These methods are explained in the FHWA report (*5*). One significant advantage in these methods besides their convenience is that testing is in situ; consequently, the actual strengths developed in the pavement are determined. This is in contrast to conventional concrete testing, in which strengths are obtained using test cylinders. Because of their small mass, much lower heats of hydration are usually generated in the cylinders, which leads to lower early strengths than those in the structure the cylinders represent. Because of the need to open fast-track projects to traffic as soon as possible, determination of the actual early strength of the concrete in the pavement is needed, and conventional test methods are not suitable.

The data on temperature gradients are also useful in predicting the possibility of thermal cracking.

Although the maturity and pulse-velocity methods appear useful in estimating the early strength of concrete, the variability in test results, the need for specialized equipment, and the need for correlation of the pulse-velocity and conventional test results using job concretes limit their usefulness for formal acceptance testing.

Second Set of Trial Batches

The specifications required the use of grout as a bonding material and a minimum bond strength of 200 psi at 24 hr when tested in tension using the method described in ACI 503R. Most bonded fast-track overlays have used a bonding grout, but ACPA representatives indicated that a satisfactory bond could be achieved without a grout. Thus, in May 1990, more trial batches were made to determine whether a bonding material was necessary, and also to determine the workability and finishing characteristics of the concrete using admixtures available commercially. Tests were also conducted to determine whether a type or brand of cement other than that used in the paving concrete and with a higher w/c than the 0.45 maximum specified was adequate for the bonding material should it be required. A WR from one producer and WR + R at two different dosages from another producer were tried. Thus, three batches of concrete were prepared using the job proportions presented in the following table. The maximum w/c of the overlay concrete was 0.42. A 3.5-in. overlay was placed in three sections (see following table) over an existing concrete slab at the plant. The surface of the slab was shot-blasted in the same manner as it would be in an actual job to properly clean the surface of the base concrete. The grout was prepared using two different proportions and two different cements (Type I and Type II), as shown in the following table, and was pumped and scrubbed on the surface. Grout in Section 1 had 5 gal of water for 1 bag of cement (w/c = 0.44), which met the specifications (maximum w/c = 0.45), but was difficult to pump. Therefore, in other sections, 6 gal of water for 1 bag of cement (w/c = 0.53) was used. The following table presents grout proportions and type of cement.

Section	*w/c*	*Cement*
1	0.44	Type I
2	0.53	Type I
3	0.53	Type II

At an age of 24 hr, the compressive strengths of the concretes were determined at the plant. The results are summarized in Table 1 and indicate that 3,000 psi could be achieved in 24 hr. Some of the 4-in. × 8-in. specimens were kept in an insulated box; others were left under the curing blanket. As expected, the retention of heat was an important factor in achieving the early strengths. The specimens in the insulated box had about 37 percent higher strength than the ones under the blanket. The temperature of the insulated box was about 120°F at 24 hr, whereas the 4-in. × 8-in. specimens under the blanket had lower temperatures (see Figures 1 and 2, which display the temperature of the air, the mid-depth of the slab, and the specimens in sections 1 and 2). The contractor selected the use of WR + R at the lower dosage rate of 25 oz/yd³ (Section 1) for economic reasons and to minimize possible retardation. The temperature profiles in the overlays for sections 1 and 2 indicate a delay of about 3.5 hr before a temperature rise occurred.

TABLE 1 24-hr COMPRESSIVE STRENGTH FOR TRIAL SECTIONS

Section	Admixture	Insulated Box	Under Blanket
1	WR + R	4,020[b]	2,950
2	WR	4,460	3,200
3	WR + R[a]	—	3,000

[a]Twice the dosage rate used in Section 1.
[b]Test values are averages of two cylinders for those in the insulated box and three for those under the blanket.

To determine the effects of bonding material, two methods of testing were used. In one (the shear test), 4-in.-diameter cores were drilled from the concrete test slab, and then the bond area was sheared. In the other (the pull-off test), 2-in.-diameter cores were drilled through the overlay and into the base concrete to a depth slightly below the bond interface. A cap was attached to the top of the core by an epoxy resin, and a load was applied to pull off the cap. This procedure applies a direct tensile stress to the bond area. The tests were conducted 24 hr after placement. Because of difficulties in controlling the rate of loading on the machine at the plant, a definite conclusion could not be drawn in the shear test. With the direct tension test, it was difficult to apply a uniaxial load on the cap and a continuous rate of loading. In view of the difficulties in controlling tests in the plant environment, it was decided to discontinue bond testing at that site. However, having abandoned the plant bond tests, it was still necessary to evaluate the need for grout on the project. Therefore, in a final effort to determine the bond strength, 4-in.-diameter cores were drilled from the test slabs at the plant and brought to the research council for shear tests at an age of 2 days. The results (summarized in Table 2) show that satisfactory and comparable bond strengths (exceeding 200 psi) were achieved with and without a bonding grout. The results also show that the type and brand of cement can be different than that in the overlay and the w/c in the grout can be higher than that in the overlay. These findings were supported by a petrographic examination of lapped vertical slabs cut from the cylinders and examined at the research council. The examination indicated that adequate bonding was achieved in all of the specimens. Thus, based on the limited lab results, it was decided that bond strength with and without the grout would be evaluated in the field. The job grout with a w/c of 0.53 and Type I cement was used for half of the overlay, and the other half was placed without a bonding material. The shear test was used to determine the bond strength.

JOB CONCRETE

The PCC overlay was placed using mixture proportions designated as job concrete that were presented previously. Concretes were air entrained with a commercially available neutralized vinsol resin. A WR + R was added at a dosage of 25 oz/yd³.

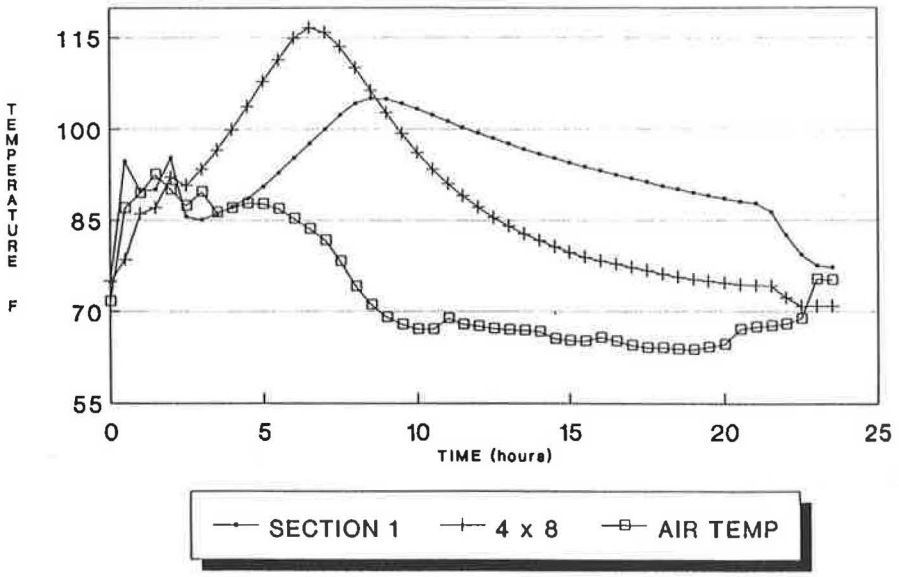

FIGURE 1 Temperature data for trial, Section 1.

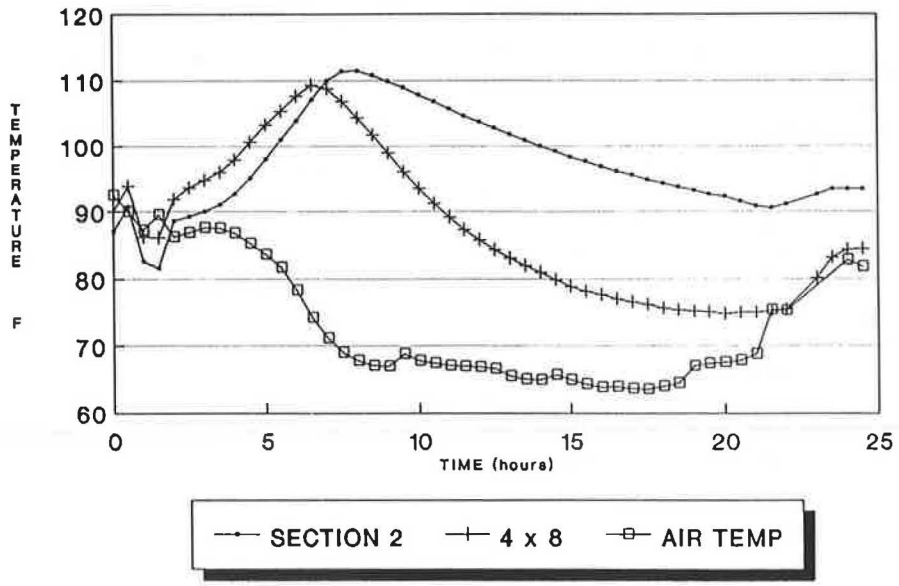

FIGURE 2 Temperature data for trial, Section 2.

TABLE 2 2-DAY BOND STRENGTH FOR TRIAL SECTIONS

Section	Grout	Specimen 1	Specimen 2	Average
2	Type I	215	365	290
2	None	395	275	335
3	Type II	430	265	345

NOTE: Strength values are in pounds per square inch.

The overlay was placed June 14 and 15, 1990. Concrete placed each day was tested for compressive strength (AASHTO T 22), splitting tensile strength (ASTM C496), flexural strength (ASTM C 78), and rapid chloride permeability (AASHTO T 277). The specimens from each of the two batches were cured under blankets near the pavement. For the first batch, additional cylinders were made to determine the compressive strength using the temperature-matched curing concept (TMC).

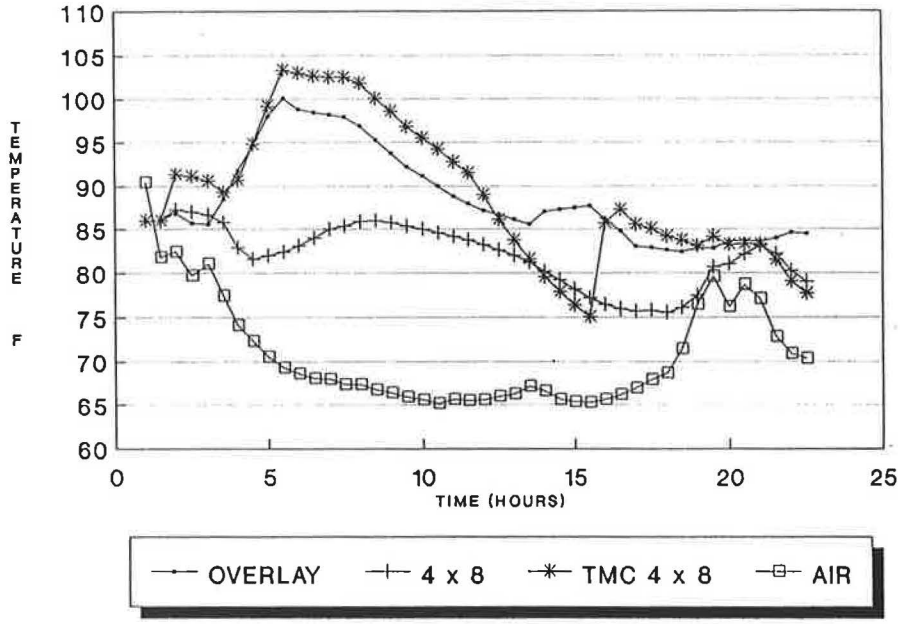

FIGURE 3 Temperature data from job.

Special molds with heating elements were used to match the temperature of the 4-in. × 8-in. specimen in the mold with that of the concrete by monitoring the mid-depth temperature of the overlay with a thermocouple. At the same time, air temperature, wind velocity, and relative humidity were continuously measured. The temperatures of the air, at mid-depth of the overlay, in the 4-in. × 8-in. cylinder kept under the insulating blankets and in the specimen in the TMC mold are shown in Figure 3. The data on environmental conditions (air temperature, relative humidity, and wind velocity) given in Figures 3–5 indicate that favorable conditions existed for placement of concrete. The rate of evaporation from the concrete surface was minimal, and the air temperatures were high enough to provide an adequate rate of hydration. The temperature data indicate that, initially, the TMC molds follow the actual temperature of the overlay closely but are several degrees above the overlay temperature. However, about 12 hr after placement, failure of a generator resulted in a drop in the temperature in the TMC molds. The temperature profile for the 4-in. × 8-in. cylinders shows that the same temperature rise achieved in the overlay or the TMC mold was not obtained by curing under the insulating blankets.

The compressive strength values given in Table 3 indicate that 3,000 psi were easily achieved in less that 24 hr. In the TMC mold, higher early strengths were obtained than with the regular molds cured under blankets. This was expected

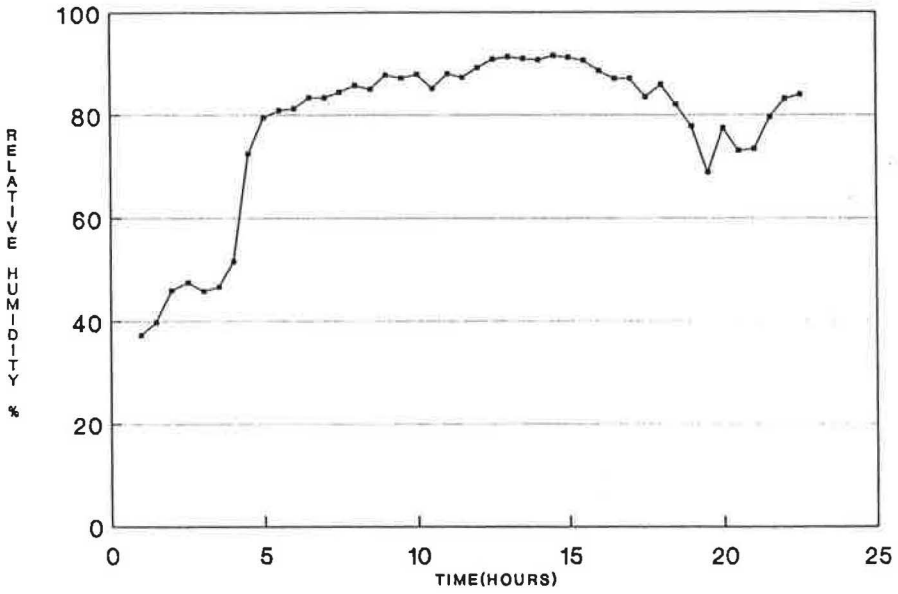

FIGURE 4 Relative humidity data from job.

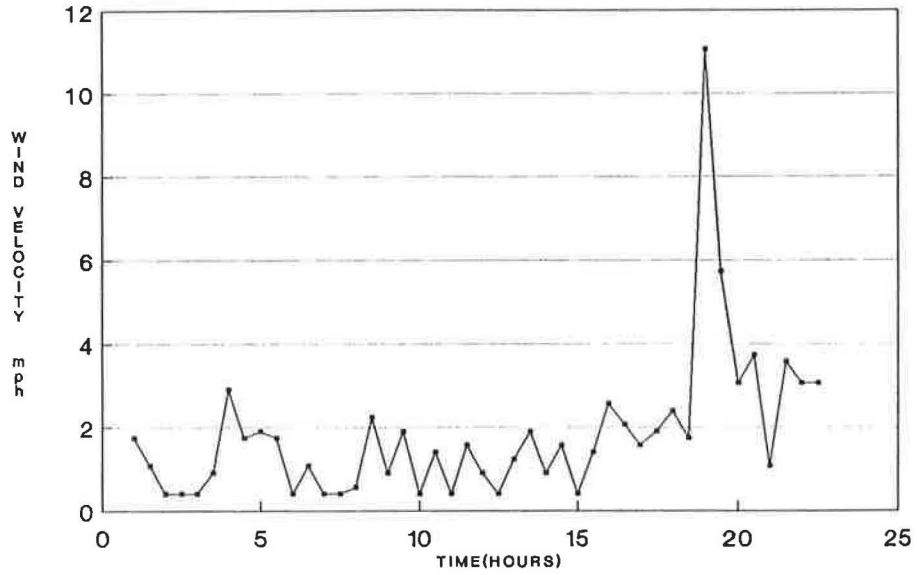

FIGURE 5 Wind velocity data from job.

because higher temperatures were developed in the TMC molds. The different strength tests for various ages summarized in Table 3 were all satisfactory. The chloride permeability (coulomb) values at 28 days were in the high range, but, at 90 days, they were either in or close to the moderate range. The temperature data indicate that the job concrete temperature rise occurred at about 3.5 hr after batching as it did in the trial batches. This is a considerable delay, and should concretes with higher early strengths than required in this project be desired, the possibility of using an accelerator instead of a retarder should be considered.

Half of the overlay was placed without a bonding agent, and half was placed with a grout that contained Type I cement at a w/c ratio of 0.53. To determine the bond strengths at different sections with and without the bond, cores were taken and tested for shear strength at 7 days in the laboratory. The results are summarized in Table 4. These results indicate that excellent bond strengths are achieved with and without the grout, and that 7-day bond strengths at the interface were close to the shear strengths of both the base concrete and the overlay concrete.

TABLE 3 TEST RESULTS FOR JOB CONCRETE

	No. of Specimens	B1	B2
Air content, %	1	5.4	5.7
Slump, inch	1	2.8	2.2
Compressive strength, psi:			
TMC 17 hour	2	3,450	—
TMC 24 hour	2	4,040	—
17 hour	2	2,940	—
18 hour	2	—	3,560
24 hour	2	3,760	4,090
7 day	2	5,240	5,590
28 day	2	6,060	6,750
Splitting tensile strength, psi:			
24 hour	2	360	345
7 day	2	460	475
28 day	2	545	550
Flexural strength, psi:			
28 day	3	835	795
Permeability, coulombs:			
28 day	2	5,290	4,220
90 day	2	4,070	2,590

CONSTRUCTION OPERATIONS

Traffic Control

Traffic control was accomplished through the provision of temporary detours on each end of the 1-mi-long site. The detours set up the two northbound lanes on the four-lane, divided highway for two-way operation to accommodate the southbound traffic during working hours. During the initial pavement preparation and the final finishing work after the overlay, southbound traffic was permitted to use the test site during nonworking hours, generally overnight and on weekends.

Preparation of Existing Pavement

Pavement Repairs

The preparation of the existing pavement began in spring 1990 with the removal and replacement of concrete considered to

TABLE 4 SHEAR STRENGTHS AT 7 DAYS

Specimen	Bonded With Grout	Bonded Without Grout	Base Concrete	Overlay
1	595	650	835	765
2	605	760	630	775
3	900	740	940	680
Average	700	715	800	740
Standard Deviation	173	59	158	52

be too badly damaged to leave in place under the overlay. Replacement concrete was standard pavement repair concrete with design strength of 3,000 psi in 24 hr. Compressible material ½-in. wide was placed on one side of each repair in the old pavement. All joints in the old pavement were cleaned and resealed with hot-poured joint sealing materials conforming to AASHTO Specification M173.

Surface Preparation

Preparation of the surface of the existing concrete pavement to ensure full bonding of the thin overlay was a major issue throughout the planning and conduct of the project. As was finally agreed on and specified, final preparation was accomplished through the use of shotblasting machines traveling in tandem, triplicate, or quadruple. In order to preclude surface contamination by traffic, actual sandblasting operations did not begin until the lanes were closed to traffic early on the first day of the placement of the overlay. Each machine covered approximately an 18-in.-wide path with each pass. Although some trial and error was necessary to achieve the texture finally agreed on by all parties, once the speed of the machines and other details were established, no further problems occurred in that operation. The texture was considered to be acceptable when coarse aggregate particles in the existing surface had a clean exposed face. Final touch-up of the surface was by use of a portable sandblasting machine placed about 100 ft ahead of the paving machine in order to catch oil spills and the like from the paving operation. Adequate bond strengths were obtained both with and without the application of a grout.

Paving

Placement of Concrete

Paving with a Gomaco slip form paver began at 1:00 p.m. June 14, 1990. Concrete was deposited from 8 yd^3 transit mix trucks in front of the paver directly on the existing pavement. Once the paver had moved forward enough to carry a "head" of concrete, the portland cement slurry grout (where used) was sprayed from a grout machine onto the surface immediately in front of the paver and then swept into place with brooms. For approximately the second half of the project, the grout was omitted.

Early in the paving operation, plywood pads were used to cover the shotblasted old pavement as a protection against oil drippings and the like from the concrete trucks. Soon, however, it became clear that the pads were not needed because the trucks were relatively new and well maintained. Because use of the pads was cumbersome, the contractor was glad to discontinue that portion of the operation.

During placement, two major difficulties were encountered in the supply of concrete. First, the supply was somewhat slow because of the number of trucks assigned to the project. Although the haul distance was short, project layout was such that trucks furnishing concrete early in the work had to back most of the 1-mi length of the project. In the grouted section, delays in concrete delivery caused some concern that the grout might dry out before concrete placement. This was soon overcome by a decision to rake concrete from the paver head forward to cover the grout until delivery resumed. A second concrete supply problem occurred for a short time when the mixture contained excessive water, and several loads had to be rejected because of high slump.

Finishing

In general, the mixture was of such a consistency that the paver, with spud vibrators at about 18-in. centers, produced an overlay with well-formed edges requiring little handwork. Magnesium floats were used to close the surface while some hand work was done on the edges. A fine texture was applied by means of a burlap drag attached to a hand-operated bridge, which was moved at intervals judged by the finishers. The transverse tining specified by VDOT (⅛in. × ⅛-in. with ¾-in.-wide land areas) was applied by a hand-held wire tine.

Curing

Liquid membrane-curing compound was applied from a rolling bridge as soon as the tining was completed. This was followed by the application of a curing blanket having a minimum R value of 0.5 and intended to hold the heat of hydration and contribute to early strength development. As noted earlier, air temperatures, relative humidities, and wind velocities were such that curing was not considered to be a major concern on the project.

Joint Sawing and Sealing

The virtual certainty that all joints and cracks in the underlying old pavement will reflect through the overlay in a short time dictated that a great deal of attention be paid to ensure that the new cracks were directly above the old. With the help of project inspectors, the contractor used a stringline across each transverse joint and crack to place paint marks on each shoulder where a second stringline could be stretched after the overlay.

As soon as the overlay was sufficiently hardened to hold the equipment, the second stringline was used to mark the locations of early saw cuts. These cuts, approximately ⅛-in. wide, accommodate the early shrinkage cracking and prevent the formation of random or uncontrolled cracks. The location, configuration, and depths of these saw cuts were the subject of a preconstruction discussion and ultimately were done in compliance with ACPA suggestions. Transverse sawcuts were ½-in. deeper than the thickness of the overlay to ensure positive control. On the other hand, because of the difficulty in precisely locating longitudinal joints in the old pavement after application of the overlay, the decision was made to saw the overlay to a depth of only 1¾-in. over those joints. The thinking in this case was that the provision of some room for vertical "wander" of the reflection crack could prevent twin cracking, which might occur if a full-depth sawcut was to miss the joint in the underlying pavement.

At the earliest possible time, most transverse joints were resawed and sealed with preformed compression seals. Longitudinal joints and transverse joints over repair joints containing expansion material were sealed with a hot-poured rubberized asphalt joint-sealing material.

OPENING TO TRAFFIC

The project was opened to traffic 58 hr after the first load of concrete appeared on the job. Although this length of time did not meet the 48-hr target, project personnel were convinced that only a few logistical modifications in the transportation of concrete and sawing operations would have permitted that target to have been met easily.

EARLY PERFORMANCE

Roughness tests conducted on the project at an age of about 1 week showed that the original international roughness index of some 160 in./mi was not substantially changed by the provision of the 3½-in overlay. This finding was not surprising to project personnel in view of the relatively good original ride and in view of the frequent interruptions in the paving operation because of the erratic supply of concrete.

A thorough evaluation of the project in March 1991 revealed only one narrow uncontrolled crack. The slight spalling of some sawed joints appeared related to the harsh texture and not to a materials or structural condition. All joint seals appeared to be in excellent condition. Early performance of the project was judged to be excellent.

CONCLUSIONS

The following conclusions are based on the construction experience from this project, during which there were favorable weather conditions, and on the observations of early performance.

1. Concrete overlays achieving compressive strengths of 3,000 psi within 24 hr can be placed using either Type III or finely ground Type II cements with a w/c of 0.42 or less.
2. The generation of external heat or retention of the heat of hydration of the concretes assists in faster strength development at early ages.
3. Overlays can be bonded to properly prepared base concrete with or without the bonding grout.
4. Thin-bonded concrete overlays applied in a fast-track mode appear to be a suitable alternative for rehabilitation of jointed concrete pavements when those pavements are not seriously distressed but are in need of structural enhancement.
5. Nondestructive test methods of maturity and pulse velocity can provide rapid evaluations of in situ concrete strengths. When using the maturity method, information on temperature gradients is also obtained, which indicates whether there is a possibility of thermal cracking.

ACKNOWLEDGMENTS

The authors gratefully acknowledge the contributions of numerous field and central office personnel in bringing the fast-track project to a successful conclusion. Not the least of those responsible was R. R. Long, Jr., former research scientist, who, through his rapport with many of the design and construction personnel, played a major role in bringing the project about. He was assisted in project development by Gary Jarrell of the maintenance division, Corky Cutright of the materials division, and by numerous others in the Suffolk District and Accomac Residency offices. Will Cumming, Kenny Wright, Kenny Marshall, and Randolph Wiggins were especially helpful in bringing the project into being and in the actual construction.

REFERENCES

1. P. L. Melville. Whitetopping—A Feasibility Study. Unpublished report. Virginia Transportation Research Council, Charlottesville, 1987.
2. *NCHRP Synthesis of Highway Practice 99: Resurfacing With Portland Cement Concrete.* TRB, National Research Council, Washington, D.C., 1982.
3. S. D. Tayabji and C. D. Ball. Field Evaluation of Bonded Concrete Overlays. In *Transportation Research Record 1196,* TRB, National Research Council, Washington, D.C., 1988.
4. J. D. Grove. Blanket Curing To Promote Early Strength Concrete. In *Transportation Research Record 1234*, TRB, National Research Council, Washington, D.C., 1989.
5. *Phase I Report: Mix Design and Trial Batches.* Demonstration Project No. 75: "Field Management of Concrete Mixes" and Special Project No. 201: "Accelerated Rigid Paving Techniques." FHWA, U.S. Department of Transportation, May 1989.

Publication of this paper sponsored by Committee on Mechanical Properties of Concrete.

Twenty-Year Performance of Latex-Modified Concrete Overlays

MICHAEL M. SPRINKEL

Fourteen bridge decks with latex-modified concrete (LMC) overlays ranging in age from 2 to 20 years and two overlays without latex were studied, and their general condition was found to be good. The half-cell and chloride data indicate that the overlays are performing satisfactorily. Rate-of-corrosion data indicate that the overlays can be used to extend the life of decks suffering from chloride-induced corrosion of the top mat of the rebar even though corrosion continues under the overlay. The permeability to chloride ions was an average of 630 coulombs (very low) for a 1.25-in.-thick LMC overlay and 5,274 coulombs (high) for the base concretes. The 2-in.-thick overlays with and without latex had permeabilities of 101 and 1,305 coulombs, respectively. Adequate shear and tensile rupture strength at the bond interface was obtained and maintained. The data indicate that LMC overlays placed on decks with less than 2 lb/yd³ of chloride ion at the rebar can be expected to have a service life of more than 20 years. The study provided the opportunity to evaluate two overlays with latex and two without latex that were installed as part of two bridges constructed in 1974. When data from these bridges were obtained in 1990 and compared with data obtained from earlier evaluations, the high quality portland cement concrete overlays without latex showed greater negative increases in half-cell potentials, greater increases in chloride content, and a higher percentage of higher rates of corrosion than the LMC overlays. Also, for these two bridges, higher shear and tensile rupture strengths were obtained at the bond interface with LMC than with concrete without latex. Higher rupture strengths were not obtained on the other bridges because of the low strength of the scarified surface of the base concrete.

Latex-modified concrete (LMC) is a portland cement concrete (PCC) in which an admixture of latex dispersed in water is used to replace a portion of the mixing water. This type of concrete has been used on highway bridges during the past 30 years (*1*) and was first used on a bridge deck in Virginia in 1969 (*2*).

The Virginia Department of Transportation's (VDOT's) special provision for LMC overlays requires 3.5 gal of styrene butadiene latex (46.5 percent to 49.0 percent solids) per bag of cement (*3*). Other VDOT requirements are minimum cement content of 658 lb/yd³, maximum water content of 2.5 gal per bag of cement, water/cement ratio (w/c) of 0.35 to 0.40, air content of 3 to 7 percent, slump of 4 to 6 in. when measured 4.5 min after discharge from the mixer, and cement/sand/coarse aggregate ratio by weight of 1.0/2.5/2.0. By comparison, the requirements for class A4 concrete used in bridge decks include minimum cement content of 635 lb/yd³, maximum w/c of 0.45 (0.47 from 1966 to 1983), air content of 5 to 8 percent, and slump of 2 to 4 in. (*4*). Thus, it can be seen that, by design, the LMC is batched with more cement, less water, less air, and at a higher slump than A4 concrete.

In 1974 VDOT installed overlays on two new bridges near Berryville, Virginia (*5*). One overlay on each bridge contained latex, and one was a high-quality PCC overlay without latex. The overlay without latex was designed to have minimum cement content of 705 lb/yd³, maximum w/c of 0.41, air content of 4 to 8 percent, and maximum slump of 2.5 in. Before the overlays were placed, the base deck (which was 2 days old) was sandblasted and moistened to achieve a saturated surface dry condition. Just ahead of the high-quality concrete placement, a portland cement slurry with a w/c of 0.40 was broomed onto the base deck. By comparison, for the LMC overlays, the mortar fraction of the overlay concrete was broomed onto the base decks.

As compared with A4 bridge deck concrete and high-quality PCC, the LMC is reported to be more resistant to the intrusion of chlorides, to have higher tensile, compressive, and flexural strengths, and to provide better freeze-thaw performance (*1*). The greater resistance to chloride intrusion is said to be attributable to the lower w/c and a plastic film the latex produces within the concrete, which inhibits the movement of chlorides. The concrete is reported to have a higher strength because the w/c is lower and because the plastic film produces a higher bond strength between the paste and aggregate. Its freeze-thaw performance is said to be superior because the lower permeability helps keep water out of the concrete and because the concrete is more flexible and therefore able to withstand the expansion and contraction associated with freezing and thawing (*1*). Although high-quality PCC overlays without latex have been used by VDOT, the LMC overlay has been the standard protective system for the rehabilitation of bridges in Virginia since the mid-1970s.

PURPOSE AND SCOPE

The purpose of this research was to evaluate the performance of LMC overlays. It consists of evaluations of 3 test areas on each of 12 bridge decks with LMC overlays and 2 test areas on each of 2 decks (1 overlay with latex and 1 without on each deck). The same test areas on 11 of the decks had been evaluated 7 years earlier (*6*). Each test area consisted of the travel lane and shoulder of a 50-ft segment of one span or the entire length of spans less than 50 ft long.

Because the principal purpose of the use of an LMC overlay is to inhibit the penetration of chloride ions to the reinforcing steel, permeability tests were conducted on 3 cores removed from each of the 14 bridges. For 12 of the bridges, 1 core was

Virginia Transportation Research Council, Box 3817 University Station, Charlottesville, Va. 22903-0817.

removed from the shoulder of 1 test area, the right wheel path of the next test area, and the center of the travel lane of the third test area. In addition, because the strength of the bond between the overlay and the base concrete is a factor in service life, three other cores were taken from the center of the travel lane of one test area on each bridge and subjected to a shear force directed through the bond line to measure the shear bond. The ACI 503R tensile adhesion test was also used to measure the tensile bond strength at seven locations in the left and right wheel paths of the same test area on each deck from which cores were taken for shear bond tests. Four 2.25-in.-diameter cores approximately 6.5 in. long were also removed from the wheel path of the same test area on each deck and used to measure the compressive strength of the overlays and the base concretes. In addition, the chloride (Cl^-) content was determined, and the electrical half-cell potentials and the rate of corrosion of the top mat of rebar were measured for the shoulder and travel lane of the other two test areas on each bridge. The data were compared with data collected before the placement of the overlays and at later ages. For the LMC overlays on bridges 1B and 1D and the overlays without latex on bridges 1A and 1C, all measurements were made in one test area.

These data were used to quantify the performance of the overlay on the basis of its having maintained satisfactory bond and compressive strengths and having prevented the infiltration of chloride, a negative increase in half-cell potentials, and high rates of corrosion. The data were also used to determine whether it is an acceptable practice to place LMC overlays on concrete having Cl^- contents in excess of 2.0 lb/yd^3 at the level of the top rebar.

RESULTS

Data supplied by the district bridge engineers in Virginia for the 14 bridges selected for study are presented in Table 1. The LMC overlays on bridges 1B, 1D, and 2 and the overlays

TABLE 1 GENERAL INFORMATION ON DECKS

Bridge No.	Structure No.	Route	District (City or County)	Type Superstructure	Date Overlay Placed	Original Date Constr.	Contractor	Latex	Deck Condition	Cost $/yd^2
1A, 1B	1052	Rte. 7, EBL, over N&WRR	Staunton (Clarke)	3-50' steel (latex on 1B)	6/1974	6/1974	Moore Bros. Const. Co.	Dow	Good	24.00 (1A-15.00)
1C, 1D	1053	Rte. 7, WBL over N&WRR	Staunton (Clarke)	3-50' steel (latex on 1D)	6/1974	6/1974	Moore Bros. Const. Co.	Dow	Good	24.00 (1C-15.00)
2	1124	Rte. 29, NBL over 29	Lynchburg (Pittsylvania)	Steel, 3 span 35', 120', 35'	11/1974	11/1974	English Const. Co.	Dow	Good	32.27
3	1030	Rte. 29, NBL over Otter Rr.	Lynchburg (Campbell)	Steel, 7 span	5/1975	4/1953	Lanford Brothers	Dow	Good	40.00
4	1029	Rte. 29, NBL, over So. R.R.	Lynchburg (Campbell)	5 steel spans (latex on A,B,C)	5/1970	8/1950	Dow	Dow	Fair	9.00
8	2032	Rte. I81, NBL, over 683	Bristol (Smyth)	3 conc. spans 32' to 47'	1982	1964	Ramco	Polysar	Good, Cracked	35.26
9	2033	Rte. I81, SBL, over 683	Bristol (Smyth)	3 conc. spans 32' to 47'	1982	1964	Ramco	Polysar	Good, Cracked	29.02
10	2000	Rte. I81, NBL over Rte. 640	Salem (Roanoke)	3-39' conc. tee beam spans	1983	1962	Whitting Turner	Dow	Good	30.70
11	2900	Rte. I66, WBL over Bull Run	Culpeper (Fairfax)	3 steel spans	1980	1961	Central Atlantic Wagman	Dow	Good	21.00
12	2024	Rte. I81, NBL, over Narrow Passage Cr.	Staunton (Edinburg)	5-70' prest. I-beams	1979	1966	Central Atlantic	Dow	Good	26.00
13	2000	Rte. I-81, NBL, Rte. 100 and Rte. 11	Salem (Pulaski)	4 steel spans, 55'	1980	1959	Chapin	Dow	Good	21.97
14	1043	Rte. 501, over Banister River	Lynchburg (Halifax)	15-50' steel spans	1979	1958	Lanford Brothers	Dow	Good	32.10
17	1045	Rte. 29 NBL over Banister River	Lynchburg (Pittsylvania)	6 steel spans 32' - 85'	1988	1948	Lanford Brothers	Dow	Good	42.19
18	1006	Rte. 340 SBL over Hawksbill Creek	Staunton (Rockingham)	3 concrete spans 32'	1986	1939	Lanford Brothers	Dow	Good	46.94

without latex on bridges 1A and 1C were placed as part of the construction of a new deck. The overlays on the other 11 bridges were used to rehabilitate older decks. Bridges 1-A, 1-B, 1-C, and 1-D are separate spans of 2 bridges. Spans 1-B and 1-D have 2-in.-thick LMC overlays, and spans 1-A and 1-C have 2-in.-thick PCC overlays without latex (2-in. maximum slump). The LMC overlays on bridges 2 and 4 do not contain coarse aggregate. Bridge 4 has five spans. Spans A, B, and C were overlaid with LMC, and spans 4-D and 4-E were completely replaced with A4 concrete. Unless indicated otherwise, the data refer to spans A, B, and C. Bridge 17 was evaluated because two liquid membrane curing materials were used to cure four experimental areas of the overlays (*7*). Bridge 18 was evaluated because it was Virginia's first high-early-strength LMC overlay (*8*).

Permeability

The rapid permeability test (AASHTO T-277) was used to measure the permeability to chloride ions of the top 2 in. and the next 2 in. of each of three cores removed from each overlay. For bridges 8, 9, and 10 it was necessary to cut and test sections from the cores at greater depths from the top for determining the permeability of the base concrete because the LMC overlays were thicker than 2.0 in. No acceptable base concrete specimens were obtained for bridge 10 because the LMC overlay was 4.7 in. thick. The results of the tests are shown in Figure 1.

Permeability of Base Concrete

The permeability values provide an indication of the differences between the base concretes. One possible explanation for the differences is that the requirements for bridge deck concrete in Virginia have changed over the years, and a significant change was made in 1966. In that year, cement content was increased from 588 to 634 lb/yd^3, w/c was reduced from 0.49 to 0.47, slump was changed from 0 to 5 in. to 2 to 4 in., air content was changed from 3 to 6 percent to 5 to 8 percent, and 28-day strength was increased from 3,000 to 4,000 psi. The base concretes of bridges 1A, 1B, 1C, 1D, 2, and 12 were constructed in 1966 or later and exhibited an average permeability of 4,476 coulombs as compared with 5,806 coulombs for the older bridges. Average values of 3,862 coulombs (1966 or later) and 5,068 coulombs (before 1966) were obtained for the base concretes in 1983 (*6*). Although the cause of the improvement in permeability cannot be determined because of the many requirements that were changed, it appears that concrete produced after the 1966 specifications were implemented has a lower permeability on the average than concrete produced before that time. The average permeability of the base concrete was 5,274 coulombs. An average of 4,590 coulombs was obtained in 1983 (*6*).

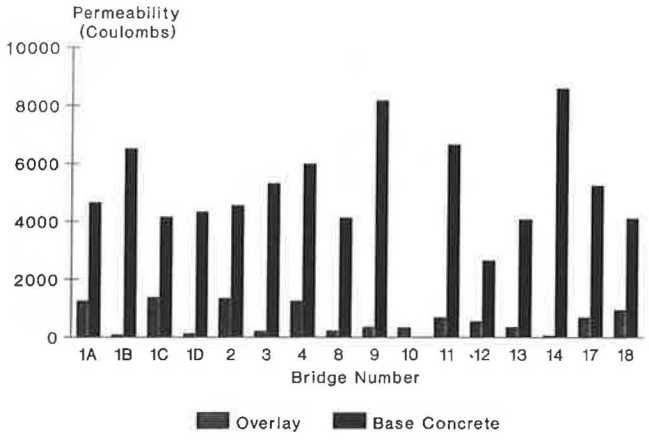

FIGURE 1 Permeability to chloride ion.

Permeability of Top 2 in.

The permeability of the top 2 in. was significantly less than the permeability of the conventional A4 base concrete for all bridges. Overlays 2 in. thick without latex on 1A and 1C had a permeability of 1,305 coulombs. Overlays 2 in. thick with latex on 1B and 1D had a permeability of 101 coulombs. The LMC overlays without coarse aggregate on bridges 2 and 4 had an average permeability of 1,288 coulombs and an average thickness of 1.4 in. The LMC overlays on the other bridges had an average permeability of 375 coulombs and an average thickness of 1.7 in.

It is believed that the principal reason for the differences in the permeability of the top 2 in. of the cores from the LMC overlays is the thickness of the overlay. Figure 2 shows the relationship between permeability and overlay thickness. The best fit of the data shows that for a typical deck with a 1.25-in.-thick LMC overlay, the average permeability of the top 2 in. is 630 coulombs, which is similar to the average value of 773 obtained in 1983 (*6*). The data for bridges 1A, 1C, 2, and 4 were omitted from the best fit.

Bond Strength

Shear Bond Strength

Three cores were removed from each of the 14 LMC overlays and the 2 overlays without latex and subjected to shear tests.

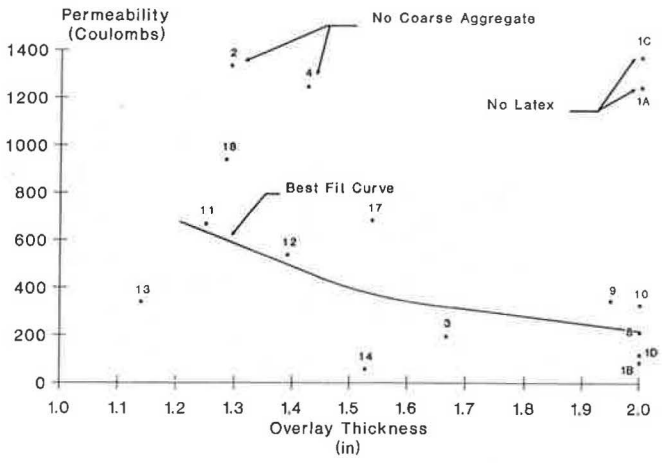

FIGURE 2 Relationship between permeability and thickness of overlay.

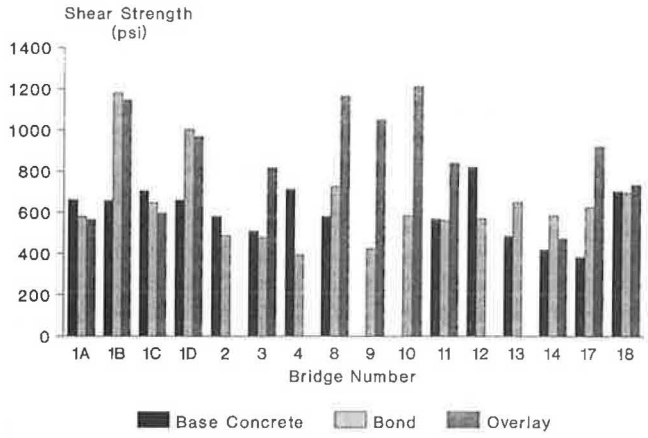

FIGURE 3 Shear strength.

The shear force was first directed through the bond interface of each core to provide an indication of its shear bond strength. The shear force was then directed through the base concrete and through the overlay to provide an indication of their shear strengths. The results of these tests are shown in Figures 3 and 4. Figure 3 shows the shear strength, and Figure 4 shows the location of the failures in the vicinity of the bond interface.

The average shear bond rupture strength of the LMC overlays was 640 psi, with 71 percent of the failures in the base concretes. For bridges 1B and 1D, the average shear bond rupture strength was 1,092 psi, with 72 percent of the failures in the base concretes. For the overlays without latex on bridges 1A and 1C, the shear bond rupture strength was 614 psi, with 1 percent of the failures in the base concrete. The average shear strength for the LMC overlays was 931 psi as compared with 581 psi for the overlays without latex. The average shear strength of the base concretes was 603 psi.

Tensile Bond Strength

Seven ACI 503R tensile adhesion tests were conducted on each of the 14 LMC overlays and the 2 overlays without latex. The results are shown in Figures 5 and 6. The results do not include tests in which the adhesive failed unless the rupture strength was higher than the average for the overlay.

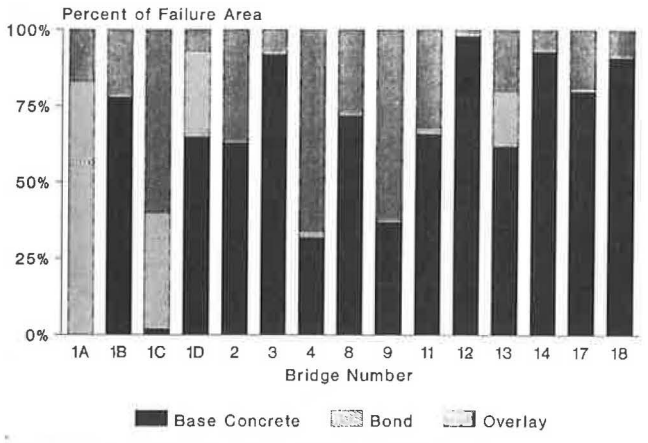

FIGURE 4 Location of failures in shear tests.

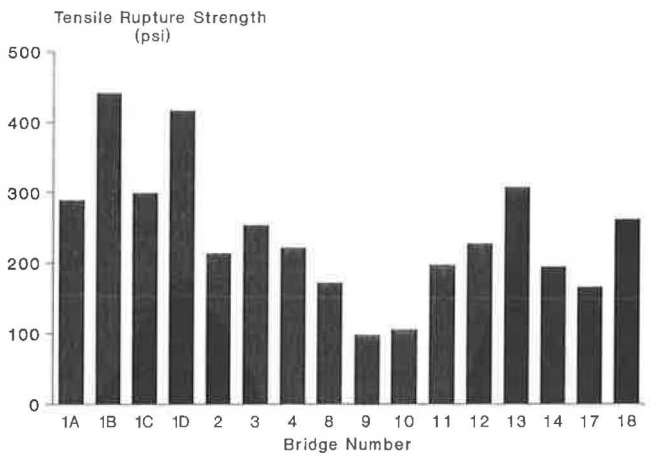

FIGURE 5 Tensile rupture strength.

The average tensile rupture strength of the LMC overlays was 233 psi with 68 percent of the failures in the base concretes. For bridges 1B and 1D the average tensile rupture strength was 428 psi with 59 percent failure in the base concrete, as compared with 294 psi with no failure in the base concrete of the overlays without latex on bridges 1A and 1C. The tensile bond strength data agree with the shear bond strength data.

Bond Strength

Based on the data in Figures 3 and 5, it can be concluded that the shear and tensile bond strengths of the LMC overlays and the overlays without the latex are high, and the strength of the bond interface is usually as high or higher than that of the base concrete. From Figures 4 and 6, it can be concluded that the majority of failures were in the base concrete, which is reasonable, because the base typically exhibited a lower strength than the bond interface (see Figure 3). The data for bridges 1A, 1B, 1C, and 1D show that higher shear and tensile rupture strengths at the bond interface can be obtained with LMC than those obtained with concrete without latex. However, the data for the other bridges show that the higher rupture strengths are not typically obtained in the rehabilitation of bridges because of the lower strength of the older

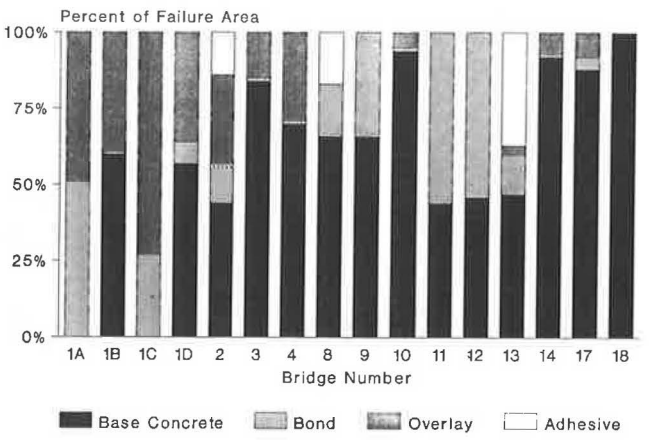

FIGURE 6 Location of failures in tensile rupture tests.

base concrete and the damage caused by the preparation of the surface of the old concrete. In addition, it can be concluded that adequate bond strengths are typically obtained with LMC overlays and overlays without latex and that the strengths can be maintained for 16 to 20 years.

Compressive Strength

Four cores that had diameters of 2.25 in. and were approximately 6.5 in. long were removed from each of the 14 LMC overlays and the 2 overlays without latex. The cores were sawed perpendicular to the length before testing for compressive strength. The length of the base concrete specimens ranged from 2.5 to 4.0 in. and that of the overlay specimens from 2.0 to 3.9 in.

The compressive strength data are shown in Figure 7. Compressive strength results could not be obtained for all overlays and for the base concrete in bridge 10 because specimens with a height of at least 2 in. could not be obtained.

The compressive strength of the base concretes ranged from 2,860 to 6,400 psi, with an average of 4,500 psi. The compressive strength of the LMC overlays ranged from 5,450 to 7,330 psi, with an average of 5,950 psi for the overlays on rehabilitated decks and 5,740 psi for the overlays on new decks. The compressive strength of the overlays without latex ranged from 4,280 to 4,900 psi; the average was 4,590 psi.

Chloride Ion Content

Chloride ion content greater than 1.3 lb/yd^3 at the level of the reinforcing steel can cause corrosion in the presence of oxygen and moisture. Table 2 and Figure 8 show the average chloride ion content (AASHTO T260) in 1983 for the shoulder and travel lane based on one sample from each of three spans

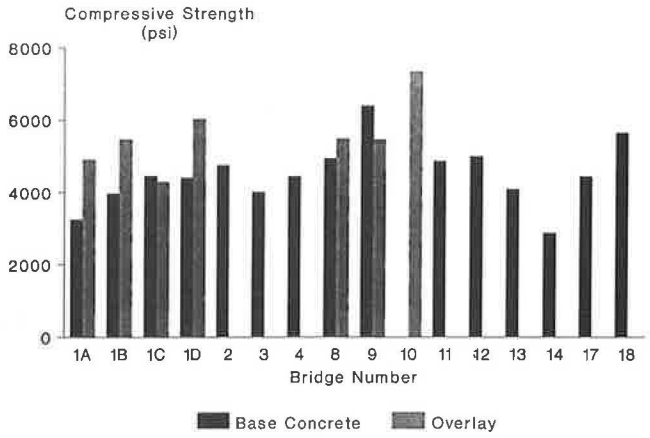

FIGURE 7 Compressive strength.

of each of the bridges and in 1990 based on one sample from the travel lane of each of two spans. Where available, data determined by district personnel before the installation of the overlays are shown. (Data for bridges 1A, 1B, 1C, and 1D were obtained by research council personnel.) Reasonable estimates of the background chloride that can be attributed to the aggregates are also reported. The depth of the reinforcing steel based on measurements made at the time the samples were taken are also shown in Table 2. Table 3 shows the chloride content as a function of depth for samples taken at each location in 1990.

From Table 2 and Figure 8, it can be concluded that there was reasonable agreement between the chloride ion contents determined before 1983 and those determined by council personnel in 1983. Also, it can be concluded that there was sufficient chloride in the vicinity of the steel in bridges 3, 4, 8, 9, and 11–14 to cause corrosion. With the exception of bridges 4, 8, 9, and 12, 1 lb or less of additional chloride has reached

TABLE 2 CHLORIDE ION CONTENT DATA

Bridge Number	Overlay Placement Date	Date of Background Data	Overlay Thickness (in)	Depth of Top Rebar (in)	Depth of Chloride 1983 (in)	Depth of[a] Chloride 1990 (in)	Chloride Content (lb/yd^3) Due to Aggregate	Prior to Overlay Placement	1983	1990	Change in Chloride Content (lb/yd^3) 1983–Prior to Overlay Placement	1990–Prior to Overlay Placement	1990–1983
1A[b]	1974	1975	2.0	2.3	2.0	2.0	0.4	0.4	0.9	0.5	0.5	0.1	−0.4
1B	1974	1975	2.0	2.3	2.0	2.0	0.4	0.4	0.4	0.6	0.0	0.2	0.2
1C[b,c]	1974	1975	2.0	2.3	--	2.0	0.4	0.4	--	1.1	---	0.7	---
1D[c]	1974	1975	2.0	2.3	--	2.0	0.4	0.4	--	0.5	---	0.1	---
2[d]	1974	---	1.3	3.3	3.1	3.5	0.1	0.1	0.1	0.5	0.0	0.4	0.4
3[d]	1975	---	1.7	3.0	2.9	3.5	0.5	--	1.8	1.1	---	---	−0.7
4[d]	1970	---	1.2	2.2	2.1	2.0	0.1	--	1.4	2.9	---	---	1.5
8	1982	1981	1.6	4.0	2.3	2.5	0.4	3.5	3.3	5.7	−0.2	2.2	2.4
9	1982	1981	1.8	3.5	2.3	2.5	0.4	1.2[e]	4.5	5.8	3.3	4.6	1.3
10	1983	---	4.4	3.3	2.3	2.5	0.4	3.0	0.4[f]	0.3	−2.6	−2.7	−0.1
11	1980	1979	1.2	3.5	2.3	2.0	0.3	4.7	4.6	4.2	−0.1	−0.5	−0.4
12	1979	1977	1.1	1.8	2.0	2.0	0.2	0.3	0.8	1.5	0.5	1.2	0.7
13	1980	---	1.1	2.5	2.0	2.5	0.3	2.4	0.6[g]	1.6	−1.8	−0.8	1.0
14	1979	1977	1.5	2.7	2.5	2.5	0.5	3.6	3.6	2.5	0.0	−1.1	−1.1
17[c,d]	1988	---	1.5	2.9	--	2.0	0.5	--	--	0.7	---	---	---
18[c,d]	1986	---	1.4	3.8	--	3.0	0.2	--	--	0.6	---	---	---

[a]See Table 3 for chloride contents at other depths
[b]High quality 2.5–in maximum slump PCC overlay
[c]Bridge was not tested in 1983
[d]Chloride data not available prior to latex installation
[e]All samples taken along edge of parapet
[f]Chloride sample taken from latex concrete used for class II repair
[g]Chloride sample taken from A4 concrete used for class II repair

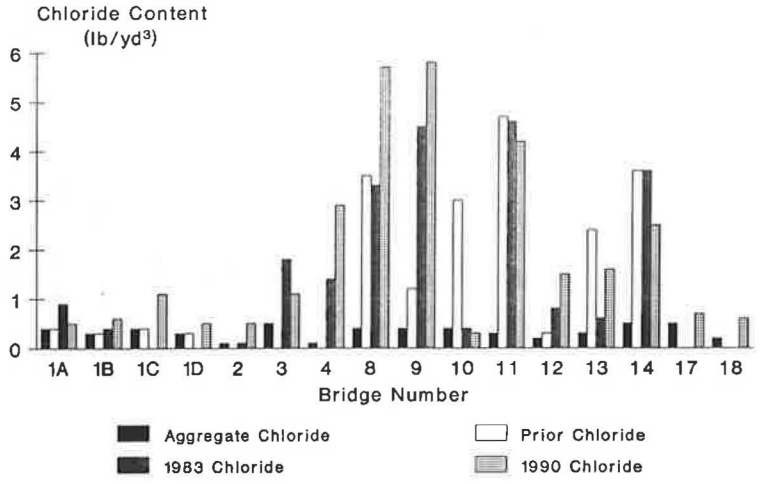

Chloride contents prior to latex overlay are unavailable for bridges 3, 4, 17, and 18. Bridges 1C, 1D, 17, and 18 were not tested in 1983.

FIGURE 8 Chloride ion content near rebar.

the level of the top rebar since the overlays were installed or since the 1983 survey. The greater increase for bridges 8 and 9 can be attributed to the large number of cracks in the overlays. The greater increase for Bridge 4 can be attributed to its higher-than-usual permeability. The overlay on Bridge 4 does not contain coarse aggregate.

Figure 9 shows the average annual change in chloride ion content as a function of depth for selected combinations of the overlays. The cracked LMC overlays showed the greatest increases. The chloride ion contents in the vicinity of the rebars have not changed significantly. Also, Figure 9 and Table 3 show that, after 16 years, the LMC overlays on bridges 1B and 1D have restricted the infiltration of chloride ion much more than the high-quality PCC overlays without latex on bridges 1A and 1C.

Half-Cell Potential

Copper sulfate half-cell potentials (ASTM C876-77) were measured at grid points 5 ft apart over the shoulder and travel lane of three spans of each bridge in 1983 and two spans in 1990 and are presented in Table 4. Also shown are the results of the measurements made by district personnel before the installation of the overlays that were constructed as part of the rehabilitation of older bridges and the results of the measurements made by council personnel shortly after the installation of the overlays on bridges 1A, 1B, 1C, and 1D. The data taken before 1983 generally agree with the data taken in 1983. Data taken in 1991 are not significantly different from data taken in 1983. It is interesting to note that even on bridges 4, 9, 11, and 13, on which there was greater than 95 percent

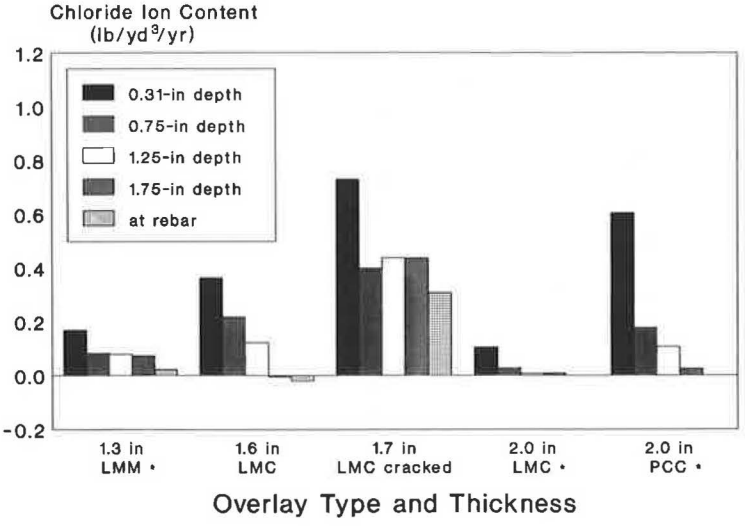

• new deck

FIGURE 9 Average annual change in chloride ion content.

TABLE 3 1990 CHLORIDE ION CONTENT DATA

Bridge Number +	Span	Chloride Content (lb/yd^3) at Depth (in) 1/8 – 1/2	1/2 – 1	1 – 1 1/2	1 1/2 – 2	2 – 2 1/2	2 1/2 – 3	3 – 3 1/2	3 1/2
1A		11.523	1.567	1.974	0.531 *				
1B		2.924	1.152	0.487	0.566 *				
1C		8.654	4.934	2.255	1.115 *				
1D		1.259	0.541	0.552	0.536 *				
2	B	2.847	1.436	1.417	0.777			0.629 *	
2	C	2.776	1.422	1.311	1.773			0.320 *	
3	C	4.999	1.225	1.227	2.129			1.509 *	
3	D	1.820	0.222	0.851	0.709			0.679 *	
4	A	8.259	5.855	3.496	3.108 *				
4	B	6.172	3.224	2.488	2.603 *				
8	B	5.279	1.689	1.577	6.190	5.246		4.217 *	
8	C	4.579	2.173	3.344	3.296	6.164			6.928*
9	A	5.170	3.761	5.615	6.856	5.474			3.246*
9	B	12.911	8.366	6.856	4.921	6.126 *			
10	1	2.462	0.874	0.140	0.289	0.350 *			
10	2	3.561	0.960	0.246	0.399	0.328			0.369*
11	1	4.869	3.544	4.980	3.583			2.594 *	
11	2	6.628	5.621	6.459	4.776 *				
12	1	8.214	5.609	2.418	0.932 *				
12	2	9.363	4.796	2.639	2.062 *				
13	3	7.430	5.498	2.823	1.500	1.975 *			
13	4	10.759	8.395	6.619	2.667	1.255 *			
14	F	0.923	0.981	2.275	2.583	3.633 *			
14	G	1.549	0.673	1.325	2.899		1.401 *		
17	A	0.652	0.252	0.681	0.674 *				
17	B	0.328	0.163	0.302	0.520 *				
17	C	1.271	0.202	0.824	0.789 *				
18	B	5.172	2.903	0.929	0.752		0.628 *		
18	C	5.773	2.599	0.575	0.885		0.645 *		

* chloride content closest to rebar

TABLE 4 ELECTRICAL HALF-CELL POTENTIALS, PERCENTAGE OF TOTAL NUMBER OF READINGS

Bridge Number	Overlay Placement Date	Date of Background Data	Half Cell Potential Distribution Prior to Overlay Placement, in 1983, and in 1990: % of Potentials < 0.20 Prior to Overlay Placement	1983	1990	0/20 3 % of Potentials 3 0.35 Prior to Overlay Placement	1983	1990	% of Potentials > 0.35 Prior to Overlay Placement	1983	1990
1A	1974	1975	100	75	39	0	22	54	0	3	7
1B	1974	1975	100	100	89	0	0	11	0	0	0
1C[a]	1974	1975	100	--	33	0	--	65	0	--	2
1D[a]	1974	1975	100	--	80	0	--	18	0	--	2
2[b]	1974	---	--	98	96	--	2	4	--	0	0
3[b]	1975	---	--	84	83	--	13	14	--	3	3
4[b]	1970	---	--	24	11	--	36	46	--	40	43
8	1982	1981	6	7	32	72	86	59	22	7	9
9	1982	1981	13	7	17	39	71	58	48	22	25
10	1983	---	53	30	60	32	63	39	15	7	1
11	1980	---	--	0	0	--	35	29	--	65	71
12	1979	1977	99	14	1	1	85	98	0	1	1
13	1980	---	3	33	13	71	36	58	26	31	29
14	1979	1977	66	75	96	33	21	4	1	4	0
17[a,b]	1988	---	--	--	74	--	--	26	--	--	0
18[a,b]	1986	---	--	--	0	--	--	64	--	--	36

[a]Bridge was not tested in 1983
[b]Electrical half-cell potential data not available prior to overlay installation

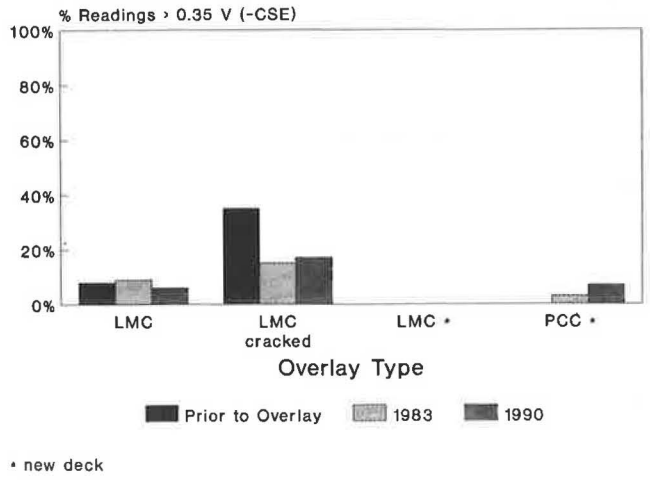

FIGURE 10 Percent of electrical half-cell potentials more negative than −0.35 V (CSE).

probability that corrosion was occurring over a large area, the overlays had no major delaminations, spalls, or patches and were providing a durable surface. It is also interesting that for bridges for which pre-1983 data were available, the scarification of the deck and installation of the overlay did not significantly change the corrosion potential of the steel.

Figure 10 shows the percentage of potentials that are more negative than −0.35V (CSE) as a function of time for selected combinations of the overlays. Figure 10 suggests the corrosion potentials have not changed much since the overlays were placed. However, the corrosion potentials for new bridges 1A and 1C without latex have become more negative than for bridges 1B and 1D, which have LMC overlays.

Rate of Corrosion

A three-point linear polarization device was used to measure the rate of corrosion of the top mat of rebar in two spans in 1990. The data are shown in Figure 11. As can be seen, no corrosion damage can be expected on any of the bridges within 2 years based on Clear's criteria (*9*). Corrosion at rates that can cause damage within 10 years is occurring in most of the decks. The data suggest that if sufficient salt is present at the rebar, corrosion occurs. Even so, overlays can be used to extend the service life of decks. Since corrosion rates for bridges 1A and 1C (without latex) are higher than for bridges 1B and 1D (with latex), a longer service life can be expected for the LMC overlays.

Shrinkage Cracks

Of the 14 bridges studied, only bridges 8 and 9 exhibited many wide plastic shrinkage cracks. Many randomly oriented hairline drying shrinkage cracks were observed in bridges 2 and 4. It is believed that these cracks were caused by the absence of coarse aggregate in the overlays. A few cracks in some of the other bridges were probably caused by drying shrinkage, reflection from the base concrete, or deck movements under traffic, but no more were noted than are typical of most A4 concrete bridge decks. These observations agree with data presented by Bishara showing that long-term shrinkage is about the same for LMC as for concrete without latex (*10*).

Spalls and Patches

The following bridges were delaminated, spalled, or patched (percentages are of the deck area evaluated): 1A: 0.3 percent, 1C: 0.6 percent, 1D: 8.7 percent, 4: 2.6 percent, 8: 20.0 percent, 9: 0.5 percent, 12: 0.5 percent; 13: 0.1 percent. The other overlays had no spalls or patches. Because of the good

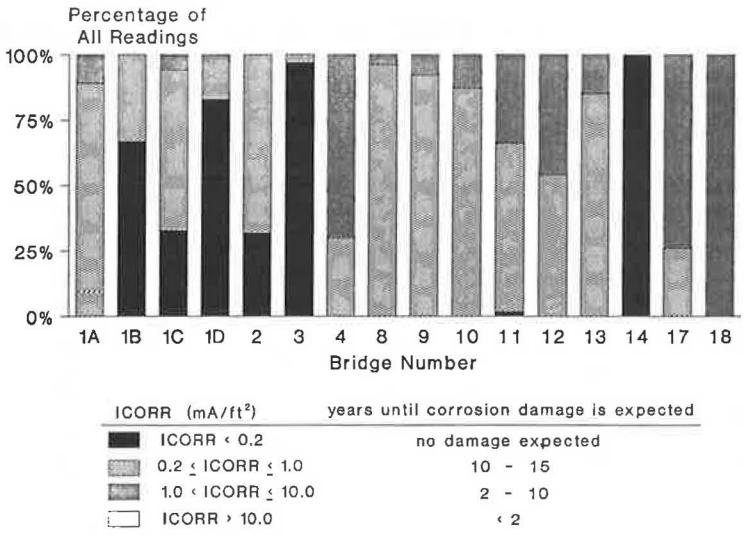

FIGURE 11 Rate of corrosion ICORR reading distribution (ICORR = corrosion current in milliamps per square foot).

bond strength of the overlays, it is believed that the spalls were caused by localized construction problems such as incorrect placement and curing of the concrete or inadequate surface preparation and concrete removal.

CONCLUSIONS

1. The average permeability to chloride ions of a 1.25-in.-thick LMC overlay was 630 coulombs, which is 12 percent of the 5,274 coulombs found to be the average permeability of the class A4 base concrete on which the overlays were placed. Two-in.-thick overlays with and without latex had permeabilities of 101 and 1,305 coulombs, respectively.

2. The shear and tensile rupture strengths at the bond interface between the LMC overlay and the base concretes were typically as good or better than the shear and tensile strengths of the base concretes, and good bond has been achieved and maintained for 20 years. Although higher bond rupture strengths can be obtained with LMC than with concrete without latex, the higher strengths are not usually obtained because of the low strength of the scarified surface of the base concrete.

3. LMC overlays have been placed over salt-contaminated concrete and steel exhibiting half-cell potentials more negative than −0.35 V CSE, and the performance of these overlays continues to be good for as long as 20 years. However, the rebar continues to corrode under the overlays, and in another 2 to 10 years spalling may occur on some bridges.

4. The half-cell potential measurements and chloride content determinations show that the LMC overlays are performing satisfactorily. The half-cell potentials and the chloride ion contents in the vicinity of the rebars have not changed significantly since the overlays were placed. However, the chloride ion contents in the overlays have increased.

5. High-quality PCC overlays without latex showed greater negative increases in half-cell potentials, greater increases in chloride content, and a higher percentage of higher rates of corrosion than similar LMC overlays.

6. LMC overlays placed on decks with less than 2.0 lb/yd^3 of chloride ion at the rebar can be expected to have a life of more than 20 years.

ACKNOWLEDGMENT

Data for bridges 1A, 1B, 1C, 1D, 11, and 12 were obtained with assistance from Larry Knab of the National Institute of Standards and Technology.

REFERENCES

1. Lower Lifetime Costs for Parking Structures with Latex Concrete Modifier. Form 173-1089-80. DOW Chemical U.S.A., Midland, Mich., 1980.
2. M. H. Hilton, H. H. Walker, and W. T. McKeel, Jr. *Latex Modified Portland Cement Overlays: An Analysis of Samples Removed from Bridge Decks.* VTRC 76-R25. Virginia Highway and Transportation Research Council, Charlottesville, Nov. 1975.
3. *Special Provision for Latex Portland Cement Concrete Bridge Deck Repairs and Widening Work.* Virginia Department of Highways and Transportation, Richmond, April 28, 1982.
4. *Road and Bridge Specifications.* Virginia Department of Highways and Transportation, Richmond, July 1, 1982, p. 180.
5. S. S. Tyson, and M. M. Sprinkel. *Two-Course Bonded Concrete Bridge Deck Construction, Interim Report No. 1, An Evaluation of the Technique Employed.* VHTRC 76-R13. Virginia Highway and Transportation Research Council, Charlottesville, Nov. 1975, p. 42.
6. M. M. Sprinkel. *Overview of Latex Modified Concrete Overlays.* VH&TRC 85-R1. Virginia Highway and Transportation Research Council, Charlottesville, July 1984.
7. M. M. Sprinkel. Use of Liquid Membrane Curing Materials to Cure LMC. Presented at 68th Annual Meeting of the Transportation Research Board, Washington, D.C., 1989.
8. M. M. Sprinkel. High-Early-Strength Latex Modified Concrete Overlay. In *Transportation Research Record 1204,* TRB, National Research Council, Washington, D.C., 1988, p. 42.
9. K. C. Clear. Measuring Rate of Corrosion of Steel in Field Concrete Structures. In *Transportation Research Record 1211,* TRB, National Research Council, Washington, D.C. 1989, p. 28.
10. A. G. Bishara. Latex-Modified Concrete Bridge Deck Overlays: Field Performance Analysis. In *Transportation Research Record 785,* TRB, National Research Council, Washington, D.C., 1980.

The opinions, findings, and conclusions expressed in this report are those of the author and not necessarily those of the sponsoring agencies.

Publication of this paper sponsored by Committee on Mechanical Properties of Concrete.

Design and Construction of Bonded Fiber Concrete Overlay of Continuously Reinforced Concrete Pavement

WILLIAM H. TEMPLE, STEVEN L. CUMBAA, AND WILLIAM M. KING, JR.

The purpose of this research was to study the design and construction of a bonded, steel-fiber-reinforced concrete overlay on an existing 8-in. continuously reinforced concrete pavement (CRCP) on Interstate 10 south of Baton Rouge, Louisiana. The existing 16-year-old CRCP, which is estimated to have carried twice its design load, contained several edge punch-out failures per mile. The research objectives were to provide an overlay with a high probability for long-term success by using a high-strength concrete mix with internal reinforcement and good bonding characteristics. A 4-in. concrete overlay containing steel fibers was designed. An inverted U-shaped reinforcing bar was added at the edge of the pavement to provide positive edge bonding. Shot blast surface cleaning of the existing tine surface easily met a specification requiring an average texture depth of 0.045 in. Water-cement grout was applied to the cleaned surface, producing bond strengths in excess of 900 psi. The concrete overlay in combination with 9-in. tied concrete shoulders reduced edge deflections by 60 percent under a 22,000-lb moving single axle load applied 2 ft from the edge. In general, the serviceability index of the pavement increased from 3.4 to 4.4, with measured profile index levels typically below the 5-in./mi specification. The bonded overlay has been in service since August 1990 and carries average daily traffic of 41,000 vehicles. Cores taken over transverse cracks in the overlay indicated reflection cracking from transverse cracks in the original pavement. Anticipation of reflective cracking was one consideration in using the steel fibers, which provide three-dimensional reinforcement.

Continuously reinforced concrete pavement (CRCP) became a standard rigid pavement design for Louisiana's Interstate construction during the 1970s. A total of 127 centerline mi was constructed on three Interstate routes 8 in. thick with identical section design details. The cross-sectional area of the steel was 0.6 percent; river gravel was used as coarse aggregate.

Performance of CRCP under heavy Interstate traffic varied, with several projects experiencing longitudinal cracking and multiple edge punch-out failures within only 5 years of service. Those pavements were typically reconstructed before they reached 10 years of age. Many of the remaining CRCP projects, including the subject overlay project, began to develop failures within 10 years of service. Previous performance has shown that this mode of failure continues at an increasing rate if not arrested.

In 1989 the Louisiana Department of Transportation and Development (LADOTD) selected a CRCP for overlay that contained several edge punch-out failures per mile and attempted to arrest the failures by thickening the 8-in. slab to a thickness sufficient to carry continued Interstate loads. The project selected for bonded concrete overlay was a 16-year-old, 4-lane section of Interstate 10, located south of Baton Rouge. The design objectives were to provide an overlay with a high chance of long-term success by providing strong concrete with internal reinforcement and excellent bond.

Louisiana Transportation Research Center, P. O. Box 94245, Baton Rouge, La. 70804–9245.

EXISTING CRCP PROJECT

The existing pavement consisted of 8 in. of CRCP constructed over a 4-in. asphaltic concrete base and lime-treated soil. The roadway contained 14-in.-thick asphaltic concrete shoulders with no provision for pavement drainage. The 1990 average daily traffic was 41,000 vehicles (22 percent being trucks), and the pavement has carried approximately twice the design load for an 8-in. CRCP since it was opened to traffic in 1974. Longitudinal cracking and edge failures were first observed in 1984, indicating that structural failures probably occurred near the time the pavement had carried its design load. Average transverse crack spacing was estimated to be 4.5 ft. Before overlay the pavement contained two to three failures per mile and had an AASHTO serviceability index of 3.4.

The location of this section of Interstate 10 is between Siegen Lane and LA 42 (Highland Road) in East Baton Rouge Parish. The total project length is 5.2 mi, with 2.2 mi of actual concrete overlay constructed. The remainder of the project consists of bridges, overpasses, and roadway transition sections that were reconstructed of jointed plain concrete pavement up to 800 ft on each end of existing structures.

OVERLAY AND SHOULDER THICKNESS DESIGN

The total projected 18-kip load for a 20-year design resulted in an estimate of 39 million applications. Calculations using Louisiana's AASHTO design procedure indicated that a thickness of 12 in. was required to satisfy anticipated loads. On the basis of these calculations a decision was made to thicken the existing 8-in slab using 4-in. of bonded concrete.

A 9-in.-thick tied concrete shoulder was designed for both the 10-ft outside and the 4-ft inside shoulders. The shoulders were designed to be tied to the original 8-in. pavement and to be jointed every 15 ft with 1 1/4-in. dowel bars spaced on 24-in. centers.

CONCRETE MIX DESIGN

Concrete mix design for the overlay included 85 lb/yd^3 of deformed steel fibers conforming to ASTM A-820, Type I or Type II. The nominal length of the fiber was specified to be not less than 1 in. and not greater than 2 in. with an aspect ratio not less than 40 and not greater than 60. The fibers selected were 1-in. long with an aspect ratio of 42. A minimum of 7.5 sacks of cement per yd^3 was required with a maximum water/cement ratio of 0.40. A slump of 1 to 2 1/2 in. was specified to be measured after adding the fibers. Both a water reducing set retarder and an air entraining agent were required. The total air content was lowered to 3.5 percent ± 0.5 percent (percent by volume) from Louisiana's typical slip-form mix specification of 5 percent ± 2 percent to minimize the chance of upward swings in air content, which may affect bond strength (*1*).

EDGE BONDING REINFORCEMENT

An edge reinforcement technique similar to curb bars was included to discourage debonding along the slab edges, which may result from curling stresses in the concrete overlay. The technique used curb-type reinforcement bars epoxied into the existing slab surface 8 in. from each outside edge (Figures 1 and 2). The inverted U-shaped bars were 4 ft long with a 2-ft spacing along the slab edge. The plans called for the bars to coincide with the center of the 4-in. overlay and therefore to be raised 2 in. above the existing surface. This was considered adequate clearance for concrete flow under the bar because the top size aggregate in the mix was limited to 1/2 in. Internal vibrators were required on each side of the edge bonding reinforcement to maximize consolidation in this area. Transverse construction joints in the overlay were required to coincide with a reinforcement bar on each slab edge to pin the overlay to the original slab at these locations.

OVERLAY CONSTRUCTION

All patching of CRCP was accomplished in accordance with standard LADOTD patching procedures where reinforcement is replaced in-kind with appropriate lapping of steel. The patches were cured a minimum of 7 days before surface preparation.

FIGURE 1 Cleaned surface with edge bonding reinforcement bars.

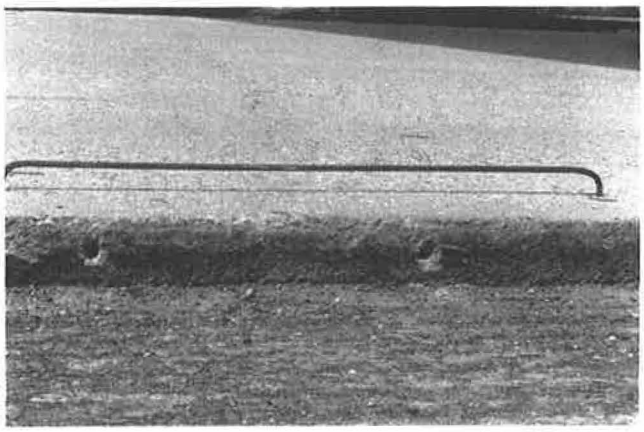

FIGURE 2 Edge bonding reinforcement bar (number 5 bar, 4-ft long, raised 2 in. above concrete).

An average texture depth of 0.045 in. was required following surface cleaning by roto-mill or shot blast. The contractor elected to use shot blast equipment with steel shot between 0.0046 and 0.0055 in. in diameter. The overall mean average texture depth achieved using the sand patch test (LADOTD TR 617) was 0.060 in. with a standard deviation of 0.009 in.

The specified minimum average texture depth was easily achievable on this project because the existing surface contained a transversely tined finish.

A stiff slurry grout consisting of 7 gal of water to one bag of cement was sprayed on the cleaned dry concrete surface just ahead of the paver. The 4-in.-thick steel-fiber-reinforced concrete overlay was then placed and finished with a slip-form paver using string line control. The concrete mix with its high cement factor provided adequate extra paste to coat the steel fibers, and the mix proved to be as constructible as normal slip-form paving concrete. Artificial turf drag was selected as the drag finish but was discontinued because of fibers catching on the material. Burlap drag was then substituted with no apparent problems, followed by transverse tinning on 1/2-in. centers. White pigmented curing compound was applied at one and a half times the normal application rate. Finally, the entire overlay paving was covered with a clear plastic membrane for a minimum of 72 hr.

Project requirements limited the temperature of plastic concrete to 90°F. This proved to be an occasional problem while the westbound roadway was being paved; however, measured concrete typically only exceeded the specification by several degrees. The contractor elected to pave the eastbound roadway during the evening to avoid upward temperature swings. Temperature restrictions on plastic concrete have subsequently been revised to a maximum of 95°F for placement of concrete overlay mixes in Louisiana.

OVERLAY BOND STRENGTH

Two methods were used to determine overlay bond strength. One was the Iowa Department of Transportation shear collar

FIGURE 3 ACI pull test was one test used to measure overlay bond strength.

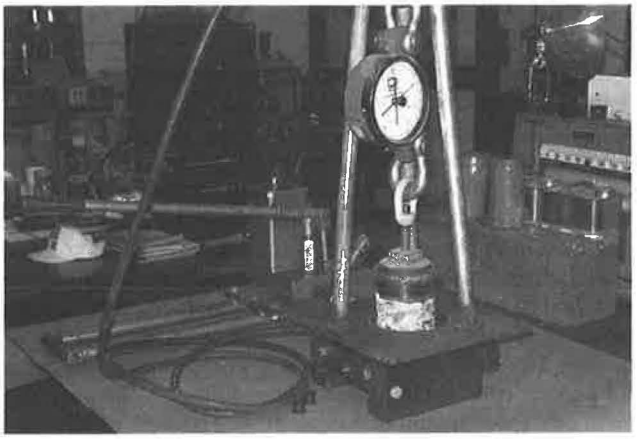

FIGURE 4 Cores of bonded overlay pull tested in laboratory.

method, in which the overlay is sheared at the bond interface using the collar device mounted in a laboratory compression tester (*2*). The other method was an American Concrete Institute (ACI) procedure that subjects the specimen to a direct pull in an attempt to disbond the overlay (Figures 3 and 4). The latter method is suitable for field evaluation because a core is drilled through the overlay and into the original pavement approximately 1 in. below the bond interface. Next, a threaded connection cap is epoxied to the top of the core and allowed to cure for several hours. Finally, the pull apparatus is screwed into the connection cap, and the force required to debond the specimen is recorded. Field tests using this procedure were unsuccessful because all failures occurred either at the epoxy bond interface or at delaminations in the original pavement layers. An additional set of cores was taken to the laboratory to repeat this test so that the epoxy could be allowed additional time to cure.

Bond strength data are presented in Table 1 for both the shear collar and pull test procedures. The average bond strength measured with the shear collar was 943 psi, which significantly exceeds the 200 psi minimum traditionally specified. The average pull strength was 128 psi, which exceeds the 100 psi minimum set forth by ACI for multicomponent epoxy adhesives used to bond fresh concrete to hardened concrete (ACI 503.2-79) (*3*).

SURFACE SMOOTHNESS AND RIDE QUALITY

Quality control measurements were conducted daily using a profilograph to check the 5-in./mi specification requirement.

TABLE 1 OVERLAY BOND STRENGTH FOR SHEAR COLLAR AND DIRECT PULL TESTS

CORE LOCATION	SHEAR COLLAR, PSI	DIRECT PULL, PSI	LOCATION OF FAILURE IN DIRECT PULL TEST
1	906	86	Field - Failed at epoxy/overlay interface.
2	832	91	Field - Failed at epoxy/overlay interface.
3	836	-	Field - Core removed by Contractor.
4	816	-	Field - Core damaged by vehicle.
5	1290	118	Field - Failed at epoxy/overlay interface.
6	736	6	Field - Failed in existing pavement.
7	1129	36	Field - Failed at epoxy/overlay interface.
8	1145	145	Field - Failed at epoxy/overlay interface.
9	1107	91	Field - Failed at epoxy/overlay interface.
10	916	95	Field - Failed at epoxy/overlay interface.
11	884	91	Field - Failed at epoxy/overlay interface.
12	868	91	Field - Failed at epoxy/overlay interface.
13	868	111	Lab - Failed at bond interface.
14	1063	159	Lab - Failed at bond interface.
15	1033	48	Lab - Failed in old concrete.
16	664	115	Lab - Failed at bond interface.
Average	943	128*	

*This average is based only on those test which failed at the bond interface.

TABLE 2 NONDESTRUCTIVE TESTING EDGE DEFLECTIONS UNDER A MOVING 22,000 lb LOAD

	AVERAGE EXPERIMENTAL RESULTS	
Stages	Pavement Deflection	Shoulder Deflection
Pre-Construction	0.0062 in.	0.0048 in.
Pre-Overlay Shoulder milled 5 in., etc.	0.0069 in.	0.0060 in.
After Concrete Overlay	0.0033 in.	0.0038 in.
Post-Construction With Tied Shoulders	0.0025 in.	0.0019 in.

On one occasion the profilograph trace indicated that the paving of an entire day was significantly out of tolerance, resulting in a profile index of 12-in./mi. A thorough examination of the paving equipment resulted in the discovery of an equipment sensor that was malfunctioning. After replacement of the sensor the profile index returned to the 5-in./mi level on subsequent paving lots. It is important to note that without daily quality control testing with the profilograph the paving equipment problem would have gone undetected during construction. The overall ride quality of the pavement increased from an AASHTO serviceability index of 3.4 to 4.4 after placement of the concrete overlay.

DEFLECTION TESTING

An indication of the reduction in edge deflection attributable to the fiber concrete overlay and to the tied concrete shoulder was provided by measuring deflections induced by a slowly moving 22,000-lb single axle load. The load was applied 2 ft from the outside pavement edge while the time-deflection profile was measured with transducers and an oscilloscope recording system. Placement of concrete overlay resulted in a reduction in edge deflection of approximately 50 percent. The 9-in. tied concrete shoulder reduced the deflection another 10 percent for a total reduction of 60 percent, as calculated from the data presented in Table 2.

OVERLAY CRACKING

A survey of transverse cracks before overlay indicated that the CRCP contained an average crack spacing of approximately 4.5 ft. Expectation of reflective cracking through the overlay was a major consideration in using steel fibers because they have the potential of providing three-dimensional reinforcement throughout the overlay. The first indications of reflective cracking became apparent 3 months after the overlay was completed. After 1 year of service, some areas of the overlay were found in which only 30 percent of the cracks reflected through and others in which essentially 100 percent of the cracks reflected through. In all locations surveyed the reflection cracks are tight and are not expected to present a problem in overlay performance.

PROJECT COSTS

The total cost for the 5.2-mi project was $5,618,356, of which $1,033,768, or $16.85/yd^2, was for the 2.2-mi-long bonded concrete overlay and $61,242, or $1.00/yd^2, was for surface preparation. Major item costs in addition to the overlay costs required to complete the project included removal and replacement of pavement for transitions at bridges, portland cement concrete shoulder construction, signs and barricades, temporary pavement markings, temporary detour roads, mobilization, and precast barriers.

CONCLUSIONS

1. A 4-in. fiber concrete overlay was successfully bonded to a 16-year-old CRCP that had carried twice its design load. The overlay was constructed in an attempt to arrest progressive development of edge failures and to provide slab thickness designed for 20 years of Interstate highway loading.
2. Design variables included to increase the probability of long-term performance include the following: (a) concrete reinforced with steel fibers and a high cement factor, (b) a clean, textured bonding surface, (c) edge bond reinforcement that pinned the overlay along slab edges, and (d) full-width tied concrete shoulders.
3. After 1 year of service varying degrees of transverse cracks have reflected through the bonded overlay; however, the cracks were anticipated and are held tight by the steel fiber reinforcement.
4. A combination of water-cement grout and a clean, textured surface provided excellent bond between fresh and hardened concrete as indicated in the results of the Iowa shear collar test.

REFERENCES

1. W. H. Temple and S. L. Cumbaa. *Thin Bonded P.C.C. Resurfacing.* Louisiana Department of Transportation and Development, Baton Rouge, 1985.
2. V. J. Bergren. *Bonded Portland Cement Concrete Resurfacing.* Division of Highways, Iowa Department of Transportation, Ames, Nov. 1990.
3. *ACI Manual of Concrete Practice.* American Concrete Institute, Detroit, Mich., 1988.

Publication of this paper sponsored by Committee on Mechanical Properties of Concrete.

Abridgment

Constitutive Relations and Failure Model for Plain Concrete and Steel-Fiber-Reinforced Concrete

M. Reza Salami

A constitutive model based on the theory of plasticity is proposed and utilized to characterize the stress-deformation behavior of plain concrete and steel-fiber-reinforced concrete. It allows for factors such as stress hardenings, volume changes, stress paths, cohesive and tensile strengths, and variation of yield behavior with mean pressure. It is applied to characterize behavior of plain concrete and steel-fiber-reinforced concrete. The constants for the model are determined from a series of available laboratory tests conducted under different initial confinements and stress paths obtained by using multiaxial and cylindrical triaxial testing devices. The model is verified with respect to observed laboratory responses. Overall, the proposed model is found suitable to characterize the behavior of plain concrete and steel-fiber-reinforced concrete.

Characterization of the stress-deformation behavior of concrete has long been a subject of active research. Linear elastic, nonlinear (piecewise linear) elastic, elastic-plastic, and endochronic models have been proposed and used by various investigators, and the literature on the subject is extensive. An excellent review of various models together with their implementation in numerical (finite element) procedures is presented by the subcommittee on the subject chaired by Chen et al. (*1*) This paper presents a general model to characterize ultimate (and failure) and hardening (softening) response in the context of the theory of plasticity.

PROPOSED MODEL

One of the functions used to define yield function in the context of incremental plasticity (*2,3*) is given by

$$J_{2D} + \alpha J_1^2 - \beta J_1 J_3^{1/3} - \gamma J_1 - k^2 = 0 \quad (1)$$

where J_{2D} is the second invariant of the deviatoric stress tensor, and α, β, γ, and k are response functions. For the behavior of plain concrete and steel fiber concrete, α, γ, and k are associated with the ultimate surface, whereas β is adopted as the growth function (hardening). Figures 1a and 1b show plots of F in the $(J_{2D})^{1/2}$ $J1$ and triaxial planes for plain concrete, respectively.

Department of Civil Engineering, North Carolina A. & T. State University, Greensboro, N.C. 27411.

To include the cohesion and the tensile strength in the ultimate criterion, a translation of the principal stress space along the hydrostatic axis is performed. A new yield function becomes

$$F = J_{2D}^* + \alpha J_1^{*2} - \beta J_1^* J_3^{*1/3} - \gamma J_1^* \quad (2)$$

For material at ultimate, Equation 2 becomes

$$J_{2D}^* + \alpha J_1^{*2} - \beta J_1^* J_3^{*1/3} - \gamma J_1^* = 0 \quad (3)$$

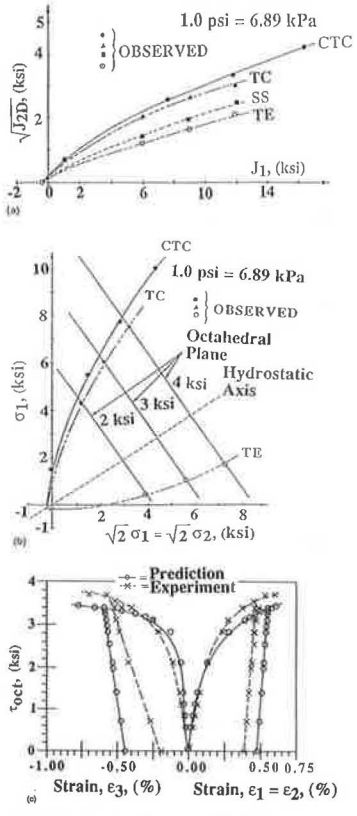

FIGURE 1 Observed ultimate surfaces: *a*, in $(J_{2D})^{1/2} - J_1$ and *b*, in triaxial plane for plain concrete; *c*, comparison of stress-strain responses of triaxial extension test for plain concrete.

where

$$J_1^* = \sigma_{11}^* + \sigma_{22}^* + \sigma_{33}^* \tag{4a}$$

$$J_{2D}^* = {}^1/_6\,[(\sigma_{11}^* - \sigma_{22}^*)^2 + (\sigma_{22}^* - \sigma_{33}^*)^2 + (\sigma_{11}^* - \sigma_{33}^*)^2] + \sigma_{12}^{*2} + \sigma_{23}^{*2} + \sigma_{13}^{*2} \tag{4b}$$

$$J_3^* = {}^1/_3\,(\sigma_{11}^{*3} + \sigma_{22}^{*3} + \sigma_{33}^{*3}) \tag{4c}$$

The resulting normal ultimate stresses σ_{11}^*, σ_{22}^*, and σ_{33}^* in equations 4a–c are then expressed as

$$\sigma_{11}^* = \sigma_{11} + R \tag{5a}$$

$$\sigma_{22}^* = \sigma_{22} + R \tag{5b}$$

$$\sigma_{33}^* = \sigma_{33} + R \tag{5c}$$

and

$$R = ap_a \tag{6}$$

where a = dimensionless number and p_a = atmospheric pressure. For cohesionless geological materials, $R = 0$, and the resulting ultimate function in Equation 2 reduces to Equation 1. If the uniaxial tensile strength (f_t) is not determined experimentally, Salami (*3*) and Lade (*4*) give an approximate formula relating f_t to the unconfined compression strength (f_{cu}) through the following power function as

$$f_t = mp_a(f_{cu}/p_a)^n \tag{7}$$

where

m and n = dimensionless numbers,
f_t = uniaxial tensile strength,
f_{cu} = unconfined compression strength, and
p_a = atmospheric pressure.

For concrete materials, $m = 0.62$ and $n = 0.68$. Once f_t is known, the value of R can be estimated. With the estimated value of R, the resulting stresses in equations 5a–c are calculated and then substituted into the expressions of the stress invariants given by equations 4a–c. The parameters a and g for the ultimate surface are determined by substituting ultimate stresses for various stress paths in equations 4a–c and then substituting them in Equation 3. Hence, a set of simultaneous equations that can be solved is obtained.

Growth Function, β

To define hardening and softening, the growth function is expressed as

$$\beta(\xi, r_D) = \beta_u\left[1 - \frac{\beta_a}{i + \xi^{\eta_1}[1 - \beta_b(r_D)^{\eta_2}]}\right] \tag{8}$$

where

$\beta_u = 3\alpha$,
β_a and η_1 = constants determined from hydrostatic compression tests,
β_b and η_1 = constants determined from shear or coupled (shear and volumetric) tests,
i = elastic limit (for material showing plastic yielding from the beginning of loading $i = 0$),
ξ = trajectory of plastic strains
$\xi = \int(d\varepsilon_{ij}^p d\varepsilon_{ij}^p)^{1/2}$ (9)
r_D = the ratio of trajectory of deviatoric plastic strains
$\xi_D = \int(dE_{ij}^p dE_{ij}^p)^{1/2}$ to ξ, and
E_{ij}^p = deviatoric plastic strain tensor.

Elastic Constants

The value of E is found as (average) slope of the unloading-reloading portion of the stress-strain curves; often the curves for the conventional triaxial compression (CTC) path are used for this purpose. The value of Poisson's ratio can be found from the measurements of the principal strains, ε_1, ε_2, and ε_3.

APPLICATIONS

The behavior of both plain and steel-fiber-reinforced concrete is verified by using the proposed model. For plain concrete, the entire hardening and ultimate responses are modeled, whereas for steel-fiber-reinforced concrete only the ultimate (failure) behavior is considered. Comprehensive laboratory tests under various stress paths (Figure 2) using the multiaxial testing device (*3*) reported by Scavuzzo et al. (*5*) and Egging (*6*) are used.

The constants for the two materials were obtained by using the foregoing procedures. Their values are presented in Tables 1 and 2.

VERIFICATION

The proposed model was verified by predicting laboratory test results under different stress paths. The incremental constitutive equations were integrated along a given stress path, starting from a given initial (hydrostatic) condition:

$$\{d\sigma\} = [C^{ep}]\{d\varepsilon\} = ([C^e] - [C^p])\,\{d\varepsilon\} \tag{10}$$

where $\{d\sigma\}$ and $\{d\varepsilon\}$ are vectors of incremental stresses and strain, respectively, and $[C^{ep}]$ is an elastic-plastic constitutive matrix with $[C^e]$ as its elastic part and $[C^p]$ as its plastic part. The latter was derived by using the theory of plasticity with F in Equation 2 as the yield function with the normality rule

$$d\varepsilon_{ij} = \lambda(\partial F/\partial\sigma_{ij}) \tag{11}$$

and the consistency condition $dF = 0$; here λ is a scalar proportionality parameter. Note that the matrix $[C^{ep}]$ is ex-

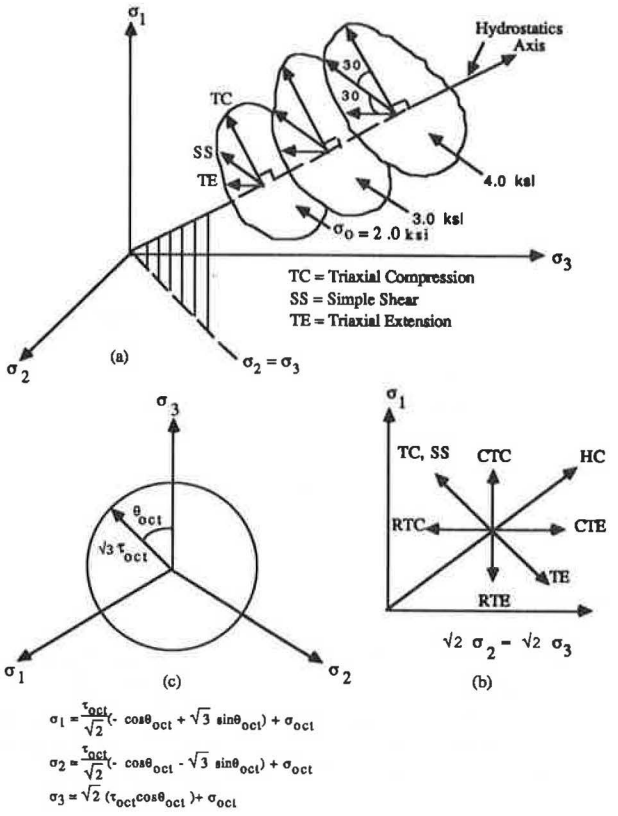

FIGURE 2 Commonly used stress paths in *a*, three-dimensional stress space and octahedral plane; *b*, triaxial plane; *c*, circular stress path with principal stress relations given (1.0 psi = 6.89 kPa) (compression stresses positive).

TABLE 1 MATERIAL CONSTANTS FOR PLAIN CONCRETE FROM DIFFERENT STRESS PATH TESTS

		English Units	SI Units
Elastic Constants	K	2000 ksi	13790 MPa
	G	1500 ksi	10343 MPa
	E	3600 ksi	24822 MPa
	ν	0.2	0.2
Constants for Ultimate Yielding	α	0.184	0.184
	γ	0.28 ksi	1.931 MPa
	δ = 3R	1.070 ksi	7.378 MPa
Constants for Hardening	β_a	4.961×10^{-3}	4.961×10^{-3}
	η_1	4.921×10^{-1}	4.921×10^{-1}
	β_b	6.2422×10^{-1}	6.2422×10^{-1}
	η_2	1.932×10^{-1}	1.932×10^{-1}

1.0 psi = 6.89 kPa

TABLE 2 ULTIMATE MATERIAL CONSTANTS FOR STEEL-FIBER-REINFORCED CONCRETE FROM DIFFERENT STRESS PATH TESTS

		English Units	SI Units
Constants for Ultimate Yielding	α	0.2215	0.2215
	γ	0.139 ksi	0.9577 MPa
	$\beta_{ult} = 3\alpha$	0.6645	0.6645
	δ = 3R	1.743 ksi	12.01 MPa

1.0 psi = 6.89 kPa

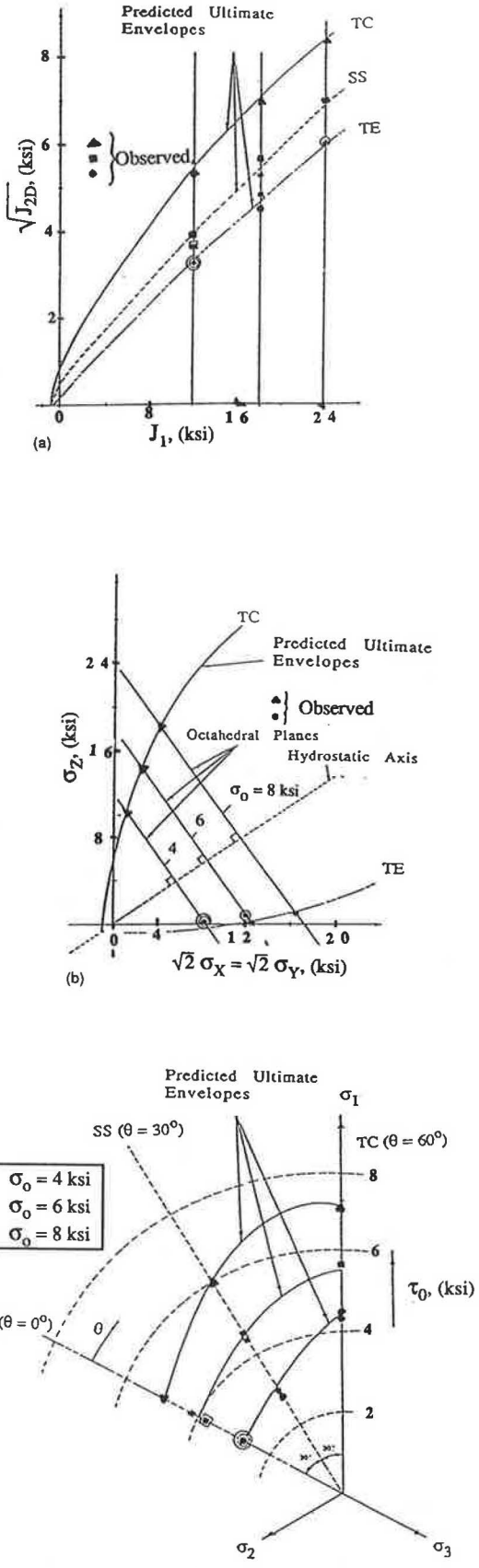

FIGURE 3 Ultimate date and predicted ultimate envelopes (1.0 psi = 6.89 kPa): *a*, in $(J_{2D})^{1/2} - J_1$ plane for steel-fiber-reinforced concrete; *b*, in triaxial plane for steel-fiber-reinforced concrete; *c*, in octahedral plane for steel-fiber-reinforced concrete.

pressed in terms of stress, stress increments, and the material constants (Tables 1 and 2).

The predicted responses for plain concrete and steel-fiber-reinforced concrete were compared with typical observed curves. Figures 1a and b show the ultimate envelopes in $[J^1 - (J_{2D})^{1/2}]$ and triaxial planes for plain concrete. Figure 1c shows comparisons between predictions and observations (plain concrete) for the triaxial extension (TE, σ_o = 6 ksi) test. Also, Figures 3a–c show comparisons between predictions and observations of steel-fiber-reinforced concrete for envelopes in the $[J_1 - (J_{2D})^{1/2}]$, triaxial and octahedral planes, respectively.

These results indicate that the model can predict the stress-strain and the volumetric behavior satisfactorily. In this study, unloading and reloading were assumed to be elastic and linear as defined by the elastic constant (E, ν).

CONCLUSION

A general, yet simplified, model is proposed and used to model behavior of geological and engineering materials such as concrete, rocks, and soils as affected by complex factors such as state of stress, stress path, and volume change. It allows for continuously yielding and stress hardening, ultimate yield and cohesive and tensile strength components. A series of multiaxial laboratory tests conducted under various stress paths and initial multiaxial laboratory tests conducted under various stress paths and initial confinements was performed. The test results were used to derive material constants. The model was verified with respect to laboratory test data used for finding the constants and a complex circular stress path test not used for finding the constants. The model was found to provide satisfactory predictions for the observed behavior of the plain concrete and steel-fiber-reinforced concrete.

ACKNOWLEDGMENTS

Part of this investigation was supported by the Air Force Office of Scientific Research, Bolling Air Force Station, Washington, D.C., and the National Science Foundation.

REFERENCES

1. Chen et al. Finite Element Analysis of Reinforced Concrete. In *Committee on Concrete and Masonry Structures*. Structural Division, ASCE, New York, N.Y., July 1982, pp. 34–137.
2. C. S. Desai and M. O. Faruque. A Constitutive Model for Geological Materials. *Journal of the Engineering Mechanics Division,* ASCE, Vol. 110, Sept. 1984, pp. 139–148.
3. M. R. Salami. Constitutive Modelling of Concrete and Rocks Under Multiaxial Compressive Loading. Ph.D. dissertation. Department of Civil Engineering and Engineering Mechanics, University of Arizona, Tucson, June 1986.
4. P. V. Lade. Three-Parameter Failure Criterion for Concrete. *Journal of the Engineering Mechanics Division,* ASCE, Vol. 108, No. EM5, Proc. Paper 17383, Oct. 1982.
5. R. Scavuzzo, H. V. Cornelius, K. H. Gerstle, H. Y. Ko, and T. Stankowski. *Stress-Strain Curves for Concrete Under Multiaxial Load Histories*. University of Colorado, Department of Civil, Environmental, and Architectural Engineering, Aug. 1983.
6. D. E. Egging. Constitutive Relations of Randomly Oriented Steel Fiber Reinforced Concrete Under Multiaxial Compression Loadings. M.S. thesis. University of Colorado, Department of Civil, Environmental, and Architectural Engineering, 1982.

Publication of this paper sponsored by Committee on Mechanical Properties of Concrete.

Effects of Aggregate, Water/Cement Ratio, and Curing on the Coefficient of Linear Thermal Expansion of Concrete

GABRIEL D. ALUNGBE, MANG TIA, AND DAVID G. BLOOMQUIST

A study to determine the coefficient of linear thermal expansion of concrete was conducted using concrete mixtures prepared with three types of coarse aggregates: porous limestone, dense limestone, and river gravel. A Type II portland cement was used at contents of 508, 564, and 752 lb/yd^3 and water/cement ratios of 0.53, 0.45, and 0.33, respectively. The concrete specimens were moist-cured and tested at 28 and 90 days. The concrete made with the porous limestone had the lowest coefficient of linear thermal expansion ($5.42-5.80 \times 10^{-6}$ in.^{2}/°F), whereas the concrete made with river gravel had the highest ($6.49-7.63 \times 10^{-6}$ in.^{2}/°F). The concrete made with dense limestone had an intermediate coefficient ($5.82-6.14 \times 10^{-6}$ in.^{2}/°F). The water-saturated concrete specimens had a lower coefficient of linear thermal expansion than the oven-dried specimens. The coefficient of oven-dried concrete decreased with moist-curing time. No significant difference between the 28-day and 90-day moist-curing was observed in the water-saturated concrete specimens.

The coefficient of linear thermal expansion of concrete is listed in the literature as varying from 4 to 8 millionths/°F (7.2 to 14.4 millionths/°C). Data on Florida concretes, which are made of predominately porous limestone, are lacking. In absence of actual data, a value of 6 millionths/°F is usually assumed. This could result in an error of 30 percent in the coefficient of linear thermal expansion and errors of more than 100 percent in the computed maximum thermal-load-induced stresses in concrete pavements. In view of the aforementioned reasons, the research reported here was started to obtain the needed data to be used in modeling and analysis of concrete pavement response and performance.

The coefficient of linear thermal expansion of concrete has been reported to be affected primarily by factors such as type and amount of aggregate and moisture content, as well as by the type and amount of cement and concrete age (*1–3*). However, the effect of the moisture content on the coefficient of linear thermal expansion applies only to the paste component as reported by one researcher (*4,5*). The variation of the coefficient of linear thermal expansion of cement paste is much greater than that of concrete (*6*). Orchard (*7*) pointed out that the coefficient of linear thermal expansion is not affected by drying wet-cured concrete specimens. Meyers (*8*) observed that the coefficient of linear thermal expansion increases with an increase in the cement content of the concrete mix and that the coefficient is dependent on the quantity of tricalcium silicate in the cement. He reported that cement with low tricalcium silicate had a low volume change with temperature variation. The type of cement does not greatly affect the coefficient of linear thermal expansion of concrete (*7,8*). Orchard (*7*) reported that the time of wet-curing (i.e., in water) has little effect on the coefficient of linear thermal expansion, whereas the time of dry-curing (i.e., in air) has little effect up to 3 months and tends to reduce the coefficient slightly between 3 months and 1 year.

G. D. Alungbe, Department of Engineering Technology, Central Connecticut State University, New Britain, Conn. 06050. M. Tia and D. G. Bloomquist, Department of Civil Engineering, University of Florida, Gainesville, Fla. 32611.

MATERIALS

The following materials and variables were used to prepare the concrete specimens for the study:

1. Three types of aggregates were used: a porous limestone (Florida Brooksville aggregate), a river gravel, and a dense limestone (Alabama aggregate). The aggregates had a maximum size of ⅜ in. because of the small size of the concrete test specimens. Although a maximum size of ¾ in. might also have been used, the ⅜ in. size was used to minimize the effects of specimen size and facilitate consolidation of the fresh concrete in the specimen molds. The physical properties of the aggregates are presented in Table 1. The fine aggregate used for all mixtures was a fine sand from Goldhead, Florida. The physical properties for the sand are as follows: bulk specific gravity = 2.50, absorption = 0.65 percent, and fineness modulus = 2.23.
2. The cement used was a Type II portland cement. The results of the physical and chemical analyses on the cement follow. Cement contents of 508, 564, and 752 lb/yd^3 were used.

TABLE 1 PHYSICAL PROPERTIES OF COARSE AGGREGATES

Property	Coarse Aggregates		
	Porous Limestone	Dense Limestone	River Gravel
Bulk specific gravity (SSD)	2.50	2.70	2.59
Absorption (%)	2.95	0.5	1.46
Unit weight (lb/ft^3)	92.0	96.82	100.38

The results of the physical tests are as follows:

- Fineness (Blaine air permeability test): 3,970 cm^2/g;
- Soundness (autoclave expansion): − 0.01 percent;
- Time of setting (Gilmore): 2 hr, 45 min (initial); 4 hr, 25 min (final);
- Compressive strength: 1,990 psi (1 day), 3,040 psi (3 days), and 4,190 psi (7 days); and
- Air entrainment: 9.1 percent.

The results of the chemical analyses (in percentages) are as follows:

- Silicon Dioxide (S_iO_2): 21.6,
- Aluminum Oxide (Al_2O_3): 4.5,
- Ferric Oxide (Fe_2O_3): 4.1,
- Magnesium Oxide (MgO): 0.6,
- Sulfur Trioxide (SO_3): 2.9,
- Loss on Ignition: 0.9,
- Insoluble Residue: 0.17,
- Alkalis (percent $Na_2O + O.658K_2O$): 0.36,
- Tricalcium Silicate: 54,
- Dicalcium Silicate: 21,
- Tricalcium Aluminate: 4.8, and
- Tetracalcium Alumino Ferrite: 12.6.

3. The water/cement (w/c) ratios were 0.33, 0.45, and 0.53.
4. The curing durations were 28 days and 3 months.
5. An admixture, Mighty RD1, was used to adjust the slump of the fresh concrete to a target slump of 3 in. This admixture meets all the requirements of ASTM C494 Type G and Type D and is classified as a water-reducer and retarder. A Darex air-entraining admixture was used. It was assumed that the small variation of admixtures used did not have any significant effects on the test results.
6. A Sikadur 32, Hi-Mod, 2-component (A and B), solvent-free moisture-insensitive structural epoxy adhesive was used to secure contact points to the concrete specimens used to determine the coefficient of thermal expansion.

EQUIPMENT

A length comparator, a water tank, and a forced draft oven were used to conduct the study on the coefficient of linear thermal expansion of concrete.

Length Comparator

The length comparator (shown in Figure 1) consists of a sensitive dial micrometer mounted on a sturdy upright support that is attached to a solid triangular base. The dial micrometer is graduated to read to 0.0001 in. The range of the scale is 0.4000 in. The dial has one large and two small count hands with needle pointers. The scale may be rotated to zero at any indication of the large needle pointer, at which point it can then be locked by a set screw. The two smaller count hands with needle pointers on the face of the large dial show the number of revolutions of the larger pointer. One of the count hands shows the reading in 0.010 in., and the other hand shows it in 0.100-in. intervals.

FIGURE 1 Length comparator.

Two anvils are fitted with collars and shaped to meet the measuring studs cast into the ends of the test concrete bars. As supplied by the manufacturer, one of the anvils is movable, whereas the other is stationary. The movable anvil is attached to the end of the indicator spindle; the stationary one is attached to the base with a threaded fastener through the base and a hex lock nut. The threaded fastener could be modified to facilitate adjustment to various heights to accommodate short specimens.

Water Tank

A water tank was constructed and used to saturate and condition the concrete specimens to the specified test temperatures. The rectangular water tank is 4 ft long × 2 ft wide × 1 ft high (see Figure 2). It was fabricated in the laboratory from 0.125-in.-thick steel. The tank was fitted with a heating element, thermometer, thermostat, and pump. Two small hollow rectangular pieces of rods were glued to the bottom of the tank for the specimens to be placed on. This helps to circulate the heated water to all surfaces of the specimens.

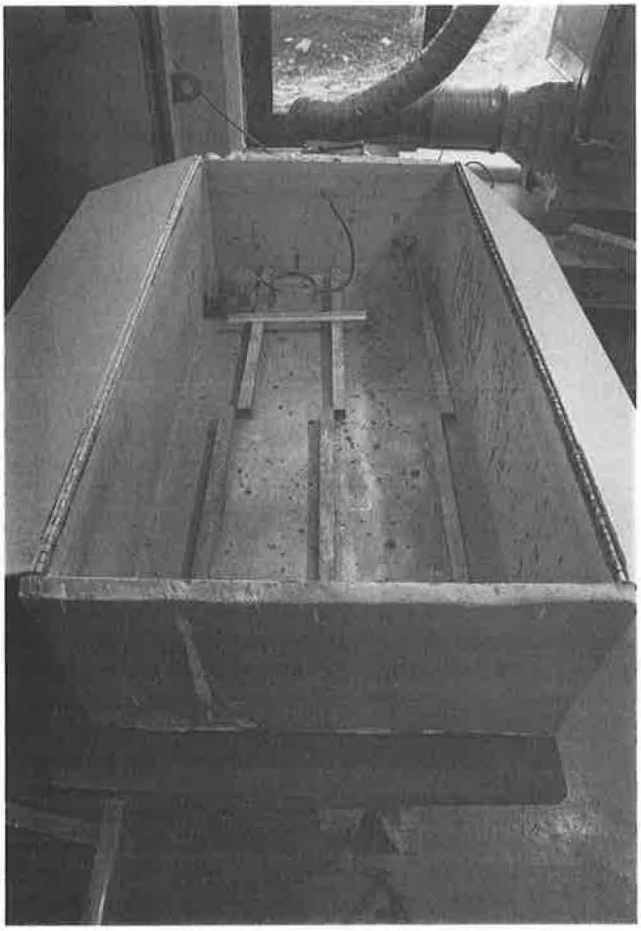

FIGURE 2 Water tank.

Forced Draft Oven

A standard laboratory oven with approximately 2 ft^3 capacity was modified in the laboratory to enable flow of warm air through the oven. The modification was performed by providing a large inlet port on one side of the oven and a small exit port on the top. A flexible aluminum duct was used to connect the two ports. A 375-cfm air booster was installed over the inlet port on the outside of the oven and connected to the duct line (see Figure 3). A thermostat and sensor were also installed to control the temperature of the oven. A small hole was made on the side of the oven so that a thermometer could be inserted to check the temperature inside the oven.

Specimen Molds

A one-compartment mold with inside dimensions of 3 in. × 11.25 in. was used to cast the test specimens. A total of ten molds were used per batch. The thickness of the steel mold is 0.5 in. (see Figure 4). Two 0.375-in.-thick, 3-in. square steel plates with a hole at the center were used to hold the contact points in place. After the concrete had set, the two steel plates were removed, leaving the two contact points embedded in the concrete specimen.

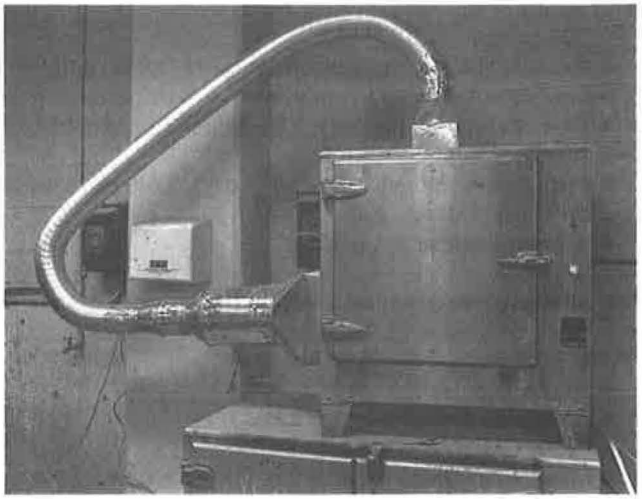

FIGURE 3 Forced draft oven.

TEST SPECIMENS

The test specimens measured 3 in. wide × 3 in. thick × 11.25 in. long. The specimens were obtained from concrete batches. Each batch varied in w/c ratio, type of coarse aggregate used, and cement content. Thermocouples were embedded in a

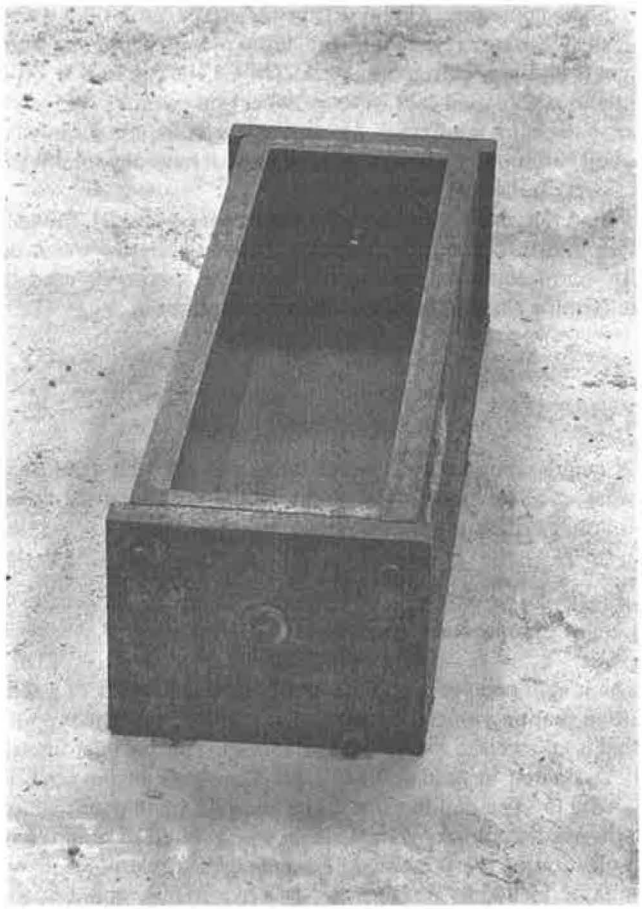

FIGURE 4 Specimen mold.

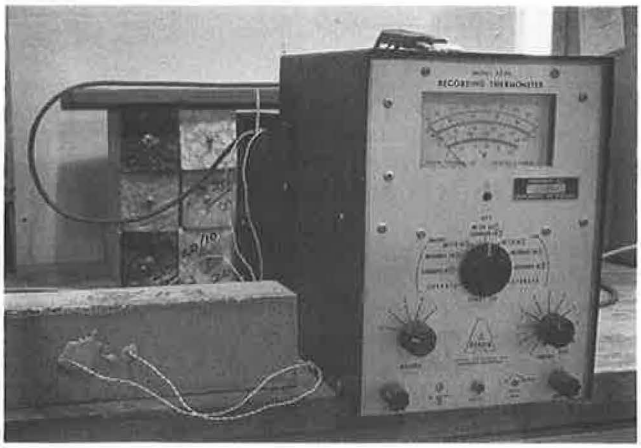

FIGURE 5 Concrete specimen with embedded thermocouples.

portion of the concrete specimens to check the temperatures in the specimen at various stages of the tests. Figure 5 is a photograph of a concrete specimen with embedded thermocouples.

EXPERIMENT DESIGN

A summary of the mix combinations is presented in Table 2. To ensure effective study of the effects of the mix parameters on the coefficient of linear thermal expansion of concrete, a factorial experiment was used. A complete factorial design facilitates statistical analyses and interpretation of the test results. The main factors and their levels under study are as follows:

- Factor A: Aggregate type:
  - –Level 1. Porous limestone,
  - –Level 2. River gravel, and
  - –Level 3. Dense limestone;
- Factor D: Curing duration:
  - –Level 1. 28-day and
  - –Level 2. 90-day; and
- Factor E: Water-Cement ratio:
  - –Level 1. 0.53,
  - –Level 2. 0.45, and
  - –Level 3. 0.33.

TABLE 2 DESIGN FOR TEST ON EFFECTS OF AGGREGATE TYPE, w/c RATIO AT VARIABLE CEMENT CONTENT, AND CURING DURATION

Aggregate	W/C = 0.53		W/C = 0.45		W/C = 0.33	
	(1) 508 lb/cy		564 lb/cy		752 lb/cy	
	(2) 28-day	90-day	28-day	90-day	28-day	90-day
Porous Limestone	X	X	X	X	X	X
River Gravel	X	X	X	X	X	X
Dense Limestone	X	X	X	X	X	X

X = Two replicate batches per cell.

Note:

(1) Cement Content

(2) Curing Durations

The following linear model was used to analyze the full factorial experiment:

$$Y_{ijklm} = \mu + A_i + E_j + (AE)_{ij} B_{(ij)k} + \delta_{(ijk)} + D_l + (AD)_{il} + (ED)_{jl} + (AED)_{ijl} + (BD)_{(ij)kl} + \varepsilon_{(ijkl)m} \quad i = 1,2,3; \quad j = 1,2,3; \; k = 1,2; \; l = 1,2; \; m = 1,2,3 \tag{1}$$

where

Y_{ijklm} = response variable of the mth specimen of the lth level of curing duration, kth batch, jth level of w/c ratio, and ith level of aggregate type;
μ = overall mean;
A_i = effect of the ith level of aggregate type;
E_j = effect of the jth level of w/c ratio;
$(AE)_{ij}$ = effect of the interaction of the ith aggregate type and the jth w/c ratio;
$B_{(ij)k}$ = effect of the kth batch nested under the ith aggregate type and jth w/c ratio;
$\delta_{(ijk)}$ = restriction error caused by subjecting samples from the same batch to different curing conditions;
D_l = effect of the lth curing duration;
$(AD)_{il}$ = effect of the interaction of the ith aggregate type with the lth curing duration;
$(ED)_{jl}$ = effect of the interaction of the jth w/c ratio with the lth curing duration;
$(AED)_{ijl}$ = effect of the interaction of the lth curing duration, jth w/c ratio, and ith aggregate type;
$(BD)_{(ij)kl}$ = effect of the interaction of the lth curing duration with the kth batch; and
$\varepsilon_{(ijkl)m}$ = effect of the mth random error within the lth curing duration, kth batch, jth w/c ratio, and ith aggregate type.

TEST PROCEDURE

Measurement of Length Change

Before length changes of the specimens were measured, a high and low reading for the standard Invar reference bar was obtained. Another high and low reference bar reading was taken at the conclusion of the measurements. This was done because the room temperature might not be constant at the location of the apparatus, and the reading was used to adjust the change in length of the reference bar. The following formula was used to correct length readings of the reference bar,

if necessary, taken at temperatures other than the standard temperature:

$$L_{\text{std. temp.}} = L_x - (T_x - \text{Std. temp.})\, G\, \alpha$$

where

$L_{\text{std. temp.}}$ = corrected length reading of the reference bar,
L_x = length reading of the reference bar taken at temperature T_x,
T_x = temperature of the room when length readings were taken,
G = gauge length, and
α = coefficient of linear thermal expansion of the reference bar material.

The coefficient of linear thermal expansion of Invar is 1.6 $\times$ 10^{-6}/°F (0.9 $\times$ 10^{-}6/°C). The correction factor for a 5°F (2.8°C) variation in temperature for the Invar bar is 0.000093.

A few trial runs with specimen embedded with thermocouples confirmed that the desired temperature can be attained within 3 hr of conditioning. However, readings were taken after at least 6 hr of conditioning.

A preliminary study was conducted to determine the reliability of the length comparator. First, the variability of the length readings from cycle to cycle was determined for the various temperatures. Then the number of cycles of readings was determined based on the variability of the data. It was observed that the variability of readings from cycle to cycle is higher when readings are taken at 140°F. For all conditions, the standard deviations are equal to or less than 0.0001 in., which is the sensitivity of the length comparator. This indicates that the method used for the measurement of the length is reliable and its precision is limited only by the precision of the length comparator. Although it could have been sufficient to use only one cycle of measurement, two cycles were used so that the mean length measurement would be more reliable and the variability of the readings could be checked. The standard deviations of the means were much less than 0.0001 in.

A conditioned specimen was brought to the instrument with the dial indicator retracted. It was carefully positioned in the lower anvil, and the indicator was released slowly and carefully to make contact with the upper anvil. The specimen was then rotated slowly while measurement of the length on each of the four sides was read aloud by one person and recorded by another or by cassette recorder. Four readings were made per cycle. A second person or cassette recorder was used to minimize the time the conditioned specimen was exposed to ambient conditions. The direction of the rotation of the specimen in the length comparator for Cycle 1 was opposite of that used for Cycle 2. Opposite directions were used to reduce the effects of the direction of rotation on the results. The specimens were placed in the length comparator with the same end pointed up each time a length measurement was made. The mean of the eight readings (four per cycle) was used as the length reading for the specimen at a given temperature.

Calculation of Coefficient of Linear Thermal Expansion

The coefficient of linear thermal expansion of each of the samples was computed from the following equation:

$$\alpha = \frac{\Delta L/L}{(T_2 - T_1)} \tag{2}$$

where

α = coefficient of linear thermal expansion of test specimen per degrees Celsius or Fahrenheit,
ΔL = change in length of the specimen from temperature T_1 to T_2,
L = original length of test specimen in inches or centimeters,
T_1 = original temperature of test specimen in degrees Celsius or Fahrenheit, and
T_2 = final temperature of test specimen in Celsius or Fahrenheit.

STATISTICAL METHODS OF ANALYSES

Analysis of Variance

The response variables were analyzed by a statistical method called analysis of variance (ANOVA). The SAS/STAT software developed by the SAS Institute, Inc., was used to perform the analyses. PROC ANOVA procedure was used. The expected mean squares presented in Table 3 enabled the construction of appropriate test statistics. In ANOVA, a *P*-value indicates the probability of error of the statement that a factor has a significant effect on the measured parameter. A lower *P*-value for a factor means that such factor has a higher level of significance. A probability of error (α) level of 0.05 was used. A factor is considered to be significant if the *P*-value of the factor is equal to or less than 0.05. It should be noted that a statistical significance may not necessarily mean a practical significance or importance and vice versa.

Before the analysis of variance, the data were screened visually by scanning and printing of the high and low values of the data. The purpose was to locate and remove outliers. The presence of outliers causes the data to depart from the basic assumptions of ANOVA, which are normal distribution, equal variances, and independent random samples. Outliers were removed before statistical analyses were performed. An assumption of independence among observations was satisfied because measurements were taken in a random order.

The Burr-Foster Q-test was used to check the assumption of homogeneity of variance, which is required in the ANOVA technique. The results of the Burr-Foster Q-test indicated no deviations from the assumptions.

Duncan's Multiple Range Test

The rejection of the null hypothesis after running ANOVA only shows that at least one pair of group means are unequal. In order to determine specifically which pair or pairs of means are unequal, multiple comparison of means was performed using Duncan's test at a significance level of 0.05.

RESULTS OF COEFFICIENT OF LINEAR THERMAL EXPANSION TEST

The mean results of the coefficient of linear expansion test on the test specimens are presented in Table 4. In water-

TABLE 3 EXPECTED MEAN SQUARE ALGORITHM FOR ANOVA MODEL

No. of levels	3	3	2	2	3	Expected Mean Square (EMS)
Type of Treatment*	F	F	R	F	R	
Subscript / Source	i	j	k	l	m	
A_i	0	3	2	2	3	$\sigma_\epsilon^2 + 6\sigma_\delta^2 + 6\sigma_B^2 + 36\sigma_A^2$
E_j	3	0	2	2	3	$\sigma_\epsilon^2 + 6\sigma_\delta^2 + 6\sigma_B^2 + 36\sigma_E^2$
$(AE)_{ij}$	0	0	2	2	3	$\sigma_\epsilon^2 + 6\sigma_\delta^2 + 6\sigma_B^2 + 12\sigma_{AE}^2$
$B_{(ij)k}$	1	1	1	2	3	$\sigma_\epsilon^2 + 6\sigma_\delta^2 + 6\sigma_B^2$
$\delta_{(ijk)}$	1	1	1	2	3	$\sigma_\epsilon^2 + 6\sigma_\delta^2$
D_l	3	3	2	0	3	$\sigma_\epsilon^2 + 3\sigma_{BD}^2 + 54\sigma_D^2$
$(AD)_{il}$	0	3	2	0	3	$\sigma_\epsilon^2 + 3\sigma_{BD}^2 + 18\sigma_{AD}$
$(ED)_{jl}$	3	0	2	0	3	$\sigma_\epsilon^2 + 3\sigma_{BD}^2 + 18\sigma_{EB}^2$
$(AED)_{ijl}$	0	0	2	0	3	$\sigma_\epsilon^2 + 3\sigma_{BD}^2 + 6\sigma_{AED}^2$
$(BD)_{(ij)kl}$	1	1	1	0	3	$\sigma_\epsilon^2 + 3\sigma_{BD}^2$
$\epsilon_{(ijkl)m}$	1	1	1	1	1	σ_ϵ^2

* F = Fixed R = Random

NOTE: See Equation 1 for model.

TABLE 4 MEAN, STANDARD ERROR OF THE MEAN, AND 95 PERCENT CONFIDENCE INTERVAL OF COEFFICIENT OF THERMAL LINEAR EXPANSION RESULTS

Condition	Moist-Curing Duration*	Mean ($\times 10^{-6}$/°F)	Standard Error of Mean ($\times 10^{-6}$/°F)	95% Confidence Interval ($\times 10^{-6}$/°F)
(a) Porous Limestone				
Water-Saturated	28- and 90-day	5.42	0.04396	5.33, 5.51
Oven-Dried	28-day	5.57	0.08999	5.39, 5.75
	90-day	5.80	0.07389	5.66, 5.94
	28- and 90-day	5.68	0.05983	5.56, 5.80
Water-Saturated and Oven-Dried	28-day	5.52	0.05749	5.41, 5.63
	90-day	5.59	0.05258	5.49, 5.69
	28- and 90-day	5.55	0.03888	5.47, 5.63
(b) Dense Limestone				
Water-Saturated	28- and 90-day	5.83	0.06828	5.70, 5.96
Oven-Dried	28-day	6.14	0.07403	5.99, 6.29
	90-day	5.83	0.10384	5.63, 6.03
	28- and 90-day	5.99	0.06793	5.86, 6.12
Water-Saturated and Oven-Dried	28-day	6.00	0.06257	5.88, 6.12
	90-day	5.82	0.07198	5.68, 5.96
	28- and 90-day	5.91	0.04873	5.81, 6.01
(c) River Gravel				
Water-Saturated	28- and 90-day	6.49	0.06904	6.35, 6.63
Oven-Dried	28-day	7.63	0.07606	7.48, 7.78
	90-day	6.77	0.12958	6.52, 7.02
	28- and 90-day	7.20	0.10389	7.00, 7.40
Water-Saturated and Oven-Dried	28-day	7.12	0.11056	6.90, 7.34
	90-day	6.58	0.08293	6.42, 6.74
	28- and 90-day	6.85	0.07547	6.70, 7.00

* Moist-curing duration for water-saturated condition is not significant.

saturated concrete, the curing duration was found to be insignificant by Duncan's Multiple Range Test. Therefore, the results from the two curing durations were combined.

STATISTICAL ANALYSES RESULTS

A Student's *t*-test analysis on the means of the coefficient of linear thermal expansion of water-saturated and oven-dried conditions showed that there is a difference between them. Hence, they were analyzed separately. The ANOVA results for water-saturated specimens are presented in Table 5. The results show that only the effect of aggregate type is significant. The results of the Duncan's test performed on the aggregate type at 5 percent alpha level show that the three aggregates are significantly different from one another (Table 6). River gravel produces the highest coefficient of linear thermal expansion (6.49–7.63 $\times$ 10^{-6}/°F) followed by dense limestone (5.82–6.14 $\times$ 10^{-6}/°F) and porous limestone (5.42–5.80 $\times$ 10^{-6}/F).

The results of ANOVA performed on data obtained from oven-dried results are summarized in Table 7. It is to be noted that, due to the presence of restriction error, the interaction term $B(A^*E)$ was used to test for the significance of factors A, E, and AE, whereas the interaction term $BD(A^*E)$ was used to test for the significance of D, AD, ED, and AED. The error term ε was used to test for the significance of $B(A^*E)$. The ANOVA results indicated that the interaction factor $B(A^*E)$ was highly significant. This meant that it could not be pooled together with the error term ε. The ANOVA results indicated that aggregate type, moist curing duration, and their interaction are highly significant. A comparison of the means of the significant effects by Duncan's multiple range test at 5 percent probability of error level was performed. The results are summarized in Table 8. At the 28-day moist curing duration, each aggregate is are significantly different from the others. At the age of 90 days, concrete made with porous limestone and dense limestone does not show significant difference in the value of the coefficient of linear thermal expansion. However, the river gravel produced a significantly higher value than the other two aggregates.

TABLE 5 RESULTS OF ANOVA ON DATA FROM COEFFICIENT OF LINEAR THERMAL EXPANSION TEST ON WATER-SATURATED CONCRETE SPECIMENS

Source of Variation#	df	SS	MS	F	P
A	2	18.40E-12	9.20E-12	34.10	0.0001**
E	2	0.84E-12	0.42E-12	1.56	0.2616
AE	4	1.43E-12	0.36E-12	1.33	0.3309
B(A*E)	9	2.43E-12	0.27E-12	-	-
D	1	0.22E-12	0.22E-12	0.51	0.4936
AD	2	0.03E-12	0.02E-12	0.04	0.9651
ED	2	0.10E-12	0.05E-12	0.12	0.8875
AED	4	1.46E-12	0.36E-12	0.85	0.5304
BD(A*E)	9	3.87E-12	0.43E-12	5.85	0.0001**
ε	67	4.93E-12	0.07E-12	-	-

R-Square = 0.858281

See Equation (1) for definition of the terms
** Significant at α = 0.01 level.

TABLE 6 GROUPING OF AGGREGATE TYPE BY MEANS OF COEFFICIENT OF LINEAR THERMAL EXPANSION OF WATER-SATURATED CONCRETE FROM DUNCAN'S TEST

Aggregate Type	Mean	Grouping*
River Gravel	6.49 x 10^{-6}/°F	A
Dense Limestone	5.83 x 10^{-6}/°F	B
Porous Limestone	5.44 X 10^{-6}/°F	C

* Note: Means with different letters are significantly different at α = 0.05 level.

TABLE 7 RESULTS OF ANOVA ON DATA FROM COEFFICIENT OF LINEAR THERMAL EXPANSION TEST ON OVEN-DRIED CONCRETE SPECIMENS

Source of Variation#	df	SS	MS	F	P
A	2	43.85E-12	21.93E-12	52.23	0.0001**
E	2	0.10E-12	0.05E-12	0.12	0.8845
AE	4	4.37E-12	1.09E-12	2.60	0.1076
B(A*E)	9	3.78E-12	0.42E-12	-	-
D	1	2.75E-12	2.75E-12	11.08	0.0088**
AD	2	5.17E-12	2.59E-12	10.41	0.0046**
ED	2	0.13E-12	0.07E-12	0.26	0.7799
AED	4	1.91E-12	0.48E-12	1.92	0.1906
BD(A*E)	9	2.24E-12	0.25E-12	2.54	0.0136*
ε	72	7.04E-12	0.10E-12	-	-

R-Square = 0.901342

See Equation (1) for definition of the terms.

* Significant at α = 0.05 level.

** Significant at α = 0.01 level.

TABLE 8 GROUPING OF AGGREGATE TYPE BY MEANS OF COEFFICIENT OF LINEAR THERMAL EXPANSION OF OVEN-DRIED CONCRETE FROM DUNCAN'S TEST

Moist Curing Duration	Aggregate Type	Mean	Grouping*
28 - day	River Gravel	7.63 x 10^{-6}/°F	A
	Dense Limestone	6.14 x 10^{-6}/°F	B
	Porous Limestone	5.64 x 10^{-6}/°F	C
90 - day	River Gravel	6.77 x 10^{-6}/°F	A
	Porous Limestone	5.85 x 10^{-6}/°F	B
	Dense Limestone	5.83 x 10^{-6}/°F	B

* Note: Means at each moist curing duration with the same letter are not significantly different at α = 0.05 level.

CONCLUSIONS

1. Aggregate type has some effect on the coefficient of linear thermal expansion of water-saturated and oven-dried concrete. Under water-saturated conditions, the three aggre-

gates are significantly different from one another. The river gravel has the highest coefficient; porous limestone has the least. Under oven-dried conditions, the three aggregates are significantly different from one another at 28-day moist-cured age. The river gravel produced the highest coefficient, followed by dense limestone; porous limestone had the least. At the 90-day moist-cured age, the porous limestone and dense limestone did not show any significant difference from each other. The river gravel, however, yielded a significantly higher coefficient than the other two aggregates.

2. The w/c ratio and the cement content did not show any effect on the coefficient of linear thermal expansion.

3. The moist-curing duration does effect the coefficient in the oven-dried condition but not in the water-saturated condition. The coefficient of concrete in oven-dried condition is significantly higher at 28-day moist curing than at 90-day moist curing.

ACKNOWLEDGMENTS

The work presented in this paper is part of a research project supported by the State of Florida Department of Transportation (FDOT) and the U.S. Department of Transportation. Torbjorn J. Larsen and Jamshid M. Armaghani of FDOT acted as technical coordinators for the study. The authors are also grateful for the assistance and cooperation of the personnel in the FDOT Materials Office in Gainesville.

REFERENCES

1. R. D. Browne. Thermal Movement of Concrete. *Concrete: The Journal of the Concrete Society (London)*, Vol. 6, Oct. 1972, pp. 51–53.
2. American Concrete Institute. *ACI Manual of Concrete Practice*, Part 1. Detroit, Mich., 1985, 209R-24–209R-25.
3. R. E. Davis. A Summary of Investigations of Volume Changes in Cements, Mortars and Concretes Produced by Causes Other Than Stress. *Proc., American Society for Testing and Materials*, Vol. 30, Part 1, 1930, pp. 149–155.
4. A. M. Neville. *Properties of Concrete*, 3rd ed. Longman Scientific and Technical, Essex, England; John Wiley and Sons, Inc., New York, N.Y., 1987.
5. A. M. Neville. *Hardened Concrete: Physical and Mechanical Aspects*. American Concrete Institute, Detroit, Mich.; Iowa State University Press, Ames, Iowa, 1971.
6. L. J. Mitchell. Thermal Expansion Tests on Aggregates, Neat Cements, and Concrete. *Proc., American Society for Testing and Materials*, Vol. 53, 1953, pp. 963–977.
7. D. F. Orchard. *Concrete Technology*, Vol. 1, 4th ed. Applied Science Publishers Ltd., London, 1979.
8. S. L. Meyers. Thermal Coefficient of Expansion of Portland Cement—Long-Time Tests. *Industrial and Engineering Chemistry*, Vol. 32, 1940, pp. 1107–1112.

Publication of this paper sponsored by Committee on Mechanical Properties of Concrete.

Abridgment

Analytical Expressions for Uniaxial Tensile Strength of Concrete in Terms of Uniaxial Compressive Strength

M. Reza Salami

For the purpose of including reasonable values of tensile strengths in the available failure criterion (for frictional materials with effective cohesion), it may be necessary to include the uniaxial tensile strength in the parameter determination. A simple expression for evaluation of the uniaxial tensile strength on the basis of the uniaxial compressive strength is proposed. Different types of geological materials were included in the study. Also, on the basis of available experimental data on flexural and splitting tensile strengths of concrete, simple expressions for evaluation of these strengths as a function of uniaxial comprehensive strength are given. The correlation between the experimental results and analytical predictions are good and provide a simple approach for developing tensile strength models for plain concrete.

The uniaxial tensile strength (f_t), split cylinder tensile strength (f'_{sp}), and flexural tensile strength (f_r) have often been expressed as a fraction of the uniaxial cylindrical compressive strength (f'_c) and uniaxial cubical compressive strength (f_c). Mitchell (*1*) indicates that f_t (given as the flexural strength, which may be higher than the true value of f_t) for cemented soils is about 1/5 to 1/3 of f'_c, whereas data compiled by Hannant (*2*) show that f_t for concrete varies between 5 and 13 percent of f'_c. However, Bortolotti (*3,4*) shows from experimental results conducted by Shah and Ahmad (*5*) that linear relationships exist among the ratios of f'_c/f_t, f_c/f_t, f'_{sp}/f'_c, and f_r/f_t as follows:

$$\frac{f'_c}{f_t} = 5.12 + 0.000844\, f'_c \tag{1}$$

$$\frac{f_c}{f_t} = 6.4 + 0.000844\, f_c \tag{2}$$

$$\frac{f'_{sp}}{f'_c} = 5.0 + 0.001\, f'_c \tag{3}$$

$$\frac{f_r}{f_t} = 1.2 + 0.0000167\, f'_c \tag{4}$$

Therefore, from Equations 1–4, the uniaxial strength tensile strength, split cylindrical tensile strength (direct tensile strength), and beam flexural tensile strength of concrete can be determined as a function of cylindrical compressive strength (f'_c) or as a function of cubical compressive strength (f_c), assuming that f'_c is equal to $0.8\, f_c$ as follows:

$$f_t = \frac{f'_c}{(5.12 + 0.000844 f'_c)} \tag{5}$$

$$f_t = \frac{f_c}{(6.4 + 0.000844 f_c)} \tag{6}$$

$$f'_{sp} = \frac{f'_c}{(5.0 + 0.001 f'_c)} \tag{7}$$

$$f_r = (1.2 + 0.0000167\, f'_c)\, f_t \tag{8}$$

where f_t, f'_{sp}, f_r, f_c, *and* f'_c are given in psi. The value of f_t differs from f'_{sp} by about 10 percent, as shown in Figure 1.

TEST DATA AND EXPERIMENTAL RELATIONSHIPS BETWEEN CONCRETE STRENGTH PARAMETERS

Figure 1 (*4,5*) shows the plot of the experimental data and equations for predicting the split cylinder strength of concrete as a function of its cylindrical compressive strength. Figure 2 (*4,5*) shows the plot of the experimental data and equations for predicting the beam flexural tensile strength of concrete as a function of its cylindrical compressive strength. Figure 3 shows a comparison of the relationships between uniaxial ten-

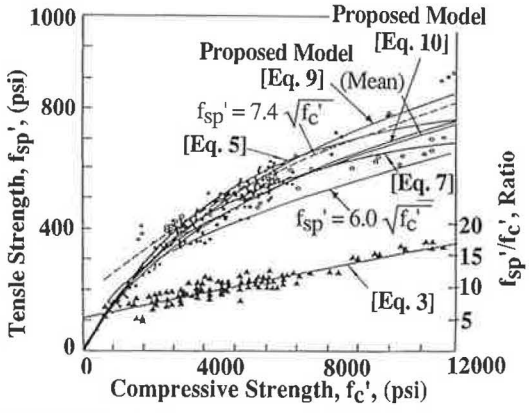

FIGURE 1 Split cylinder tensile strength (*4,5*).

Department of Civil Engineering, North Carolina A&T State University, Greensboro, N.C. 27411.

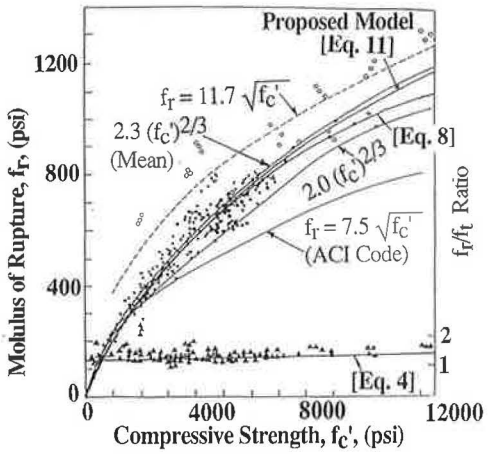

FIGURE 2 Beam flexural tensile strength (*4,5*).

sile and uniaxial compressive strengths for materials presented in Table 1.

PROPOSED TENSILE STRENGTH EXPRESSION

The proposed analytical expression of uniaxial strength (f_t) as a function of cylindrical compressive strength for concrete, on the basis of experimental results obtained by Shah and Ahmad (*5*), Salami (*6*), Salami and Desai (*7*), Egging (*8*), and Lade (*9*), is given as follows:

$$f_t = -mP_a\left(\frac{f_c'}{P_a}\right)^n \qquad \text{(compression positive)} \qquad (9)$$

where m and n are dimensionless numbers (for plain concrete $m = 0.62$ and $n = 0.68$) and P_a is atmospheric pressure in the same units as f_t and f_c'. The proposed equation is shown in Figure 1. It is evident from the figure that the prediction from the proposed model compares well with experimental results and the model proposed by Bortolotti (*4*), which is also shown in Figure 1. Values of m and n have been determined for several frictional materials, which are presented in Table 1. These values represent the best fit between experimental data and the simple expression in Equation 9. A comparison of the relationships between uniaxial compressive strengths for the materials in Table 1 is shown in Figure 3. The straight lines shown on the log-log diagram span over the ranges of uniaxial compressive strengths indicated by available data. Both relatively weak and very strong frictional materials are presented in Figure 3. Note that the lines are clustered and slope away from the line representing equal uniaxial tensile and uniaxial compressive strengths. Thus, the weak materials have relatively higher uniaxial tensile strengths than the strong materials.

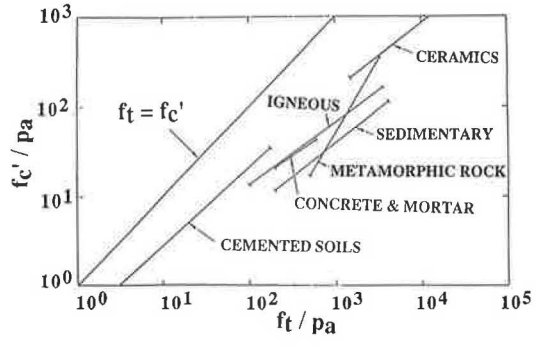

FIGURE 3 Relationships between uniaxial tensile strength and uniaxial compressive strengths for various types of frictional materials.

TABLE 1 VALUES OF PARAMETERS m AND n FOR VARIOUS TYPES OF FRICTIONAL MATERIALS

Material	m	n
Cemented soils (*1*)	0.37	0.88
Plain concrete (for f_t)	0.62	0.68
Plain concrete (for f_{sp}')	$\lambda = 0.56$	0.68
Plain concrete (for f_r)	$\alpha = 0.68$	$\beta = 0.71$
Igneous rocks (*9*)	0.53	0.70
Metamorphic rocks (*9*)	0.00082	1.60
Sedimentary rocks (*9*)	0.22	0.75
Ceramics (*9*)	1.0	0.73
Mortar (*10*)	0.61	0.67

PROPOSED EXPRESSION FOR SPLIT TENSILE STRENGTH

On the basis of experimental results obtained by Shah and Ahmad (*5*), Salami (*6*), and Salami and Desai (*7*) and Equation 9, the split tensile strength of concrete is given as follows:

$$f_{sp}' = -\lambda P_a\left(\frac{f_c'}{P_a}\right)^n \qquad \text{(compression positive)} \qquad (10)$$

where λ and n are dimensionless numbers (for plain concrete $\lambda = 0.56$ and $n = 0.68$) and P_a is atmospheric pressure in the same units as those of f_t and f_c'. The proposed equation is shown in Figure 1. It is evident from the figure that the prediction from the proposed model compares well with experimental results and the model proposed by Bortolotti (*4*), which is also shown in Figure 1.

PROPOSED BEAM FLEXURAL TENSILE STRENGTH

Based on experimental results obtained by Shah and Ahmad (*5*), Salami (*6*), and Salami and Desai (*7*) and Equation 9 the flexural tensile strength is given as follows:

$$f_r = \alpha P_a\left(\frac{f_c'}{P_a}\right)^\beta \qquad \text{(compression positive)} \qquad (11)$$

where α and β are dimensionless numbers (for plain concrete $\alpha = 0.69$ and $\beta = 0.68$) and P_a is atmospheric pressure in the same units as f_t and f_c'. The proposed equation is shown to afford a satisfactory fit of the experimental data plotted in

Figure 2. In addition, the proposed model compares well with the model proposed by Bortolotti (*4*), which is also shown in Figure 2.

CONCLUSION

For the purpose of including reasonable values of tensile strengths in the available failure criterion (for frictional materials with effective cohesion), it may be necessary to include the uniaxial tensile strength in the parameter determination. Simple expressions for evaluation of the uniaxial tensile strengths on the basis of the uniaxial compressive strength are given.

Uniaxial compressive and tensile tests were performed on plain concrete. The purpose of these tests was to acquire some understanding of the strength behavior of plain concrete subjected to compressive and tensile load histories, and the results of these tests were used to calibrate the proposed tensile strength model for predicting the tensile strength of plain concrete on the basis of experimental uniaxial compressive loading.

The proposed model has two material constants. Laboratory tests were performed to determine them. The proposed model predictions are shown in Figures 1 and 2. The correlation between the experimental results and analytical predictions are good and provide a simple approach for developing tensile strength models for plain concrete.

ACKNOWLEDGMENT

The author gratefully appreciates the support of the Department of Civil Engineering at North Carolina A&T State University. This research was funded in part by the North Carolina Board of Science and Technology and the National Science Foundation.

NOTATION

The following symbols are used in this paper:

f'_c = uniaxial cylindrical compressive strength,
f_c = uniaxial cubical compressive strength,
f_t = direct uniaxial tensile strength,
f'_{sp} = split cylinder tensile strength,
f_r = beam flexural tensile strength,
m, n = dimensionless constants,
P_a = atmospheric pressure,
λ = dimensionless constant, and
α, β = dimensionless constants.

REFERENCES

1. J. K. Mitchell. The Properties of Cement-Stabilized Soils. *Proc., Workshop on Materials and Methods for Low Cost Road, Rail and Reclamation Works,* Leura, Australia, Sept. 1976, pp. 365–404.
2. D. J. Hannant. Nomograms for the Failure of Plain Concrete Subjected to Short-Term Multiaxial Stresses. *The Structural Engineer,* Vol. 52, No. 5, May 1974, pp. 151–165.
3. L. Bortolotti. Double-Punch Test for Tensile and Compressive Strength in Concrete. *ACI Materials Journal,* Vol. 85, No. 1, Jan.–Feb. 1988, p. 26.
4. L. Bortolotti. Interdependence of Concrete Strength Parameters. *ACI Materials Journals,* Vol. 87, No. 1, Jan.–Feb. 1990, pp. 25–26.
5. S. P. Shah and S. H. Ahmad. Structural Properties of High Strength Concrete and Its Implications for Precast Prestressed Concrete. *Journal Prestressed Concrete Institute,* Vol. 30, No. 6, Nov.–Dec. 1985, pp. 92–119.
6. M. Reza Salami. Constitutive Modelling of Concrete and Rocks Under Multiaxial Compressive Loading. Ph.D. dissertation. University of Arizona, Tucson, June 1986.
7. M. Reza Salami and C. S. Desai. A Constitutive Model for Plain Concrete. *Proc., Second International Conference on Constitutive Laws for Engineering Materials: Theory and Application,* Vol. I, Tucson, Ariz., Jan. 5–8, 1987, pp. 447–455.
8. D. E. Egging. Constitutive Relations of Randomly Oriented Steel Fiber Reinforced Concrete Under Multiaxial Compression Loadings. M. S. thesis. University of Colorado, 1982.
9. P. V. Lade. Three-Parameter Failure Criterion for Concrete. *Journal of the Engineering Mechanics Division,* ASCE, Vol. 108, No. EM5, Proc. Paper 17383, Oct. 1982.
10. J. Wasliels. Behavior of Concrete Under Multiaxial Stresses, A Review. *Cement and Concrete Research,* Vol. 9, 1979, pp. 35–44.

Publication of this paper sponsored by Committee on Mechanical Properties of Concrete.

History of the Rapid Chloride Permeability Test

DAVID WHITING AND TERRY M. MITCHELL

Corrosion of reinforcing steel is recognized as the predominant cause of bridge deck deterioration. The need for a more precise method to estimate the susceptibility of a bridge to corrosion led to the development of the rapid chloride permeability test (AASHTO T 277-89 and ASTM C 1202-91). The developers of the test describe its conception, development, and applications. Concepts of permeability as applied to concrete are discussed, and the need for a rapid measure of chloride ion penetration into concrete is addressed. The authors describe the development and testing of a field method based on forcing chloride ions to migrate toward reinforcing steel maintained at a positive potential and note its limitations. Concurrent development of a laboratory procedure based on similar principles is described, and results of a round-robin statistical evaluation of method precision are presented. Further evaluations, current applications, and limitations are also discussed.

In the mid-1970s FHWA began to publish a series of comprehensive reports (*1–3*) dealing with factors involved in corrosion of reinforcing steel in concrete. Corrosion of reinforcing steel had been recognized as the predominant cause of premature bridge deck deterioration, as demonstrated by field investigations carried out at a number of agencies in the 1960s (*4,5*). The FHWA reports related the onset of corrosion to the presence of chloride ions that penetrated through the concrete cover after deicing agents were applied to the bridge surface. Other factors, such as moisture content and oxygen, were also needed to support corrosion once initiated. Finally, because the chloride ions had to penetrate through the concrete in order to reach the reinforcing steel, the permeability of the concrete cover became a determining factor in the time-to-corrosion of the reinforcement.

Recognizing that the ability to measure a number of these factors in actual structures would allow a more precise estimate of the susceptibility of a given bridge deck to corrosion, FHWA supported a series of contracts designed to develop field instruments capable of measuring these parameters. Devices to measure in situ chloride (*6*) and moisture content (*7*) were developed. A method to rapidly (and nondestructively) measure the permeability of bridge deck concrete to chloride ions was also needed, and in 1977 FHWA let a contract with Construction Technology Laboratories of Skokie, Illinois, to develop such a device. (Note: Some individuals believe the term "permeability" is not appropriate when referring to the mechanism for chloride ion movement, but instead speak of concrete's "lack of resistance to chloride ion penetration." Because the dictionary defines "permeability" as "the quality of being able to be diffused through or penetrated," the authors believe the use of that term in this context is correct.) The development of the field device and subsequent widespread use of a laboratory method based on the same principles is the subject of this paper.

D. Whiting, Construction Technology Laboratories, Inc., 5420 Old Orchard Road, Skokie, Ill. 60077-1030. T. M. Mitchell, Federal Highway Administration, HNR-30, 6300 Georgetown Pike, McLean, Va. 22101.

ORIGINS OF THE TEST METHOD

Literature Review

Considerable work in the area of concrete permeability had already been carried out at the time this research was initiated. A comprehensive literature review was conducted; much of the same material is covered in a more recent review by Collins et al. (*8*). These reviews indicate that most of the early work in permeability of concrete dealt with flow of bulk water through concrete under relatively high pressure heads, as such data were needed in design of concrete mixtures for hydroelectric and flood control projects. Classic papers in this field include those by Ruettgers et al. (*9*) and Cook (*10*). These and other studies demonstrated that the permeability of concrete could vary by as much as two orders of magnitude as the water to cement ratio (w/c) increases from 0.4 to more than 0.7.

The steady-state flow of water under a hydraulic gradient, as measured in the early studies, was deemed to be not relevant to the bridge deck situation. What was of interest was the penetration of chloride ions (derived primarily from sodium chloride deicing agents) to the vicinity of the steel. Except for the near-surface region of the concrete, where capillary forces (*11*) may be active under drying conditions, the predominant mechanism for transport of chloride ions in crack-free concrete is by ionic diffusion through the water-filled pore system. Studies by Clear (*1–3*), Monfore and Ost (*12*), Collepardi et al. (*13*), Berman and Chaiken (*14*), and Kondo et al. (*15*) have demonstrated this mechanism and again verified the influence of w/c on the rate of chloride diffusion.

These measurements, however, involved either long-term ponding with chloride solutions and subsequent measurement of chloride concentration with depth or direct measurement of diffusion using classical diffusion cell techniques (*16*), both inappropriate to rapid field testing. This is not to say that the subject of field testing of concrete permeability had been totally ignored before 1977. By the early 1970s, for example, Levitt (*17*) and Figg (*18*) had developed devices that indicate the relative permeability of concrete to water or air. However, it was not at all certain whether such techniques would cor-

relate with diffusion of chloride ions into concrete, which was the primary concern of FHWA. Highest priority was given to developing a method based on measurement of chloride ion penetration, as this would also serve as a direct field demonstration that low-permeability concretes under development at that time (*19–21*) could indeed retard the penetration of chlorides into bridge deck surfaces.

Genesis of the Method

A special case of diffusion occurs when an electric potential is applied across an electrolytic solution, free or contained within a porous material. The ions will then be transported toward the electrodes of the opposing sign (*22*). Ionic mobility is given by the following expression:

$$\mu = \frac{x}{t(dE/dx)} \tag{1}$$

where

μ = ionic mobility ($cm^2/V \cdot s$),
x = distance (cm),
t = time (sec), and
dE/dx = electric field strength (V/cm).

Using these principles, studies carried out in the mid-1970s (*23,24*) indicated that chloride could be extracted from a concrete slab quite rapidly by applying an external electric field between the concrete slab surface and the reinforcing steel.

It was reasoned that this technique could be used as a chloride permeability method if the polarity were reversed, that is, if the reinforcing steel were made anodic (positively charged); chloride ions, having a negative charge, would migrate into the concrete when the voltage was applied. After a suitable period of treatment, samples could be taken to verify the ingress of chloride by subsequent wet chemical analysis. This approach was called the applied voltage concept. A few preliminary experiments using thin membranes composed of cement pastes, aggregate materials, and mortars indicated that the concept was sound, and chloride ions could be forced to migrate through these materials in reasonably short periods of time. Furthermore, results were generally comparable to longer term experiments on the same materials that involved diffusion under conditions under which no voltage was applied across the membranes. (Note: Measuring how easily chloride ions can be forced to move through mortars or concretes electrically is not directly measuring chloride permeability; that such measurements correlate with the results of long term diffusion experiments means, however, that applied voltage methods can be regarded as indirect methods of measuring chloride permeability.) Experiments on concrete were then planned.

TEST METHOD DEVELOPMENT

Optimization of Test Parameters

The first task undertaken was optimization of the various test parameters (area of measurement, time of measurement, voltage level) within the context of a rapid and practical field method.

A drawing of the apparatus used in the preliminary studies is shown in Figure 1. A dc power supply applied a constant voltage between the copper screen and steel reinforcing mat.

Conventional reinforced concrete slabs were prepared at both high and low w/c ratios (0.35 and 0.60). Testing was conducted at voltages from 10 to 120 Vdc and over periods of time from 1 to 8 hr. Parameters evaluated included currents generated during the test, chloride content of the concrete slabs at various depths [up to 2 in. (50 mm)] after test, chloride content of the solution after test, and temperatures generated inside the slabs during test. The following conclusions were reached:

1. A test period of 6 hr at 80.0 Vdc offered the optimum test condition for distinguishing between concretes having high and low chloride permeabilities.
2. Up to 2.6 amperes of current was passed through a highly permeable concrete slab during the test period, compared with 1.8 amperes for a low-permeability slab.
3. After 6 hr of testing at 80.0 Vdc, approximately half as much chloride ion was detected ¾ in. (19 mm) below the surface of the low-permeability slab as was detected at the same depth in the high-permeability slab.
4. Whereas chloride concentration of the surface solution after testing could be measured in the laboratory, accurate field techniques did not exist at that time. Therefore, use of the change in concentration of the surface solution as a measure of permeability was abandoned.
5. Temperature rise in the slabs during testing was significant, being greatest for the high-permeability concrete. However, in full-scale bridge decks this was not expected to present a problem because of the much larger heat sink, as compared with small laboratory specimens.

Application to Other Concretes

The promising initial results led to an expanded test program on a variety of concrete slabs. These slabs were prepared by FHWA laboratories from a number of concrete types. Slabs were tested in three different states, as-received (after conventional curing for each type of concrete, e.g., 14 days with moist burlap covering for ordinary portland cement concrete),

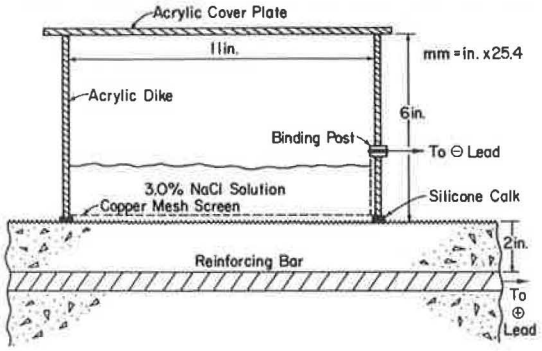

FIGURE 1 Apparatus used in preliminary studies.

after approximately 3 months of moist storage, and after 2 weeks of forced-air drying at 130°F (54°C). The test protocol throughout this phase consisted of a 6-hr application of 80.0 Vdc between a 3 percent sodium chloride solution ponded on top of the slab and a mat of reinforcing bars located 2 in. (50 mm) below the slab surface.

Representative examples of the behavior of current flowing through the slabs during the test period are shown in Figure 2. In the highest permeability concrete tested (w/c = 0.6), a peak occurred in the plot of current versus time, whereas for the other concretes current increased continuously with time. The magnitude of the current flow was generally proportional to the expected relative permeabilities of the various concretes.

The plots of current versus time were also integrated to obtain the total electric charge (in coulombs) passing through the slabs during the test period. In addition, after chloride analyses were obtained at ¼-in. (6-mm) depth increments after each test, the plots of chloride content versus depth were integrated to obtain an estimate of total integral slab chloride content. Results for the as-received slabs after testing are presented in Table 1. The various concretes were placed into four convenient major groups. The first, conventional concretes, exhibits relatively high total chloride levels and charge passed. In the next group, which encompasses latex-modified and Iowa concretes, values of total chloride and charge passed are about 20 to 30 percent lower than the best of the conventional concretes. The third group, internally sealed concretes, showed a dramatic drop in both parameters. (Internally sealed concrete was an experimental material developed in the 1970s made by mixing small, discrete wax particles into conventional portland cement concrete mixtures. After curing, the concrete was heated and the wax melted and flowed into the capillaries and bleed channels; when the heat source was removed, the wax cooled and produced a low-permeability concrete.) Note that when internally sealed concrete was not heat treated, its permeability was the same as conventional concretes. The final group, polymer-impregnated and polymer concrete, shows negligible permeability to chlorides.

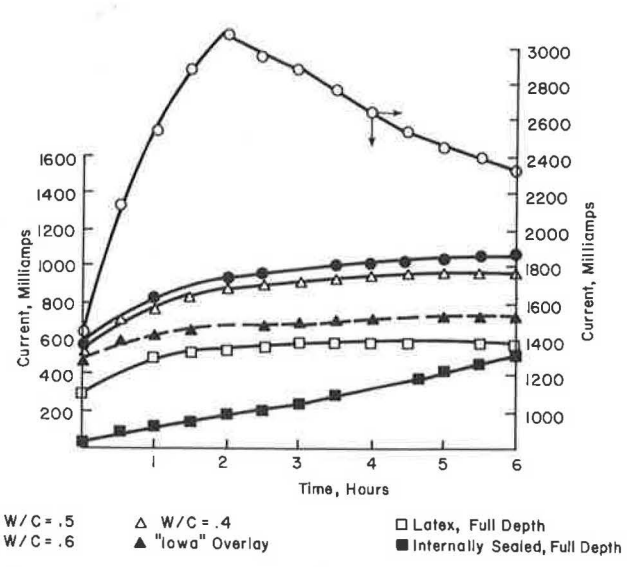

FIGURE 2 Current flow versus time through FHWA slabs.

TABLE 1 PERMEABILITY CHARACTERIZATION PARAMETERS

Description	Total Integral Chloride	Total Charge Passed (Coulombs)	Chloride Permeability
w/c = 0.60	0.77	52,570	High
w/c = 0.50	0.56	39,380	High
w/c = 0.40	0.37	20,410	High
Latex - Overlay	0.37	16,950	Moderate
Latex - Full Depth	0.27	8,670	Moderate
Iowa - Overlay	0.31	15,270	Moderate
Internally Sealed - Full Depth - Heated[a]	0.10	5,770	Low
Internally Sealed - Full Depth - Unheated	0.93	36,070	High
Internally Sealed - Overlay - Heated[a]	0.09	3,020	Low
Internally Sealed - Overlay - Unheated	0.47	22,418	High
Polymer Impregnated	--	0	Very Low
Polymer Concrete Overlay[b]	--	0	Very Low

[a]Slabs tested in moist condition only.
[b]Slabs not sampled for chloride.

Correlation with 90-Day Ponding Results

In the late 1970s, the most commonly used procedure for determining chloride permeability of concrete was that specified in AASHTO T 259, Resistance of Concrete to Chloride Ion Penetration. In T 259, concrete samples are ponded with a 3 percent sodium chloride solution for 90 days, after which the chloride content of the concrete at various levels in the sample is established by wet chemical analysis. This ponding procedure was applied to companion specimens prepared along with specimens used in the evaluation of the applied voltage test. Correlation analyses (using linear regression techniques) were performed between the data in the second and third columns of Table 1 and the results of 90-day ponding tests.

The correlations indicated that the closest relationship was between the charge passed (coulombs) in the rapid test and the total integral chloride in the 90-day test. A correlation coefficient of 0.92 was calculated. Data obtained on the moist-cured specimens were also encouraging. However, when the applied voltage technique was tested on a set of slabs subjected to forced air-drying for 2 weeks at 130°F (54°C), serious problems were encountered. The values of charged passed and total chloride were much lower than those recorded on companion slabs tested in the as-received or moist conditions. It was obvious that the drying reduced the moisture content of the concrete to such an extent that the amount of current that could be passed through the slabs was limited by the high electrical resistance caused by the drying. Therefore, a method for preconditioning the test area to a moisture content close to that of the original concrete was needed.

To develop preconditioning procedures, the test apparatus was modified to enable a vacuum of −25.5 in Hg (15.0 kPa absolute pressure) to be drawn over the surface of the slab by use of a vacuum chamber sealed to the slab surface by silicone-based caulk. Various resaturation schemes were evaluated, and the following approach was found to be most effective.

1. A vacuum is maintained over the test area for 60 min. Limewater is then introduced into the chamber, and the vacuum is maintained for another 60 min.

2. The vacuum is broken, and the limewater is heated and held at 140°F (60°C) for approximately 18 hr.
3. The limewater is removed, the 3 percent sodium chloride solution is poured into the chamber, and the applied voltage test is conducted as previously described.

This procedure was incorporated into the design of the prototype and was used in all succeeding work.

Development of Field Prototype

Many workers who routinely use the AASHTO T 277 laboratory technique are not aware that a field version of the procedure was developed and tested more than 10 years ago. This device incorporated the features of the laboratory components into a single package. The field instrumentation consisted of three separate modules, one to vacuum saturate the concrete before test, the second to apply the voltage to the salt solution on the concrete surface, and the third (the electronics package) to provide the voltage source and accumulate the data. A detailed description of the instrumentation can be found in a report by Whiting (*25*).

The field test procedure can be conveniently separated into four stages:

1. Location of reinforcing steel and bonding of test dike,
2. Vacuum saturation and heating of test area,
3. Applied voltage test, and
4. Optional chloride sampling.

Each test takes 2 full work days; if two dikes are used, four tests can be completed in 1 work week (modifying the electronics package could further increase productivity by allowing two or more tests to be conducted at the same time). Stage 2 requires overnight operations; however, the unit may be left unattended during this period.

Before proceeding to actual field testing, the prototype was tested on slabs intermediate in size between the small specimens tested in the initial phases of the project and full-scale bridge decks. This allowed evaluation using a more realistic heat sink and also allowed the evaluation of a number of variables within a single slab. Variables studied in detail were the following:

1. Concrete cover,
2. Ambient test temperature,
3. Geometry of reinforcing cages, and
4. Presence of chloride in concrete before test.

Results of these tests indicated that (a) deviations of ± 1 in. (25 mm) in concrete cover from the nominal 2-in. (50-mm) test cover caused deviations of ± 25 percent in charge passed; (b) reinforcing bar size and cage geometry had no significant effect on charge passed; (c) charge passed increased with an increase in initial slab temperature; and (d) initial slab chloride contents of up to 5 lb/yd^3 (3 kg/m^3) had little effect on charge passed.

Field testing was carried out on a conventional concrete bridge deck (just constructed) and on an older deck that had recently been overlaid with dense low-slump concrete (*26*). Results on the conventional deck fell within the ranges to be expected from a bridge deck concrete with w/c between 0.4 and 0.5, but interpretation of test results on the overlay was complicated by varying relative thicknesses of overlay and substrate at the different test locations.

In addition, the presence of chlorides in the aggregates appeared to interfere with the chloride analysis and subsequent calculation of integral chloride values. Finally, a series of four in situ tests required that one lane of traffic be closed continuously for 5 days. This is quite expensive when traffic control requirements are considered. Although workable, the field test appeared to need further development, and, in any case, was somewhat impractical in terms of operation on in-service structures. As an alternative, a laboratory test, described in subsequent sections, was developed.

ADOPTION OF A LABORATORY TEST PROCEDURE

Description of the Laboratory Method

In view of the limitations on the field device, a laboratory version of the apparatus was developed. It should be noted that the laboratory test was developed originally as an alternative to the field test, to be used in those instances when it was not practical to employ the in situ device. It was not viewed as an accurate, standard laboratory test to determine the absolute permeability of a given concrete; the objective of the original research project had simply been to develop a rugged, in situ indicator of permeability. Because the laboratory test was viewed as a fallback, it was not developed and tested nearly as thoroughly as the field method, and no systematic investigations were carried out of the many variables that might influence the test.

The new device was called the applied voltage cell and is shown in Figure 3. The cell is machined out of solid acrylic plastic (e.g., polymethylmethacrylate) and allows for two reservoirs of approximately 200 mL capacity to be fitted onto either face of a 4-in. (102-mm) diameter core by use of a rapid-setting silicone compound. One reservoir is filled with 0.3 M NaOH, the other with 3.0 percent NaCl. The core specimen [usually 2 in. (51 mm) thick] is coated on its periphery with epoxy and vacuum saturated for 18 hr before test. The core is then sealed between the cell halves, the reservoirs are filled, and the specimen subjected to an applied voltage of 60.0 Vdc for 6 hr. Current is monitored during the 6-hr period, and, as in the field test, the integral of current over time yields a value of charge passed (in coulombs) during the test.

The lab procedure was applied to cores taken from the same set of slabs used in development of the field device. In addition to the charge passed parameter, the amount of chloride ion present in the positively charged half of the cell, representing the chloride that had passed entirely through the sample during the test period, was also measured. Attempts were also made to construct chloride profiles by obtaining thin slices from the cores after the test was completed; however, this process was tedious and not appropriate for inclusion in a rapid test procedure.

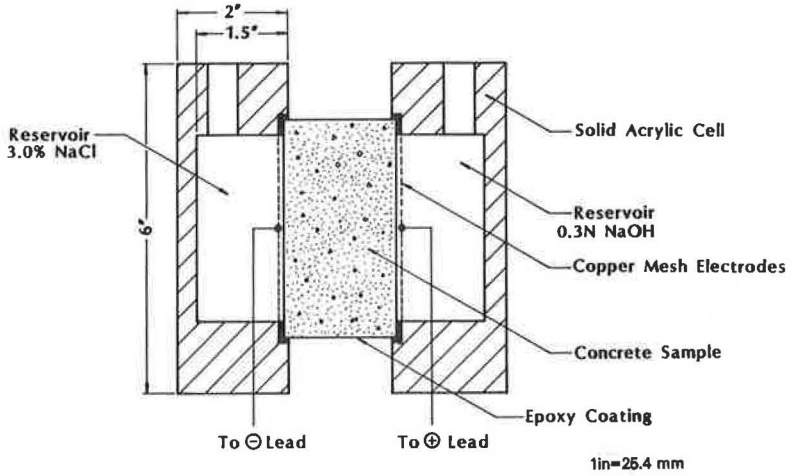

FIGURE 3 Schematic drawing of applied voltage cell.

As had been done for the slab tests, correlation analyses were run between charge passed through the cores and the results of 90-day chloride ponding on companion slabs. The correlation coefficient for the charge passed through cores compared with the integral chloride contents of the companion slabs was 0.83. This was somewhat less than the correlation coefficient for the charge passed through slabs versus integral chloride content, which was 0.92. The difference was perhaps due to the limited surface area included in the core test, as opposed to the approximately 1 ft^2 (0.09 m^2) of surface included in the slab tests. This indicated that multiple samples would need to be tested in order to obtain a more representative test area. The coefficients of variation for 6-sample groups prepared from batches of high w/c (0.6) and latex-modified concretes were each approximately 6 percent.

Standardization of the Laboratory Method

In 1982, researchers presented the laboratory method to AASHTO for consideration as a standard test method. The method had come to be referred to as the rapid chloride permeability test (RCPT), or the coulomb test, and was immediately adopted by AASHTO and given the designation T 277-83, Rapid Determination of the Chloride Permeability of Concrete. The method presented for standardization and adopted was essentially the material contained in Appendix 1 of the original FHWA report (*25*).

This version of the test method included a table to interpret the results; it is presented here as Table 2. In the AASHTO version, only the charge passed (in coulombs) is used as an indicator of permeability. Many users of the method believe that these values represent a large data base of concrete tests and are typical of what to expect in testing concretes of the types described. In fact, the table was constructed from results obtained on single cores of each concrete type, taken from the slabs originally supplied by the FHWA. As a further caution, in Appendix 1 of the FHWA report, the following advice is given: "The effect of such variables as aggregate type and size, cement content and composition, density, and other factors have not been evaluated. We recommend that persons using this procedure prepare a set of concretes from local materials and use these to establish their own correlation between charge passed and known chloride permeability for their own particular materials. The values given in Table I [Table 2 in this paper] may be used as estimates until more data has been developed by a number of agencies on a wider range of concretes." Although further testing of some of these variables has since been carried out, it has been limited, and the values in Table 2 still must be applied with extreme caution. The concretes listed in the third column were intended to serve as examples of concretes that might typically give the coulomb values in the first column. Because of the many other factors that may affect chloride permeability, this simple correspondence does not always hold true.

In late 1991 the laboratory method was also adopted by ASTM, as C 1202, Standard Test Method for Electrical Indication of Concrete's Ability to Resist Chloride Ion Penetration. Although some differences exist between the ASTM and AASHTO versions, none are significant; the basic test procedures are identical.

One important feature of both standard versions of the test method is the precision statements, which were developed from an interlaboratory study carried out in late 1985. A total of 11 laboratories participated in this round-robin study to develop values for within- and between-laboratory precision.

TABLE 2 CHLORIDE PERMEABILITY BASED ON CHARGE PASSED

Charge Passed[a] (Coulombs)	Chloride Permeability	Typical of
> 4,000	High	High water-cement ratio, conventional (≥ 0.6) PCC
2,000 - 4,000	Moderate	Moderate water-cement ratio, conventional (0.4-0.5) PCC
1,000 - 2,000	Low	Low water-cement ratio, conventional (< 0.4) PCC
100 - 1,000	Very Low	Latex-modified concrete Internally sealed concrete
< 100	Negligible	Polymer impregnated concrete Polymer concrete

[a]Coefficients of variation for replicate specimens from a single batch were approximately 6 percent.

Two conventional and two latex-modified concrete mixtures were included, and each laboratory tested triplicate specimens from each mixture. Detailed results can be found in publications by Mobasher and Mitchell (*27,28*). The following are the precision statements that were developed and are now part of both standards:

- Single-operator precision: The single-operator coefficient of variation of a single test result was found to be 12.3 percent. Therefore, the results of two properly conducted tests by the same operator on the same material should not differ by more than 35 percent.
- Multilaboratory precision: The multilaboratory coefficient of variation of a single test result was found to be 18.0 percent. Therefore, results of two properly conducted tests in different laboratories on the same material should not differ by more than 51 percent. The averages of three test results in two different laboratories should not differ by more than 29 percent.

These precision estimates (especially that for single-operator essentially a measure of within-test precision) seem somewhat high when compared with other tests that are more commonly used to assess quality characteristics of concrete. For instance ACI 214 (*29*) categorizes within-test coefficients of variation for field control testing as poor if they exceed 6.0 percent. Mobasher and Mitchell (*27*) suggest the variabilities from the round-robin may have been higher than they should have been because laboratories deviated from details of the AASHTO T 277 procedure and from the round-robin instructions. Several of the laboratories were relatively new users of the method and apparently did not recognize the importance of some aspects of the test.

Although Hooton (*30*) notes that permeability of concrete is, in general, a more variable quantity than strength, there is reason to believe that significant improvements can be made in the precision of the test. Because the test is now an ASTM standard, laboratories will presumably more closely follow the detailed ASTM version of the method. Between-laboratory variations would likely be reduced if the method were added to the list of those inspected by laboratory evaluators such as the Cement and Concrete Reference Laboratory during their periodic tours. Finally, after researchers evaluate the ruggedness of various test parameters and make additional refinements in the procedure, improved precision would be expected and another interlaboratory study might be appropriate.

Current and Future Applications of the Method

Since its adoption by AASHTO as an interim test method in 1983, the RCPT has come into increasing use in the areas of concrete materials research, development and testing of concrete mixtures, and acceptance of job-site concrete. The technique apparently gives users the ability to measure a property of concrete that heretofore has been relatively difficult and time-consuming to determine. The availability of commercial instrumentation designed specifically to conduct AASHTO T 277 or ASTM C 1202 now makes it possible for almost any test lab to obtain a permeability value. A word of caution is advised, however, because the quantity measured by the RCPT is not permeability in the strictest sense, but is instead an indication of permeability based on the ability of a given concrete specimen to conduct electric current. Any materials that cause concrete to be more (or less) conductive will increase (or decrease) the value obtained using the RCPT, irrespective of the effects that such materials or treatments have on actual permeability, diffusion, or other mass transport phenomena.

In spite of these limitations, the utility of the RCPT for gaining an understanding of the effects of materials and treatments on concrete permeability has been demonstrated by the large numbers of studies where it has been successfully used. The reader is referred to its use in studies of concrete consolidation (*31*), of the effects of aggregates (*28*) and cements and pozzolans (*32,33*) on permeability, and of specialty concretes (*34–36*) and coatings and sealers (*37,38*). In these and most other studies the RCPT has been the sole method used for determination of permeability to chloride ions, other techniques being too costly or time-consuming. However, in those instances in which other measures of permeability have been used, agreement with the RCPT has generally been quite good.

Were it not for two developments, the RCPT might still be a laboratory curiosity limited to occasional research studies. The first of these, its standardization by AASHTO, has already been noted. A number of state highway agencies began to use the test immediately, especially for product and mixture design evaluation. The second development that has lead to widespread use of the method is the large growth in the use of silica fume as a concrete admixture in the mid- to late 1980s. Holland (*39*) noted that more than 350,000 yd^3 (270,000 m^3) of silica fume concrete was placed in 1986 alone, and its use is expected to increase annually. Its primary application is for reducing permeability of concrete to chloride ions in such structures as bridge decks and parking garage slabs. Although the RCPT is an indirect method, Luther (*40*) noted that since 1986 it has increasingly been specified for use in parking garage slab placements and on shotcrete repair jobs. In many cases, an arbitrarily chosen value of charge passed (in coulombs) is selected as the maximum design value, usually between 700 and 1,000 coulombs. Trial mixtures are usually tested to see if this limit can be met. On the actual job, samples are obtained either in the form of cast cylinders or as cores taken from the cured slabs. Testing is carried out at various ages, from 28 to 90 days, with a 42 days apparently the most common. Accelerated curing, using techniques similar to ASTM C 684-89, Standard Test Method for Making, Accelerated Curing, and Testing Concrete Compressive Test Specimens—Procedure B—Boiling Water Method has been used. Acceptance is based on the average value of charge passed being less than the specified limit. Statistically based acceptance schemes are nonexistent. In the authors' opinion, further work on definition of acceptable limits, development of statistical acceptance schemes, and improvement in the precision of the test must be done before this technique can be equitably applied to acceptance of silica-fume and other types of concrete. Users must also recognize that chloride permeability depends not only on the mix design and the component materials, but also on such aspects of construction as degree of consolidation and type and extent of curing.

SUMMARY

In the late 1970s, in response to the needs of the highway engineering community, a method was developed that afforded an in situ indication of the chloride permeability of reinforced portland cement concrete bridge structures. Although results obtained via this method correlated well with long-term ponding of chloride solutions, practical considerations made it more pragmatic to obtain cores from the structure of interest and test these cores using a laboratory version of the method. This laboratory version was standardized by AASHTO in the early 1980s, and with the increasing use of silica fume in the latter half of the decade has been increasingly applied to design, testing, and acceptance of such mixtures. Comparison studies have shown the test method, at least in its original version, to be less precise than methods generally used in acceptance of concrete, such as compressive strength. Although the method is adequate for research and materials development purposes, further standardization and development of statistically based decision schemes are needed before the technique can be equitably applied as an acceptance tool.

ACKNOWLEDGMENTS

Over the years, many people have contributed to the initial conception, development, standardization, and application of the method discussed here. Many are recognized as sources of reference for this paper. Others involved in the initial development include William F. Perenchio, who codeveloped the initial concept; Robert Carver, who designed and assembled the electronic instrumentation package; and Kenneth C. Clear, who assisted in many technical aspects of the FHWA effort. The authors also acknowledge the many insights gained by the users of the method, and especially would like to thank Mark Luther and Neal Berke for their constructive criticisms based on their opportunities to apply the method in a variety of circumstances.

REFERENCES

1. K. C. Clear and R. E. Hay. *Time-to-Corrosion of Reinforcing Steel in Concrete Slabs, Vol. 1, Effect of Mix Design and Construction Practices.* FHWA-RD-73-32. FHWA, U.S. Department of Transportation, April 1973.
2. K. C. Clear and R. E. Hay. *Time-to-Corrosion of Reinforcing Steel in Concrete Slabs, Vol. 2, Electrical Potential Data.* FHWA-RD-73-33. FHWA, U.S. Department of Transportation, April 1973.
3. K. C. Clear. *Time-to-Corrosion of Reinforcing Steel in Concrete Slabs, Vol. 3, Performance after 830 Daily Salt Applications.* FHWA-RD-76-70. FHWA, U.S. Department of Transportation, April 1976.
4. *Durability of Concrete Bridge Decks—A Cooperative Study, Final Report.* Report EB-67.01E. Portland Cement Association, Skokie, Illinois, 1970.
5. D. L. Spellman and R. F. Stratfull. Chlorides and Bridge Deck Deterioration. In *Highway Research Record 328,* HRB, National Research Council, Washington, D.C., 1970, pp. 38–49.
6. J. R. Rhodes, J. A. Stout, R. D. Sieberg, and J. S. Schindler. *In Situ Determination of the Chloride Content of Portland Cement Concrete Bridge Decks.* FHWA/RD-80/030. FHWA, U.S. Department of Transportation, 1980.
7. G. A. Matzkanin, A. DeLos Santos, and D. A. Whiting. *Determination of Oxygen and Moisture Levels in Structural Concrete.* FHWA-FH-11-9487. FHWA, U.S. Department of Transportation, 1981.
8. J. F. Collins, K. N. Derucher, and G. P. Karfiatis. Permeability of Concrete Mixtures, Part I: Literature Review. *Civil Engineering for Practicing and Design Engineers,* Vol. 5, 1986, pp. 579–638.
9. A. Ruettgers, E. N. Vidal, and S. P. Wing. An Investigation of the Permeability of Mass Concrete with Particular Reference to Boulder Dam. *Proc., American Concrete Institute,* Vol. 31, 1935, pp. 382–416.
10. M. K. Cook. Permeability Tests of Lean Mass Concrete. *Proc., ASTM,* Vol. 51, 1951, p. 1,156.
11. E. N. Washburn. The Dynamics of Capillary Flow. *Physical Review,* Series 2, 17, 1921, pp. 273–283.
12. G. E. Monfore and B. Ost. Penetration of Chloride into Concrete. *Journal of the PCA Research and Development Laboratories,* Vol. 8, No. 1, Jan. 1966, pp. 46–52.
13. M. Collepardi, A. Marcialis, and R. Turriziani. The Kinetics of Penetration of Chloride Ions into Concrete. *Journal of the American Ceramic Society,* Vol. 55, No. 10, 1972, p. 534.
14. H. A. Berman and B. Chaiken. Techniques for Retarding the Penetration of Deicers into Cement Paste and Mortar. *Public Roads,* Vol. 38, No. 1, June 1974, pp. 9–18.
15. R. Kondo, M. Satake, and H. Ushiyama. Diffusion of Various Ions in Hardened Portland Cement. In *Review of the 28th General Meeting Technical Session,* The Cement Association of Japan, Tokyo, Japan, May 1974, pp. 41–43.
16. A. R. Gordon. The Diaphragm Cell Method of Measuring Diffusion. *Annals of the New York Academy of Sciences,* Vol. 46, 1945, pp. 285–308.
17. M. Levitt. The ISAT—A Non-Destructive Test for the Durability of Concrete. *British Journal of Non-Destructive Testing,* Vol. 13, No. 4, July 1971, pp. 106–112.
18. J. N. Figg. Methods of Measuring the Air and Water Permeability of Concrete. *Magazine of Concrete Research,* Vol. 25, No. 85, 1973, pp. 213–219.
19. W. C. Smoak. Surface Impregnation of New Concrete Bridge Decks. *Public Roads,* Vol. 40, No. 1, July 1976, pp. 1–6.
20. K. C. Clear and B. H. Chollar. *Styrene-Butadiene Latex Modifiers for Bridge Deck Overlay Concrete.* FHWA-RD-78-35. FHWA, U.S. Department of Transportation, April 1978.
21. G. H. Jenkins and J. M. Butler. *Internally Sealed Concrete.* FHWA-RD-75-20. FHWA, U.S. Department of Transportation, Jan. 1975.
22. F. Daniels and R. Alberty. *Physical Chemistry,* 3rd ed., Wiley, New York, N.Y., 1967, Chapter 11, p. 394.
23. J. Slater, D. Lankard, and P. J. Moreland. Electrochemical Removal of Chlorides from Concrete Bridge Decks. *Materials Performance,* Vol. 15, No. 11, 1976, pp. 21–26.
24. G. L. Morrison, Y. P. Virmani, F. W. Stratten, and W. J. Gilliland. *Chloride Removal and Monomer Impregnation of Bridge Deck Concrete by Electro-Osmosis.* FHWA-KS-RD-74-1, Kansas Department of Transportation, Topeka, 1976.
25. D. Whiting. *Rapid Determination of the Chloride Permeability of Concrete.* FHWA/RD-81/119. FHWA, U.S. Department of Transportation, 1981.
26. G. Calvert. The Iowa Method of Bridge Deck Resurfacing. *Concrete Construction,* Vol. 23, No. 6, June 1978, pp. 323–328.
27. B. Mobasher and T. Mitchell. *Precision Data for Test for Determining the Chloride Permeability of Concrete.* Report RR # C-9-1004. ASTM, Philadelphia, Pa., 1986.
28. B. Mobasher and T. Mitchell. Laboratory Experience with the Rapid Chloride Permeability Test. In *Special Publication SP-108: Permeability of Concrete* (D. Whiting and A. Walitt, eds.). American Concrete Institute, Detroit, Mich., 1988, pp. 117–144.
29. Recommended Practice for Evaluation of Strength Test Results of Concrete (ACI 214–77). In *Manual of Concrete Practice Part I,* American Concrete Institute, Detroit, Mich., 1988, pp. 214-1–214-14.
30. R. D. Hooton. Problems Inherent in Permeability Measurement. In *Advances in Cement Manufacture and Use* (E. Gartner, ed.). Engineering Foundation, New York, N.Y., 1989, pp. 143–154.
31. D. Whiting, G. W. Seegebrecht, and S. Tayabji. Effect of Degree of Consolidation on Some Important Properties of Concrete. In *Special Publication SP-96: Consolidation of Concrete* (S. Gebler,

ed.). American Concrete Institute, Detroit, Mich., 1987, pp. 125–160.
32. C. Ozyildirim and W. Halstead. Resistance to Chloride Ion Penetration of Concretes Containing Fly Ash, Silica Fume, or Slag. In *Special Publication SP-108: Permeability of Concrete* (D. Whiting and A. Walitt, eds.). American Concrete Institute, Detroit, Mich., 1988, pp. 35–61.
33. P. Plante and A. Bilodeau. Rapid Chloride Ion Permeability Test: Data on Concretes Incorporating Supplementary Cementing Materials. In *Special Publication SP-114: Fly Ash, Silica Fume, Slag, and Natural Pozzolans in Concrete* (V. M. Malhotra, ed.), Vol. 1. American Concrete Institute, Detroit, Mich., 1988, pp. 625–644.
34. D. Whiting and L. Kuhlmann. Curing and Chloride Permeability. *Concrete International—Design and Construction,* Vol. 9, No. 4, April 1987, pp. 18–21.
35. L. A. Kuhlmann and N. C. Foor. Chloride Permeability versus Air Content of Latex Modified Concrete. *Cement, Concrete, and Aggregates,* Vol. 6, No. 1, Summer 1984, pp. 11–16.
36. M. M. Sprinkel. *Comparative Evaluation of Concrete Sealers and Multiple Layer Polymer Concrete Overlays.* FHWA/VA-88/R2. FHWA, U.S. Department of Transportation; Virginia Transportation Research Council, Charlottesville, Va., Sept. 1987.
37. R. M. Rollings and B. Chojnacki. *A Laboratory Evaluation of Concrete Surface Sealants—Phase 2.* Report MI-127. Ontario Ministry of Transportation, Toronto, Canada, Nov. 1988.
38. D. Whiting. Application of the Rapid Chloride Permeability Test to Evaluation of Penetrating Sealers for Concrete. *Cement, Concrete, and Aggregates,* Vol. 9, No. 1, Summer 1987, pp. 49–51.
39. T. C. Holland. Practical Considerations for Using Silica Fume in Field Concrete. In *Transportation Research Record 1204,* TRB, National Research Council, Washington, D.C., 1988, pp. 1–7.
40. M. D. Luther. Silica Fume (Micro Silica) Effects on Concrete Permeability and Steel Corrosion. In *Recent Advances in Concrete Technology: Concrete Durability and Repair* (P. Soroushian and S. Ravanbakhsh, eds.). Michigan State University, E. Lansing, Feb. 1990, pp. 5-1–5-19.

Publication of this paper sponsored by Committee on Chemical Additions and Admixtures for Concrete.

Aspects of Concrete Strength and Durability

JAMSHID M. ARMAGHANI, TORBJORN J. LARSEN, AND DAVID C. ROMANO

Research is under way to study the strength and durability of concrete in Florida. Results of the first phase of this research are presented. Twenty-two concrete mixtures were prepared and tested for compressive strength, water permeability, chloride permeability (AASHTO T277), and corrosion resistance. Four groups of concrete mixtures that covered a wide range of materials and mixture proportions were included. Water/cementitious ratios used were 0.45, 0.38, and 0.33, corresponding to cementitious contents of 564, 658, and 752 lbs/yd^3, respectively. Different combinations of fly ash and silica fume were used. Fly ash content ranged between 10 and 50 percent by weight of the total cementitious material. Silica fume was included in proportions between 5 and 15 percent. Effects of fly ash and silica fume on strength and permeability of concrete and on corrosion of steel in concrete are discussed. Correlation is established between results of the Florida water permeability test and results of the AASHTO T277 chloride permeability test. It is also shown that concrete mixtures with equal compressive strengths do not necessarily produce equal levels of permeability, especially when fly ash and silica fume are included in the mixture. This lack of correlation continues until the strength reaches about 8,000 psi. At and beyond 8,000 psi, a well-defined trend is observed. With increased concrete strength, the permeability becomes consistently low to very low according to both AASHTO T277 and water permeability classifications. Findings from this phase of the research affirm the need to develop specifications for concrete durability based on requirements for both compressive strength and permeability of concrete.

Quality and performance of concrete have traditionally been assessed by its compressive strength. However, in marine structures, problems associated with poor durability, such as corrosion of the reinforcement, are by far more prevalent than problems related to strength. Thus when structures in aggressive environments (such as sea water) are considered, emphasis is placed not only on achieving a concrete with optimum strength but also, and more important, on ensuring a highly durable concrete. In these situations testing for and evaluating concrete durability become equally, if not more, important as testing for strength. Durability is better evaluated from permeability and strength tests than from a strength test alone. Resistance to freezing and thawing is another indication of durability. However a freeze-thaw test of concrete was not considered in this study because Florida is not concerned with freezing temperatures.

In most specifications, permeability has not been established as a requirement for concrete durability. Material specifications address the durability aspect by requiring a low water/cement ratio (w/c) and the use of pozzolanic materials and admixtures. Low w/c and the use of such pozzolanic materials as fly ash, blast-furnace slag, and silica fume are design parameters that can contribute to improved strength and long-term performance of concrete.

It is generally assumed that achieving a specified target strength in concrete would also imply a given level of durability. The problem is how to accurately evaluate and ensure an acceptable level of durability in a given mixture when its compressive strength has met the specified strength requirement. Durability is greatly influenced by concrete permeability. Many mixtures, designed with widely different materials and mixture proportions, can produce concretes with equal strength but different permeability levels. Concrete that meets only the strength requirement may fail to develop the expected durability if the permeability is high. Against this background, the Florida Department of Transportation (FDOT) has embarked on a major research effort to study strength and durability of concrete. The overall objective of this research is to develop an advanced understanding of the relationship between concrete durability and strength. The goal is to develop specifications for testing and classifying durability of concrete using test data related to aggressiveness of the environments.

Findings from the first phase of this extensive research program are presented in this paper. Work discussed here was limited to one source of Florida limestone aggregate. Different proportions of cement, fly ash, and silica fume were used in the concrete mixtures. Results of the compressive strength, permeability, and corrosion tests are correlated to assess the durability of different concrete mixtures. A water permeability classification for concrete is developed based on correlation between results of the water permeability test, developed in Florida (*1*), and of the rapid chloride permeability test (AASHTO T277).

EXPERIMENTAL PROGRAM

Materials

Type II cement was used throughout this phase of the investigation. The chemical and physical properties of the cement are shown in Tables 1 and 2, respectively. Class F fly ash and silica fume in slurry form were used primarily as partial replacements for the cement. However, in two mixtures, silica fume and fly ash were added to the cement content. The chemical composition and physical properties of fly ash are presented in Tables 1 and 2.

Florida Department of Transportation, Materials Office, P.O. Box 1029, Gainesville, Fla. 32602.

TABLE 1 CHEMICAL COMPOSITION

Constituent Percent	Type II Cement	Class F Fly Ash
Calcium Oxide (CaO)	63.23	4.71
Silicon Dioxide (SiO_2)	20.21	
Aluminum Oxide (Al_2O_3)	5.53	86.53
Ferric Oxide (Fe_2O_3)	4.32	
Magnesium Oxide (MgO)	0.62	
Sulfur Trioxide (SO_3)	2.67	1.24
Loss on Ignition	1.69	2.88
Insoluble Residue	0.33	
Alkalis ($Na_2O + 0.658K_2O$)	0.48	
Tricalcium Silicate (C_3S)	52.84	
Dicalcium Silicate (C_2S)	18.07	
Tricalcium Aluminate (C_3A)	7.34	
Tetracalcium Aluminoferrite (C_4AF)	13.16	

TABLE 2 PHYSICAL TESTS RESULTS

Test	Type II Cement	Fly Ash
Fineness -		
Blaine, m^2/kg	383	
Retained on Mesh 325, %		23.63
Soundness	0.02	0.01
Pozzolanic Activity Index @ 28 Days		84.90
Specific Gravity	3.15	2.47
Gillmore Setting Time -		
Initial Set, Minutes	120	
Final Set, Minutes	245	
Compressive Strength, psi -		
1 Day	2038	
3 Day	3188	
7 Day	4319	

1 psi = 0.0069 MPa

The coarse aggregate was crushed limestone, and the fine aggregate was silica sand. Both aggregates were obtained from sources in Florida. Table 3 presents the physical properties and gradation of the aggregates.

Mixture Proportions

Table 4 presents the concrete ingredients for the 22 mixtures batched during this study. Four primary groups are included.

TABLE 3 PROPERTIES AND GRADATION OF AGGREGATE

Property	Coarse Aggregate	Fine Aggregate
Specific Gravity, Dry	2.32	2.61
Specific Gravity, SSD	2.45	2.63
Absorption, %	5.3	0.7
Unit Weight lb/cu.ft	88	----
Fineness Modulus	7.13	2.43

Gradation Sieve	% Passing	Sieve	% Passing
1 in	100	3/8 in.	100
3/4 in	96	#4	99
1/2 in	62	#8	98
3/8 in	23	#16	85
#4	3	#30	54
#8	3	#50	19
		#100	2

1 lb/ft^3 = 16.02 kg/m^3, 1 in = 25.4 mm

Mixtures in Group A were basically designed with water cementitious ratio (w/ct) of 0.45, and cementitious content of 564 lb/yd^3. The fly ash content in this group was between 10 and 30 percent by weight of the cementitious material. Group B mixtures had w/ct of 0.38, and a cementitious content of 658 lb/yd^3. The fly ash content was similar in percentages to those in Group A. Group C included 6 mixtures. Each mixture was designed with 0.33 w/ct and contained 752 lbs/yd^3 of the cementitious material. In this group, the percent fly ash in the cementitious material ranged between 10 and 50.

In Group D mixtures, the cementitious material included both silica fume and fly ash. The silica fume was in slurry and, according to the supplier, contained an unspecified ASTM Type G high-range water-reducer (HRWR). The basic design for mixtures D1 through D6 was similar to the control mixture (C1) with respect to w/ct and the total weight of the cementitious material. The difference was the use of silica fume as part of the cementitious content. Mixtures D1, D2, and D3 used silica fume, respectively, at 5, 10, and 15 percents by weight of the total cementitious material. Mixtures D4 to D6 included 20 percent fly ash with 5, 10, and 15 percent silica fume.

The last two mixtures in this group were different from the rest. In mixtures D7 and D8, the fly ash and silica fume were additions to the cement content. This increased the total weight of the cementitious materials in a cubic yard of concrete from 752 lb to 826 lb for D7, and to 977 lb for D8. The water content was held constant at 248 lb/yd^3, similar to the water content in Group C and mixtures D1 through D6. However, because fly ash and silica fume were in addition to the cement the w/ct was reduced to 0.30 for D7 and 0.25 for D8.

It should be noted that the weight of the coarse aggregate was kept constant at 1,682 lb/yd^3 for all mixtures in this study, allowing fluctuation to occur in weight of the fine aggregate only. Also, the coarse aggregate stockpile was kept in "wet" condition up to the time of batching, using a sprinkler system operating intermittently. This was in accordance with the standard operating procedure of FDOT to account for the high absorption of the coarse aggregate (see Table 3). Adjustment to the batch weights were subsequently made based on the moisture content of the wet aggregate.

Chemical admixtures were used in all mixtures. Water reducing and retarding admixture, meeting ASTM requirements (ASTM C494) as Type D, was used in every mixture at a constant rate of 7.5 fl oz/100 lb of cement. HRWR, classified as ASTM C494 Type F, was used in some mixtures to supplement the Type D in achieving the target slump of 2 to 4 in. Rates of HRWR were between 1 and 5 fl oz/100 lb of cement. It should be noted that no air-entraining admixture was used in any of the mixtures. The size of each concrete batch was 14 ft^3. The materials were batched and mixed in a 24 ft^3 size pan mixer.

Properties of Plastic Concrete

Tests performed on plastic concrete included slump, air content (volumetric method), and unit weight. Two operators performed these test simultaneously, each using a different set of equipment for each test. Averages of the two test results for each property are presented in Table 4. A slight increase

TABLE 4 MIXTURE PROPORTIONS PER ONE CUBIC YARD OF CONCRETE

Mix name	Water To Cementitious ratio (W/CT)	Cementitious Material (lb)			Aggregate		Plastic properties		
		Cement	Fly Ash	Silica Fume	Fine (lb)	Mix Water (lb)	Slump (in)	Air (%)	Unit Wt. lb/ft³
A1	0.45	564 (100)	--	--	1398	254	2.1	3.7	141.7
A2		508 (90)	56 (10)	--	1387		3.4	3.0	141.8
A3		451 (80)	113 (20)	--	1375		3.3	2.2	142.1
A4		395 (70)	169 (30)	--	1362		3.8	2.9	142.5
B1	0.38	658 (100)	--	--	1329	250	2.3	3.0	142.7
B2		592 (90)	66 (10)	--	1316		2.6	3.1	143.2
B3		526 (80)	132 (20)	--	1300		2.6	3.0	141.7
B4		461 (70)	197 (30)	--	1287		4.5	2.8	140.8
C1	0.33	752 (100)	--	--	1257	248	4.0	3.2	141.4
C2		677 (90)	75 (10)	--	1242		2.4	2.4	143.7
C3		602 (80)	150 (20)	--	1226		3.6	2.1	143.1
C4		526 (70)	226 (30)	--	1208		2.5	2.1	144.7
C5		451 (60)	301 (40)	--	1193		1.9	2.0	142.7
C6		376 (50)	376 (50)	--	1177		2.5	2.1	142.6
D1	0.33	714 (95)	--	38 (5)	1246	248	2.5	2.7	143.6
D2		677 (90)	--	75 (10)	1232		3.5	2.2	144.5
D3		639 (85)	--	113 (15)	1221		7.5	1.8	145.2
D4		564 (75)	150 (20)	38 (5)	1213		3.4	2.2	143.4
D5		527 (70)	150 (20)	75 (10)	1200		3.6	2.2	144.7
D6		489 (65)	150 (20)	113 (15)	1188		4.0	2.2	144.1
D7	0.30	752	--	75	1170	248	3.3	1.9	144.7
D8	0.25	752	150	75	1013	248	3.3	2.3	144.6

Note: Number in parentheses is percent ratio of total cementitious material

can be observed in unit weights of Group D mixtures. This increase is probably a result of concrete densification caused by silica fume in the mixture.

Specimen Preparation and Curing

Three 6- × 12-in. concrete cylinders were prepared for each compression test. Two 4- × 8-in. cylinders were cast for each water permeability test, one of which was also used in the rapid chloride permeability test. Three 4- × 5¾-in. cylinders were prepared for each corrosion test. Each cylinder had a ½-in.-diameter reinforcing bar embedded along its central axis.

The molds were filled with two layers of concrete; each layer was consolidated using a vibrating table. Vibrating time was approximately 45 sec. After 24 hr, the molds were removed, and the specimens were placed in lime-saturated water for curing. Water curing continued until the time of testing.

TESTS AND RESULTS

Compressive Strength

Testing for compressive strength was performed according to ASTM C39. Three concrete cylinders were tested at ages 3, 7, 28, and 91 days. Neoprene pads in steel controllers were used for capping ends of the tested specimen. Compressive strength at each age was determined by averaging strength results from the three tested specimens. Test results of the compressive strengths for concrete at ages 3, 7, 28, and 91 days are presented in Table 5. Each compressive strength at 3, 7, and 91 days was also presented as a percent ratio of the 28-day strength of the same mixture. The overall average strength gains, with respect to the 28-day strength, for all mixtures at 3, 7, and 91 days were 71, 84, and 111 percent, respectively.

In Table 6 each strength value is presented as a percent ratio of the 28-day strength of Mixture C1. This manipulation

TABLE 5 COMPRESSIVE STRENGTH OF CONCRETE

Mix Name	Compressive Strength (psi)			
	Age - Days			
	3	7	28	91
A1	4380 (75)	5210 (89)	5860	6210 (106)
A2	4010 (73)	4540 (82)	5520	6240 (113)
A3	3590 (67)	4360 (81)	5370	6340 (118)
A4	3300 (64)	4290 (83)	5170	6150 (119)
B1	4350 (73)	5430 (91)	6000	6680 (112)
B2	4720 (74)	5620 (88)	6400	7070 (111)
B3	4600 (71)	5550 (85)	6500	7470 (115)
B4	4050 (70)	4770 (82)	5810	6950 (120)
C1	5350 (81)	6140 (93)	6570	7140 (109)
C2	5310 (80)	5670 (85)	6670	7410 (111)
C3	5060 (81)	5640 (90)	6250	7430 (119)
C4	4550 (72)	5360 (85)	6300	7590 (121)
C5	3830 (62)	4710 (76)	6170	6920 (112)
C6	3470 (59)	4320 (73)	5920	6700 (113)
D1	6140 (75)	7130 (87)	8180	8450 (103)
D2	6220 (73)	7580 (90)	8470	8510 (101)
D3	5600 (65)	6030 (70)	8650	9150 (106)
D4	5310 (69)	6550 (85)	7720	8100 (105)
D5	5270 (67)	6550 (83)	7870	8500 (108)
D6	4960 (62)	6740 (84)	8040	8660 (108)
D7	6850 (80)	7628 (89)	8580	8990 (105)
D8	6170 (72)	7414 (86)	8580	8880 (104)

Note: Numbers in parentheses are ratios of the 28-day strength.

1 psi = 0.0069 MPa

TABLE 6 COMPRESSIVE STRENGTH AS PERCENT OF THE 28-DAY STRENGTH OF MIXTURE C1

Mix Name	% of C1-28 Day Compressive Strength			
	3 Day	7 Day	28 Day	91 Day
A1	67	79	89	94
A2	61	69	84	95
A3	55	66	82	96
A4	50	65	79	94
B1	66	83	91	102
B2	72	86	97	108
B3	70	84	99	114
B4	62	73	88	106
C1	81	93	100	109
C2	81	86	101	113
C3	77	86	95	113
C4	69	82	96	116
C5	58	72	94	105
C6	53	66	90	102
D1	93	108	124	129
D2	95	115	129	130
D3	85	92	132	139
D4	81	100	117	123
D5	80	100	120	129
D6	76	103	122	132
D7	104	116	131	137
D8	94	113	131	135

of the data allows more direct comparison between strengths at various ages, within and among different groups.

TABLE 7 RESULTS OF WATER PERMEABILITY, RAPID CHLORIDE PERMEABILITY (AASHTO T277), AND CORROSION TESTS

Mix Name	28 Day		91 Day		Corrosion, Days To Failure
	K-H2O in/s (E-12)	K-Cl Coulombs	K-H2O in/s (E-12)	K-Cl Coulombs	
A1	8.88	6913	7.18	5712	15
A2	8.92	4971	8.69	4788	7
A3	3.64	4262	3.68	3279	11
A4	4.30	3606	3.96	1963	10
B1	6.76	5575	6.18	6943	17
B2	4.61	5524	4.77	2725	18
B3	4.83	3684	3.79	2343	25
B4	3.17	2561	2.32	1696	22
C1	4.98	5709	4.30	5999	30
C2	4.95	4860	4.21	3244	22
C3	4.24	3965	3.12	2496	35
C4	2.31	3188	2.36	971	40
C5	2.62	2458	2.35	1017	68
C6	2.30	1887	2.16	931	38
D1	1.30	1170	1.12	1238	90
D2	1.37	510	1.40	691	100
D3	1.41	668	1.13	369	120
D4	1.09	869	1.10	1053	48
D5	1.00	680	1.43	466	95
D6	1.53	319	1.22	212	120
D7	2.29	427	2.15	695	120
D8	1.02	444	1.02	446	120

Note : Test was terminated at 120 days for D3,D6,D7,& D8
K-H2O = Water permeability, K-Cl = Chloride permeability
in/s = 0.0254 m/s

Permeability

Concrete permeability was determined using two test methods. The first was the rapid chloride permeability test (AASHTO T277). This is an indirect test for permeability. It is based on chloride diffusion into a 4- × 2-in. slice of a concrete cylinder or core. A potential of 60 V is applied across the concrete specimen. The total charge (determined in coulombs) that passes through the specimen during a 6-hr period is used as the indicator of concrete permeability.

The second method was the water permeability test, which was developed at the University of Florida. The procedure for water permeability test is described elsewhere (*1*). In this test water under 100 psi pressure is forced into a 2-in.-thick specimen cut from a 4- × 8-in. cylinder or core. The amount of water flowing into the specimen is plotted against time. The average rate of flow into the specimen is obtained from the segment of the curve where flow rate is constant. Darcy's formula is then applied to determine the water permeability of concrete. Table 7 presents the permeability test results for different concrete mixtures at 28 and 91 days. The water permeability values are averages of two specimens, whereas the chloride permeability values represent single test results.

Corrosion

Resistance to corrosion was determined from Florida's Impressed Current test (*2*). The following is a summary of this test procedure. Three 4- × 5¾-in. concrete cylinders are prepared, with a 12-in.-long and ½-in.-diameter reinforcing bar embedded along the longitudinal axis at 1¾ in. from the cylinder bottom. The specimens are demolded after 24 hr, and then moist cured for 28 days. This is followed by additional 28 days of conditioning in a 5 percent NaCl solution. The test begins with the specimens partially submerged in a 5 percent NaCl solution and connected to a constant voltage rectifier. Direct current is passed from the rectifier to the specimen rebar, through the surrounding concrete and the chloride solution, into the ½-in.-diameter reinforcing bar (cathode) in the tank, and back to the rectifier. The rectifier is adjusted to maintain a 6-V direct current. The current, in milliamperes, that passes through each specimen is monitored daily. Testing continues until the specimen fails. Failure time is defined as the time when a large increase in current is measured. This is normally followed by staining and cracking of the concrete.

Average resistance to corrosion (in days) for the different concrete mixtures is presented in Table 7. The test was terminated for specimens that had not failed after 120 days to make space in the tank for new specimens.

DISCUSSION OF TEST RESULTS

Effect of Fly Ash

The rate of strength development at early ages is lower for concrete with fly ash than for similar concrete without fly ash (Table 5). Greater reduction in strength gain can be observed in mixtures with fly ash content of 40 percent (C5) and 50 percent (C6). Delay in the hydration process of fly ash at early ages is responsible for the slower growth in strength.

However, the early reduction in compressive strength is later recovered with the gradual increase in the rate of hydration of the cementitious material. At 91 days, the strength gain with respect to the 28-day strength is slightly higher for mixtures with fly ash, except for concrete with 40 and 50 percent fly ash content.

The percent difference in compressive strengths of concrete with and without fly ash can be determined from Table 6. At 3, 7, and 28 days, the strength of concrete without fly ash is greater than that of concrete with fly ash (except for Group B). For example, the difference at 3 days between C1 and C6 is 28 percent. However, this trend is reversed at 91 days. Concrete mixtures C2, C3, and C4 show strength 4 to 7 percent higher than that of C1. For mixtures C5 and C6, with 40 and 50 percent fly ash respectively, the strengths at 91 days were still 4 to 7 percent lower than the control mixture (C1). When all results of this study are considered, one can conclude that the substitution of fly ash for cement does not cause significant change in concrete strength at 28 and 91 days.

Fly ash can cause significant reduction in concrete permeability. Evidence of substantial reduction in permeability is shown in Table 7 and in Figure 1. The water permeability at 91 days was reduced by as much as 50 percent in some mixtures. As an example, with respect to Mixture C1, the reduction at 91 days in water permeability was 27 percent for Mixture C3 (with 20 percent fly ash), and 50 percent for Mixture C6 (with 50 percent fly ash).

In spite of some inconsistencies in the corrosion data, a general trend indicates good improvement in the corrosion resistance of concrete with fly ash. The most obvious improvement in corrosion resistance was observed in the fly ash concrete in Group C, as shown in Table 7. Lower w/ct and the use of higher fly ash contents contributed to lower permeability and better corrosion resistance. Results of this study show that the benefits to concrete durability from use of fly ash in concrete outweigh the slight reduction in strength.

Effect of Silica Fume

Concrete mixtures with silica fume (Group D) showed significant improvement in compressive strength, impermeability, and corrosion resistance over similar mixtures with no silica fume. The 28-day compressive strength of silica fume mixtures (D1, D2, and D3) was between 24 and 32 percent higher than that of Mixture C1 (with no silica fume), as shown in Table 6. In fact, the 3-day compressive strength of D2 (10 percent silica fume) reached 95 percent of the 28-day strength of Mixture C1. In mixtures D4, D5, and D6, 20 percent fly ash was also included in the cementitious material of the mixture. The fly ash did slow down the rate of strength development at 3 days by an average of 12 percent. However, after 7 days, the compressive strength increased by 20 percent, reaching a strength equivalent to the 28-day strength of Mixture C1. This shows that fly ash can be used with silica fume in concrete mixtures without causing significant reduction in early strength. In fact, the fly ash may actually provide advantages to silica fume concrete mixtures in terms of lower cost and lower heat of hydration.

In mixtures D7 and D8, silica fume and a combination of silica fume and fly ash were used as additions to the cement content. The 28-day strength for D7 and D8 was slightly higher than the strength of D2 and D5. However, this strength increase over mixtures with fly ash and silica fume as replacements is not considered significant enough to warrant the use of silica fume and fly ash as additions to a concrete mixture with a high cement content. Benefits from slight increase in strength may be outweighed by increase in the cost of concrete.

Improved durability is an important advantage of using silica fume in concrete. This widely acknowledged fact is clearly demonstrated by the results of permeability tests and corrosion tests of the mixtures in Group D, as shown in Table 7.

Figure 2 is a graphical representation of the water permeability test results of Group D mixtures. From Figure 2 it can be observed that silica fume decreases the 91-day concrete permeability by as much as 75 percent. This substantial reduction is almost identical in silica fume contents of 5, 10, and 15 percent.

Figure 2 and Table 7 highlight an important fact about the role of fly ash in silica fume concrete. It is clear that the use of fly ash in the mixture does not seem to further reduce the permeability of silica fume concrete. This can be realized

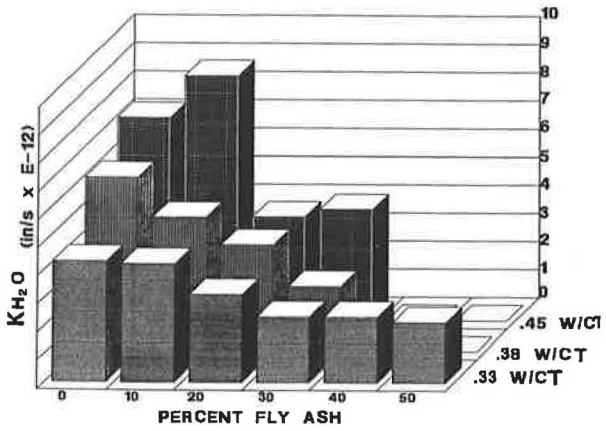

FIGURE 1 Effect of fly ash on water permeability of concrete at 91 days.

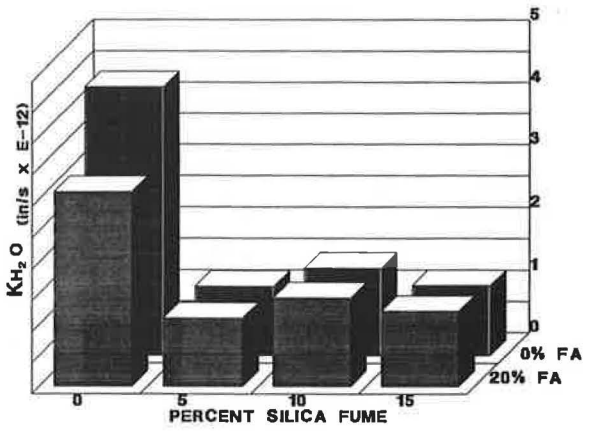

FIGURE 2 Effect of silica fume on water permeability of concrete at 91 days (FA = fly ash).

when comparing mixtures D4, D5, and D6 with D1, D2, and D3.

Silica fume also causes substantial increase in the corrosion resistance of concrete. This improvement in corrosion resistance correlates well with the significant drop in permeability, as shown in Table 7 and Figure 3. The silica fume/fly ash concrete mixtures in Group D showed remarkable resistance to corrosion compared with mixtures C1 (with only cement) and in C3 (with cement and fly ash). Tests on some Group D specimens had to be terminated after 120 days because no sign of corrosion was detected.

Correlation of Water and Chloride Permeability Tests

The AASHTO T277 rapid chloride permeability test is the only permeability test currently recognized in national specifications. An attempt was made to correlate results of the water permeability test developed in Florida with results of the chloride permeability test. Figure 4 shows the correlation between results of the two tests. By means of statistical regression analysis, a linear relation was established between the two tests. The equation is as follows:

$$K_{(H_2O)} = 9.02 \times 10^{-13} + 9.47 \times 10^{-16} K_{(Cl)}$$

R-square = 0.77

where $K_{(H_2O)}$ is water permeability and $K_{(Cl)}$ is chloride permeability. This simple relation can be used to correlate the results of the two permeability tests.

AASHTO T277 identifies 5 chloride permeability classifications and establishes criteria for these classifications based on charge passed through the specimen, as shown in Table 8. In this study, similar criteria based on water permeability were also established for the AASHTO classifications, as shown in the last column of Table 8. The water permeability criteria were derived from the correlation established between water and chloride permeabilities, as shown in Figure 4. Table 8 can now be used to determine permeability classification for a given concrete mixture based on results of either one of the two tests. This classification can be used to directly assess the durability of laboratory-produced concrete mixtures. Future work will be focused on developing criteria for permeability classification for field-produced concrete mixtures and for in-service structures.

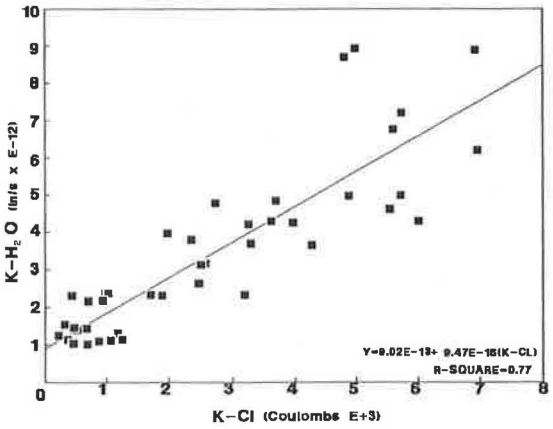

FIGURE 4 Relationship between water and chloride permeability test results.

Permeability and Compressive Strength

Water permeability values are plotted against the corresponding compressive strengths in Figure 5. Different classifications of water permeability are also plotted on the same figure. Compressive strength values are between 5,200 and 9,000 psi. Water permeability values are between 1.0×10^{-12} and 9×10^{-12} in./sec. The data points in Figure 5 represent all the mixtures including those with fly ash and silica fume.

It is clear from Figure 5 that concrete mixtures producing a given strength do not necessarily fall in the same permeability classification. There does not appear to be a clear correlation between strength and permeability. Lack of correlation is most obvious for concrete mixtures with compressive strengths between 5,000 and 7,500. Within this strength range, a concrete with low strength can have a lower permeability than that of a higher-strength concrete. This situation prevails until the compressive strength approaches 8,000 psi. At 8,000 psi and beyond, the permeability of concrete becomes low and remains within the low classification. A similar trend can also be observed in the relationship between chloride permeability and compressive strength, as shown in Figure 6.

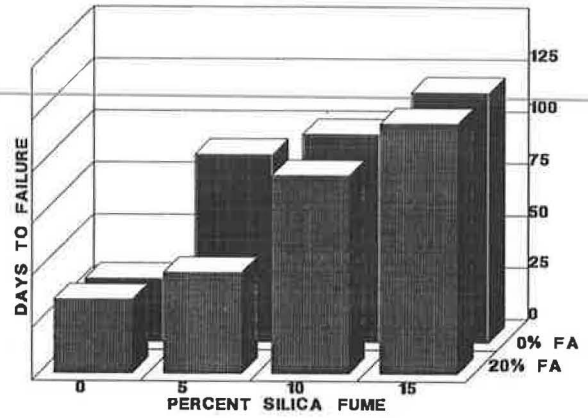

FIGURE 3 Time to corrosion (days) for concrete mixtures with silica fume (FA = fly ash).

TABLE 8 CLASSIFICATION OF CONCRETE PERMEABILITY

Permeability Classification, AASHTO T-277	Criteria	
	Chloride Permeability, Coulombs	Water Permeability, in/s x 10^{-12}
Negligible	< 100	------
Very Low	100 - 1000	< 1.0
Low	1000 - 2000	1.0 - 2.5
Moderate	2000 - 4000	2.5 - 4.5
High	> 4000	> 4.5

1 in/s = 0.0254 m/s

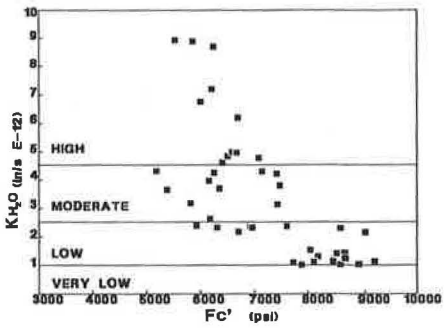

FIGURE 5 Correlation between water permeability and compressive strength.

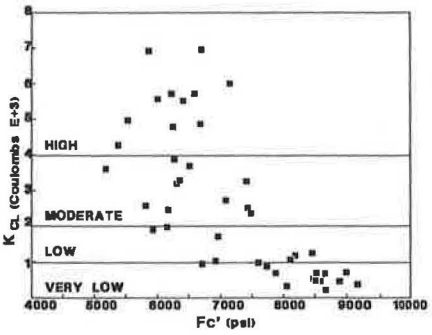

FIGURE 6 Correlation between chloride permeability and compressive strength.

In view of the poor correlation between strength and permeability, and the fact that permeability is an important indicator of durability, durability specifications should be developed for concrete to include requirements for both strength and permeability. These requirements can then be applied to improve the durability in concrete mixtures and ensure better-performing concrete structures.

CONCLUSIONS

Based on test results from this study the following conclusions are drawn:

1. Fly ash in concrete is effective in reducing permeability and improving corrosion resistance of concrete. Concrete with 20 to 30 percent fly ash shows the best overall results with respect to strength, permeability, and corrosion resistance.
2. Silica fume in concrete increases the compressive strength by up to 30 percent and lowers concrete permeability by as much as 70 percent.
3. High-performance concrete with respect to strength and durability can be produced from mixtures with w/c ratios at or below 0.35, and having at least 650 lb of cementitious material, including 20 to 30 percent fly ash and 5 to 10 percent silica fume.
4. A useful relationship is established between results of water permeability and the AASHTO T277 rapid chloride permeability tests for laboratory-produced concrete.
5. Concrete mixtures with similar compressive strength do not necessarily have similar level of permeability.
6. Durability specifications should be developed for concrete used in aggressive environments. These specifications should be based on requirements for both strength and permeability to ensure better performing and longer lasting concrete structures.

ACKNOWLEDGMENTS

The authors wish to thank M. Tia and P. Amornsrivilai for their contributions to this study. The assistance of R. Powers and J. Bachman in the corrosion tests is much appreciated.

REFERENCES

1. P. Soongswang, M. Tia, D. Bloomquist, C. Meletiaou, and L. Sessions. An Efficient Test Setup for Determining the Water-Permeability of Concrete. In *Transportation Research Record 1204,* TRB, National Research Council, Washington, D.C., 1988, pp. 77–82.
2. R. Brown and R. Kessler. *An Accelerated Laboratory Method for Corrosion Testing of Reinforced Concrete Using Impressed Current.* Research Report 206. Bureau of Materials and Research, Florida Department of Transportation, Gainesville, Oct. 1978.

Publication of this paper sponsored by Committee on Chemical Additions and Admixtures for Concrete.

Abridgment

Nondestructive Testing of Concrete Block Foundations for Telecommunication Towers

T. REZANSOFF, K. W. NASSER, AND P. S. H. LAI

The long-term performance of concrete blocks more than 25-years-old that anchored the guy wires bracing telecommunication towers was evaluated. Tasks included on-site visual inspection and nondestructive field and laboratory tests. Laboratory tests on drilled cores permitted correlation of nondestructive tests to the concrete compressive strength. Test results were analyzed, and recommendations were made to provide guidelines for evaluating the performance of similar concrete structures.

Although the deterioration of concrete is a common problem, severe service conditions, such as exposure to sulfates, deicing salts, and freezing and thawing, can be accommodated with proper design. Because many concrete structures are approaching their serviceability limit because of neglect or improper design, appropriate nondestructive testing procedures to evaluate their structural integrity are continuing at the University of Saskatchewan. The most common nondestructive testers available on the market are the rebound hammer, and the ultrasonic pulse velocity and pin penetration testers. Nondestructive field tests were compared with laboratory tests made on core samples obtained from the same structure, and guidelines for evaluating in situ strength of similar concrete structures are presented here.

INVESTIGATION

Saskatchewan Telecommunications, because of concerns about the integrity of concrete blocks used to anchor transmission towers, commissioned the investigation of three sites located near three communities in the Province of Saskatchewan, Canada. The below-ground anchor blocks, with dimensions of 60 × 36 × 72 in. in the community of Swift Current, 30-in. diameter × 70-in. depth in Rosetown, and 72-in. diameter × 50-in. depth in Oxbow, were made of concrete produced on site and are more than 25 years old. Another anchor block near the Oxbow site, which was only 5 years old, was also included in the study in order to increase the data base. The blocks were excavated to permit visual inspection and in-place testing.

Visual inspection of the anchor blocks revealed some spotty minor deterioration on the top surface of the concrete. The overall quality and condition of the blocks appeared to be satisfactory. No evidence of reinforcing steel corrosion was observed on the surface of the blocks.

University of Saskatchewan, Saskatoon, Canada, S7N 0W0.

The rebound hammer (ASTM C805) and the ultrasonic pulse velocity (ASTM C597) tests were chosen to investigate the condition of the concrete blocks. Results obtained from in situ nondestructive tests were compared with data from cores that were tested in the laboratory using the same nondestructive tests. The cores were then failed by either compression (ASTM C39) or splitting tension (ASTM C496). The air void systems of the hardened concrete were determined by the linear traverse modified point-count method (ASTM C457).

Because soils in most areas of Saskatchewan are known to contain sulfates that may affect the long-term durability of concrete, samples taken from each location were tested to determine sulfate content.

NONDESTRUCTIVE TEST DETAILS

Rebound Hammer

After the exposed surfaces were cleaned, ground relatively smooth, and marked with a grid pattern, surface hardness of the in-place concrete was determined by a rebound hammer to provide a relative measure of the quality of the surface concrete. Eight readings in the vicinity of a grid point were averaged to give one rebound number. In laboratory testing, the cores were lightly loaded in a compression testing machine, and the rebound hammer tests were performed on the circumferential surface.

Ultrasonic Pulse Velocity

Pulse velocity measurements were taken using a "V" meter. Depending on the arrangement of the transducers on the concrete surfaces, the transmission may be direct, indirect, or semidirect. In the direct transmission method, the transmitter and receiver are positioned on two opposite parallel faces; longitudinal pulses leaving the transmitter are propagated in the concrete in a direction normal to the transducer faces to provide maximum sensitivity along a well-defined path length. The indirect transmission method, in which both transducers are placed on the same concrete face, is the least satisfactory because, apart from its relative insensitivity and less well-defined path length, it gives pulse velocity measurements that are influenced by the concrete layer near the surface, and this layer may not be representative of the concrete

in deeper layers. Intermediate accuracy is obtained by using semidirect transmission by placing the transmitting transducer on a face perpendicular to the receiving transducer.

Direct transmission longitudinally through the cores was used in the laboratory tests, whereas in the field all three measurements were used. Grease was used as a coupling medium between transducers and concrete. Because the amount of reinforcing steel in the blocks was minimal, no attempt was made to locate it.

ANALYSIS OF TEST DATA

Laboratory Calibration Tests

Part of the evaluation program was based on testing 4- × 8-in. cores that were drilled from the concrete block foundations. For each core, measurements were made to determine density, water absorption, pulse velocity, rebound number, and pin penetration. Most cores were then failed in compression; the remaining cores were failed in splitting tension. Average results for each site are presented in Table 1, and individual core compressive strengths are shown in Figure 1.

Regression analyses were performed on the data obtained from the core tests to correlate compressive strength with measured pulse velocity (Figure 1). A correlation curve from a previous study (*1*) is also shown.

Analysis of the rebound hammer data from the cores showed unsatisfactory correlation of strength with the rebound hammer number. It is possible that cored surfaces do not provide reliable readings.

Field Tests

Field pulse velocity test data were converted to concrete compressive strength data using the correlation curves obtained from the core tests. Rebound hammer field data were converted to concrete strength using the calibrations provided with the hammer, because rebound hammer tests on the cores did not provide a reasonable correlation curve. A statistical summary of the estimated strength data is provided in Table 1.

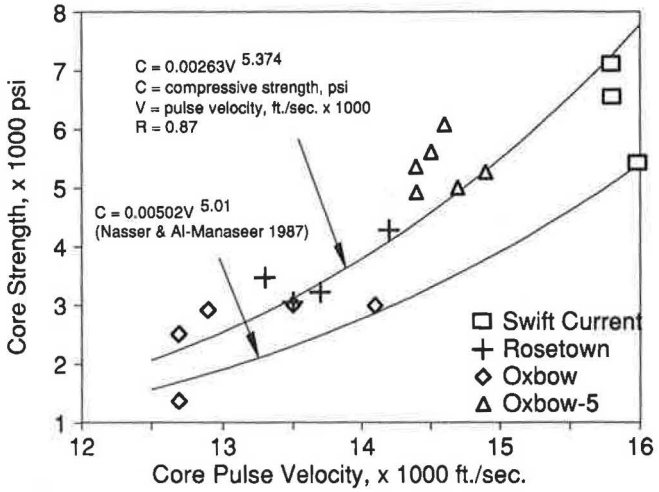

FIGURE 1 Relationship between core pulse velocity and core strength of concrete.

Pulse Velocity Tests and Data

The high ranges and coefficients of variation common in much of the strength data predicted from pulse velocities in Table 1 do not necessarily reflect the variation of the concrete strength through the various anchor blocks. Much of the pulse velocity data recorded is unreliable, because readings were attempted under conditions beyond the capabilities of the equipment.

TABLE 1 SUMMARY OF TEST DATA

	Core Tests				Field (In-situ) Tests								
Site	SC*	R	O	O-5	SC			R			O		
Pulse Velocity	D**	D	D	D	D**	S	I	D	S	I	D	S	I
No. of tests	4	5	7	8	3	21	12	6	14	15	3	17	16
Comp. Strength													
Mean, psi	7110	3530	2640	4700	3110	4080	2070	3500	2760	1360	2790	700	100
Maximum, psi	7780	4100	3120	5300	4760	6560	3380	4420	5500	4930	4250	1450	494
Minimum, psi	6120	2880	2250	4420	770	21	770	1660	810	390	1320	44	2
Coef. of Var. %	9.9	13.1	17.1	6.6	67	43	35	28	52	84	74	66	148
Rebound													
No. of tests	4	5	7	8		32			22			21	
Comp. Strength													
Mean, psi	1700	2800	1700	3500		4750			2070			1570	
Maximum, psi	1800	3000	1800	4200		6690			3700			2200	
Minimum, psi	1500	2800	1000	2800		2570			1100			1100	
Coef. of Var. %	9.2	3.2	17.5	14.2		4.6			8.1			5.5	
Core Comp.													
No. of tests	3	4	6	6									
Comp. Strength													
Mean, psi	6830	3510	2590	5390									
Maximum, psi	7130	4290	3010	6100									
Minimum, psi	5440	3060	1370	4920									
Coef. of Var. %	13.5	15.6	24.0	8.1									

Other Core Tests	SC	R	O
WaterAbsorption %	1.2	3.7	3.5
Density, lb./cu.ft.	147.3	142.8	141.7
Rebound Number	24	30	24
Splitting Tension, psi	564	421	353
Modulus of Elasticity, x 10^6 psi	2.70	1.35	1.17
Air Content %	5.5	5.2	4.9
Air-void Spacing Factor, in.	0.015	0.015	0.037

* SC = Swift Current, R = Rosetown, O = Oxbow, O-5 = Oxbow-5 year old concrete block
** D = direct transmission, S = semi-direct transmission, I = indirect transmission

Detailed examination of the concrete strengths estimated from the pulse velocities revealed that unrealistically low strengths usually resulted from semidirect transmission if one or both of the concrete surfaces on which the sending and receiving transmitters were placed were not formed but the concrete was simply cast against a plastic sheet separating the concrete block from the clay excavation. Although the unformed surfaces were ground to remove some roughness, apparently the coupling of the transducer with the concrete was not adequate for semidirect transmission. Only with direct transmission could reasonable results be obtained with an unformed surface. If both faces were formed or troweled, semidirect transmission usually gave a reasonable strength prediction.

With indirect transmission, unrealistic results were often obtained even if both faces were formed, and even if the distances between the transmitters were short. Because strength (f'_c) is a function of pulse velocity (V) raised to a high power ($f'_c = aV^b$, with b ranging from 5 to 6, where a and b are calibration constants), extreme caution is needed in evaluating the statistics. Even a small error in pulse velocity will indicate a large error in predicted strength. Although other factors, such as voids in the concrete along the transmission path, or the presence of reinforcing steel, can invalidate pulse velocity data, in the current study it appears that rough concrete surfaces or long transmission paths make much of the semidirect and indirect pulse velocity data suspect.

In two of the three sites investigated (Rosetown and Oxbow), the mean concrete strength predicted from direct transmission pulse velocity measurements lay within the range of strengths measured from compression tests on the cores and were relatively close to the mean strengths of all cores from the site considered (Table 1). At the Rosetown site, a large amount of the semidirect pulse velocity data was obtained between two smooth faces over relatively short distances. One was a formed vertical face, whereas the second face was the troweled top face of the block. These data yielded better correlation with the core strengths than the limited data that were recorded from direct transmission pulse velocities. The low value of 770 psi obtained from one of the three pulse velocities recorded by direct transmission was between two rough unformed surfaces separated by a relatively long (5 ft) transmission path.

Rebound Hammer Tests and Data

Compressive strengths obtained from rebound hammer numbers are summarized in Table 1. The calibration data obtained from the Schmidt hammer were applied directly, because the calibration using the data obtained from the 4- × 8-in. cores was unsuccessful. The mean strength predicted at each site from the rebound hammer data was only on the order of 60 to 75 percent of the measured average compressive strengths obtained in cores from the corresponding sites.

Accurate correlation was not expected because the rebound hammer approach is known not to provide accurate assessment of strength in old, hardened concrete. However, that the rebound numbers provided some correlation with concrete strength, in samples that were different in design, materials used, service location, and strength, shows potential for field evaluation of old concretes.

Other Tests and Measurements

The sulphate contents (percent by weight of dry soil as SO_4) were negligible at the Swift Current site, 0.31 percent at Rosetown, and 0.016 percent at Oxbow. Design records showed that the concrete blocks were made with ASTM Type V sulphate resisting cement, thus the high sulphate content in the Rosetown area did not cause significant deterioration of the concrete block as witnessed during the visual inspection.

The water absorption, density, modulus of elasticity, and splitting tensile strength presented in Table 1 for the various cores indicated that the core strength increased with concrete density and decreased with the degree of water absorption. Modulus of elasticity and splitting tensile strength were related to the compressive strength of the cores.

The air contents determined from cores (Table 1) show approximately 5 percent air, although it is believed that air-entraining agents were not used in the mix designs. The relatively high air-void spacing factors, exceeding the 0.1-in. value recommended as a maximum by Powers (2) for ensuring frost resistance under severe exposure, suggests that the air content is entrapped air only.

RECOMMENDATIONS

Recommendations for investigating the integrity and condition of buried concrete structures are as follows:

1. A visual inspection is needed for preliminary information on the surface condition and defines the field testing required.
2. The limitations of the nondestructive tests that will be used in the investigation must be known in advance. A minimum of two nondestructive tests are recommended for estimating in situ strength. Testing of representative cores is essential to ensure that reasonable calibration curves are used for evaluating field data.
3. For rough concrete surfaces (e.g., concrete cast against an excavated clay wall), direct transmission with the pulse velocity test yields representative results. Semidirect transmission may be unreliable with rough surfaces. Indirect transmission may be unreliable with all surfaces.

ACKNOWLEDGMENTS

The authors are grateful to SaskTel Corporation for assistance and for granting permission to publish this article. Thanks are also extended to D. Stott and H. Tala for performing some of the laboratory testing.

REFERENCES

1. K. W. Nasser and A. A. Al-Manaseer. Comparison of Nondestructive Testers of Hardened Concrete. *ACI Journal,* Vol. 84, No. 5, 1987, pp. 374–380.
2. T. C. Powers. The Air Requirement of Frost-Resistant Concrete. *HRB Proc.*, Vol. 29, 1949, pp. 184–201.

Publication of this paper sponsored by Committee on Mechanical Properties of Concrete.